

# Verification of a One-Dimensional, Unsteady-Flow Model for the Fox River in Illinois

United States  
Geological  
Survey  
Water-Supply  
Paper 2477

Prepared in cooperation  
with the Illinois Department  
of Natural Resources,  
Office of Water Resources  
and the Du Page County,  
Department of  
Environmental Concerns



---

## AVAILABILITY OF BOOKS AND MAPS OF THE U.S. GEOLOGICAL SURVEY

---

Instructions on ordering publications of the U.S. Geological Survey, along with prices of the last offerings, are given in the current-year issues of the monthly catalog "New Publications of the U.S. Geological Survey." Prices of available U.S. Geological Survey publications released prior to the current year are listed in the most recent annual "Price and Availability List." Publications that may be listed in various U.S. Geological Survey catalogs (see **back inside cover**) but not listed in the most recent annual "Price and Availability List" may be no longer available.

Order U.S. Geological Survey publications **by mail** or **over the counter** from the offices given below.

### BY MAIL

#### Books

Professional Papers, Bulletins, Water-Supply Papers, Techniques of Water-Resources Investigations, Circulars, publications of general interest (such as leaflets, pamphlets, booklets), single copies of Earthquakes & Volcanoes, Preliminary Determination of Epicenters, and some miscellaneous reports, including some of the foregoing series that have gone out of print at the Superintendent of Documents, are obtainable by mail from

**U.S. Geological Survey, Information Services  
Box 25286, Federal Center, Denver, CO 80225**

Subscriptions to periodicals (Earthquakes & Volcanoes and Preliminary Determination of Epicenters) can be obtained **ONLY** from the

**Superintendent of Documents  
Government Printing Office  
Washington, DC 20402**

(Check or money order must be payable to Superintendent of Documents.)

#### Maps

For maps, address mail orders to

**U.S. Geological Survey, Information Services  
Box 25286, Federal Center, Denver, CO 80225**

### OVER THE COUNTER

#### Books and Maps

Books and maps of the U.S. Geological Survey are available over the counter at the following U.S. Geological Survey Earth Science Information Centers (ESIC), all of which are authorized agents of the Superintendent of Documents:

- **ANCHORAGE, Alaska**—Rm. 101, 4230 University Dr.
- **LAKEWOOD, Colorado**—Federal Center, Bldg. 810
- **MENLO PARK, California**—Bldg. 3, Rm. 3128, 345 Middlefield Rd.
- **RESTON, Virginia**—USGS National Center, Rm. 1C402, 12201 Sunrise Valley Dr.
- **SALT LAKE CITY, Utah**—Federal Bldg., Rm. 8105, 125 South State St.
- **SPOKANE, Washington**—U.S. Post Office Bldg., Rm. 135, West 904 Riverside Ave.
- **WASHINGTON, D.C.**—Main Interior Bldg., Rm. 2650, 18th and C Sts., NW.

#### Maps Only

Maps may be purchased over the counter at the following U.S. Geological Survey offices:

- **ROLLA, Missouri**—1400 Independence Rd.
- **STENNIS SPACE CENTER, Mississippi**—Bldg. 3101

# Verification of a One-Dimensional, Unsteady-Flow Model for the Fox River in Illinois

By AUDREY L. ISHII and MARY J. TURNER

Prepared in cooperation with the  
Illinois Department of Natural Resources,  
Office of Water Resources and the  
Du Page County Department of  
Environmental Concerns

U.S. GEOLOGICAL SURVEY WATER-SUPPLY PAPER 2477

U.S. DEPARTMENT OF THE INTERIOR  
BRUCE BABBITT, Secretary

U.S. GEOLOGICAL SURVEY  
Gordon P. Eaton, Director



Any use of trade, product, or firm names in this publication is for descriptive purposes only and does not imply endorsement by the U.S. Government.

UNITED STATES GOVERNMENT PRINTING OFFICE, WASHINGTON: 1997

---

For sale by the  
U.S. Geological Survey  
Information Services  
Box 25286  
Federal Center  
Denver, CO 80225

**Library of Congress Cataloging in Publication Data**

Ishii, Audrey L.

Verification of a one dimensional, unsteady-flow model for the Fox River in Illinois  
/ by Audrey L. Ishii and Mary J. Turner.

p. 65 cm.—(U.S. Geological Survey water-supply paper; 2477)

“Prepared in cooperation with the Illinois Department of Natural Resources, Office of Water Resources and the Du Page County, Department of Environmental Concerns.”

Includes bibliographical references.

Supt. of Docs. no.: I 19. 13:2477

1. Stream measurements—Fox River (Wis. and Ill.) 2. Stream measurements—  
Illinois. I. Turner, Mary J. II. Illinois. Office of Water Resources.

III. Du Page County (Ill.). Dept. of Environmental Concerns. IV. Title.

V. Series.

GB1225.I27184 1996  
551.48'3'09773—dc20

96-38748  
CIP

# CONTENTS

- Abstract ..... 1
- Introduction ..... 2
  - Purpose and Scope ..... 2
  - Description of Study Area ..... 2
  - Acknowledgments ..... 3
- Data Collection ..... 3
- Development of a One-Dimensional, Unsteady-Flow Model ..... 8
- Implementation and Calibration of the Fox River Model ..... 9
  - Channel Geometry ..... 11
  - Control Structures ..... 15
  - Boundary and Initial Conditions ..... 16
  - Roughness Coefficient Selection ..... 17
  - Transport-Model Description ..... 20
- Verification of the Fox River Model ..... 20
  - Hydraulic Simulation Results ..... 21
  - Transport Simulation Results ..... 32
- Sensitivity Analysis ..... 39
  - Convergence ..... 43
  - Hydraulic Geometry ..... 46
  - Boundary and Initial Conditions ..... 52
  - Roughness Coefficient ..... 53
- Evaluation of the Model ..... 61
- Summary and Conclusions ..... 64
- References Cited ..... 65

## FIGURES

- 1. Map showing location of the Fox River study reach and data-collection sites in Illinois..... 4
- 2. Graph showing the Fox River study-reach bottom elevation and data-collection sites in Illinois..... 5
- 3. Model schematic of the Fox River in Illinois showing output locations..... 10
- 4. Plots of the surveyed channel cross section nearest to discharge, stage, and dye data-collection sites for the Fox River study reach in Illinois ..... 12
- 5-7. Graphs showing:
  - 5. Measured or rated and calibrated discharge and stage for the July–August 1990 calibration-check period for the Algonquin Dam headwater on the Fox River in Illinois..... 18
  - 6. Measured or rated and calibrated discharge and stage for the May–June 1991 calibration-check period at the Algonquin Dam headwater on the Fox River in Illinois ..... 19
  - 7. Measured or rated and simulated discharge and stage at data-collection sites on the Fox River in Illinois..... 22
- 8. Photographs of selected data-collection sites on the Fox River in Illinois..... 30
- 9-27. Graphs showing:
  - 9. Measured or rated and simulated stage-discharge relations at data-collection sites on the Fox River in Illinois for the October 30–November 11, 1990, study period..... 33
  - 10. Measured and simulated dye concentrations and discharge at data-collection sites on the Fox River in Illinois..... 40
  - 11. Effect of varying the convergence criterion on simulated discharge and stage at Huntley Road Bridge at Carpentersville, Ill. .... 44

12. Effect of varying the temporal-integration weighting factor on simulated discharge and stage at Huntley Road Bridge at Carpentersville, Ill. ....	45
13. Simulated discharge and stage for maximum computational intervals of 5 minutes, 15 minutes, and 1 hour at Huntley Road Bridge at Carpentersville, Ill. ....	47
14. Effect of varying computational distance step on simulated discharge and stage at selected sites on the Fox River in Illinois ....	48
15. Effect of varying computational parameters on model error ....	49
16. Effect of bridge and cross-section geometric data on simulated discharge and stage at selected sites on the Fox River in Illinois ....	50
17. Effect of bridge head-loss coefficients on simulated discharge and stage at the Railroad Bridge at Carpentersville, Ill. ....	51
18. Effect of boundary-datum error on simulated discharge and stage at Huntley Road Bridge at Carpentersville, Ill., for discharge-stage (Q-Z) and stage-stage (Z-Z) boundary conditions ....	52
19. Effect of boundary-datum error at the Elgin Dam crest on simulated discharge and stage upstream and downstream from the dam for discharge-stage (Q-Z) and stage-stage (Z-Z) boundary conditions on the Fox River study reach in Illinois ....	54
20. Upstream and downstream boundary conditions for 5-minute, 1-hour, 6-hour, and mean daily time intervals for the Fox River study reach in Illinois ....	55
21. Effect of boundary-condition data time resolution on simulated discharge and stage at Huntley Road Bridge at Carpentersville, Ill. ....	56
22. Effect of input-data time resolution and maximum computational interval on simulated discharge and stage at Huntley Road Bridge at Carpentersville, Ill. ....	57
23. Effect of varying initial conditions on simulated discharge and stage at Huntley Road Bridge at Carpentersville, Ill. ....	58
24. Effect of varying the roughness coefficient by 30 percent upstream from Algonquin Dam on the Fox River in Illinois on simulated discharge and stage at selected sites upstream and downstream from the dam ....	59
25. Effect of varying the roughness coefficient by 30 percent downstream from the Algonquin Dam on the Fox River in Illinois on simulated stage and discharge at selected sites upstream and downstream from the dam ....	60
26. Effect of linear variation in the roughness coefficient from 0.030 at 4-ft depth to 0.130 at 0-ft depth at selected sites of the Fox River study reach in Illinois. ....	62
27. Effect of varying the roughness coefficient by 30 percent throughout the Fox River study reach on simulated dye concentration at selected sites in Illinois ....	63

## TABLES

1. Data-collection sites for the Fox River study reach in Illinois ....	6
2. Tributary areas and scaling ratios for estimating inflow to the Fox River in Illinois. ....	17

## CONVERSION FACTORS AND VERTICAL DATUM

<b>Multiply</b>	<b>By</b>	<b>To obtain</b>
foot (ft)	0.3048	meter
mile (mi)	1.609	kilometer
square mile (mi <sup>2</sup> )	2.590	square kilometer
cubic foot per second (ft <sup>3</sup> /s)	0.02832	cubic meter per second
pound, avoirdupois (lb)	$453.6 \times 10^6$	microgram
foot per mile (ft/mi)	0.00019	dimensionless slope

Temperature in degrees Fahrenheit ( $\times\times\times^\circ\text{F}$ ) may be converted to degrees Celsius ( $^\circ\text{C}$ ) as follows:

$$^\circ\text{C} = 5/9 \times (^\circ\text{F} - 32)$$

**Sea level:** In this report, "sea level" refers to the National Geodetic Vertical Datum of 1929 (NGVD of 1929)—a geodetic datum derived from a general adjustment of the first-order level nets of both the United States and Canada, formerly called Sea Level Datum of 1929.

# Verification of a One-Dimensional, Unsteady-Flow Model for the Fox River in Illinois

By Audrey L. Ishii *and* Mary J. Turner

## Abstract

A one-dimensional, unsteady-flow model utilizing the Full de Saint-Venant Equations (FEQ) for one-dimensional, unsteady flow in open channels was verified for a 30.6-mile reach of the Fox River in northeastern Illinois. The model, which was calibrated prior to the verification study by the Illinois Department of Natural Resources, Office of Water Resources and the Illinois State Water Survey, was used to simulate a period of unsteady, within-bank flow induced by dam operations at the upstream end of the river reach, Stratton Dam near McHenry, Illinois, during November 1990. The river reach included three low-head dams that resulted in backwater effects where the channel slope was small. The river stages and streamflows simulated by the model, together with dye-injection rate and concentration data measured at Stratton Dam, were used as input for a transport model, the Branched Lagrangian Transport Model. The simulation results from both models were compared graphically with stage, streamflow, and (or) dye-concentration data collected during the unsteady-flow period at a total of 31 downstream sites. The celerity of the induced low-flow wave was simulated accurately, with no significant error at any location. Differences during low-flow conditions between measured and simulated stage were less than about 0.2 foot at most of the sites, although differences up to 0.8 foot resulted at four sites where depths were shallow or head losses were inadequately represented through bridges. The differences may have resulted from the increase in effective

roughness in the channel at very low depths that was not effectively modeled. Furthermore, accurate and representative measurements were difficult under some conditions of very low velocities or water-head buildup on the upstream side of bridges. The traveltime and concentration attenuation of the dye cloud were accurately simulated.

The effects of the physical and computational model parameters also were examined. The converged model was insensitive to distance-step and time-step size. The initial conditions were varied by 50 percent, and the simulated stage and discharge still converged to a common solution within twelve 1-hour time steps. The sensitivity of the model to geometric data was studied by replacing measured cross sections with interpolated cross sections within branches. The changes in distance-step size and geometric information had no effect on flood-wave celerity or discharge, but simulated stage was affected by how well the remaining cross sections represented local channel geometry. Deletion of bridge representations from the model caused no significant effects on the overall hydraulic routing, and only local effect on stage probably because the period simulated did not include high flow. Because of low-head controlling dams throughout the study reach, sensitivity to error in gage datum depended on the type of boundary condition used and whether the datum error was in the upstream or downstream boundary. The FEQ model was evaluated as accurate and robust for this application.

## INTRODUCTION

The delineation of the regulatory flood plain is an urgent need in areas undergoing rapid urbanization. The traditional application of standard step-backwater approaches with a steady-flow design discharge can incorrectly describe flood-plain hydraulics, particularly where channel storage, backwater, and backwater at junctions are important. The topography in Illinois is generally flat to gently sloping, and rivers usually have flood plains of considerable size. These conditions frequently result in flow conditions with backwater and channel or overbank storage. Therefore, the capability to do flood routing using unsteady-flow principles is a vital need for water-resources planners and regulators in Illinois.

Only thorough calibration and verification of an unsteady-flow model application with data collected in the field can ensure the reliability and value of the model results (Schaffranek, 1989, p. 1). To maximize confidence in the accuracy and robustness of both the model numerical routines and the representation of a particular river, the verification data set should be independent from the data used to calibrate the model. Independence implies that the data are collected from different time periods than those used to calibrate the model, and also, if possible, at different locations. The comparison of flow conditions at points in the stream not used in the model calibration strengthens the verification. The model robustness also should be evaluated to assist the user in parameter selection. This report is one product of a continuing study to address these needs. The study is being done in cooperation with the Illinois Department of Natural Resources, Office of Water Resources (IDNR/OWR), and Du Page County, Department of Environmental Concerns, and includes the documentation of the Full EQUations (FEQ) model for the solution of the full, dynamic equations of motion for one-dimensional, unsteady flow in open channels and through control structures (Franz and Melching, in press); the companion program the Full EQUations UTiLity model (FEQUTL) for approximating the hydraulic properties of open channels and control structures; and the data set used in this report to verify the model (Turner, 1994).

The model, FEQ, is unique in that many control structures and stream features including weirs, bridges, culverts, overbank areas, and embankments, and several dynamic controls, such as pumps and dams, may be represented by function tables that are computed by the companion program, FEQUTL, and accessed as

needed during model execution. The data collection for this verification study was planned to test several aspects of model performance, primarily by illustrating the ability of the model to route a rapid change in flow through a river system containing a large number of controlling features, such as bridges, low-head dams, and flat slopes.

## Purpose and Scope

This report documents the verification of the one-dimensional, unsteady-flow FEQ model of the Fox River in Illinois by the use of a set of field data that was collected specifically for the purpose of verifying the previously calibrated model. To provide a potential user with information regarding the accuracy, reliability, and robustness of the model, convergence testing and sensitivity analyses also are documented.

The capability of the calibrated model to reproduce a period of unsteady flow induced by dam operation at the upstream boundary is demonstrated by comparing the calibrated model results to stage and discharge data collected at 16 and 8 locations, respectively, on the mainstem of the Fox River. For the majority of the data-collection sites, no previous data were available for the calibration. The model-simulated flow field was input to a Branched Lagrangian Transport Model (BLTM), and the transport of a conservative dye was simulated and compared with collected dye-concentration data at 17 downstream locations to evaluate the total simulated flow field output by the model. The sensitivity of the model to the computational and physical model parameters is shown by varying the values for the time- and distance-step size, the temporal-integration weighting factor, the convergence criterion, the resolution of temporal and spatial data, the initial and boundary conditions, and the hydraulic geometry including bridges and the roughness coefficients; and then by comparing the results graphically.

## Description of Study Area

The Fox River is located in southwestern Wisconsin and northeastern Illinois, in an area flattened by till and outwash deposits from receding glaciers. The origin of the Fox River lies about 15 mi northwest of Milwaukee in Waukesha County, Wis. From its source, the river flows south to the Illinois-Wisconsin border through the Chain-of-Lakes in Lake and

McHenry Counties in Illinois, bends southwesterly just south of Aurora in Kane County, and continues to its junction with the Illinois River near Ottawa in La Salle County. The total length of the Fox River is about 185 mi.

The Fox River watershed covers 2,658 mi<sup>2</sup> and is a major tributary to the Illinois River. The mean annual flow for the Fox River at Algonquin, which has a drainage area of 1,403 mi<sup>2</sup>, for October 1915–September 1992 is 867 ft<sup>3</sup>/s. The mean flow for November for the same period is 784 ft<sup>3</sup>/s. The peak flow for the period of record was 6,610 ft<sup>3</sup>/s on both April 6, 1960, and April 2, 1979. The minimum daily mean flow was 12 ft<sup>3</sup>/s on August 30 and 31, 1934, and July 28, 1942. The flow range at Algonquin Dam, simulated as part of the verification study, ranged from 170 to 1,700 ft<sup>3</sup>/s.

The study area and the data-collection sites are shown in figure 1. The reach of the Fox River discussed in this report is regulated by Stratton Dam near McHenry, Ill. (river mile 97.8), and ends 30.6 mi downstream at South Elgin, Ill. (river mile 67.2). This study area includes portions of Lake, McHenry, and Kane Counties in Illinois. The minimum riverbed elevations at selected locations are shown in figure 2. The total fall of the river reach included in the study is 32.6 ft, of which 29.7 ft is below Algonquin Dam (river mile 81.6). Hence, the river reach between Stratton Dam and Algonquin Dam is relatively flat with a slope of 0.18 ft/mi (0.0034 percent). Between Algonquin Dam and South Elgin Dam the slope averages 2.06 ft/mi (0.039 percent). The incremental drainage area between Stratton Dam and South Elgin Dam is 306 mi<sup>2</sup>, with one-half of the incremental increase in drainage area above Algonquin Dam and one-half below Algonquin Dam. The river channel cross-sectional data were obtained from surveys carried out by the IDNR/OWR, the U.S. Army Corps of Engineers, and the U.S. Geological Survey.

## Acknowledgments

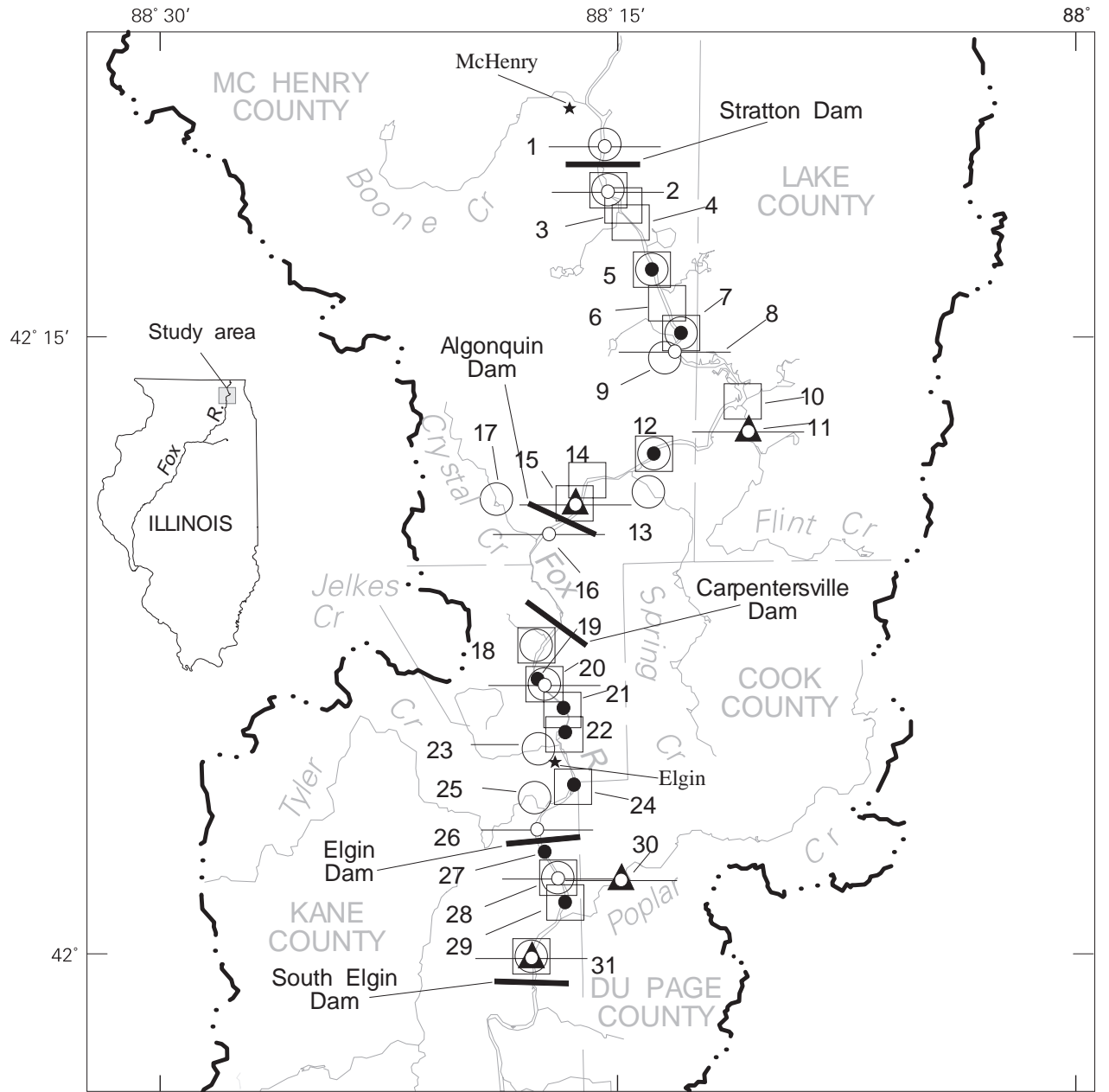
The authors are grateful to the Illinois Department of Natural Resources, Office of Water Resources, particularly William R. Rice and Rita M. Lee for providing model data sets, survey data, and technical advice.

## DATA COLLECTION

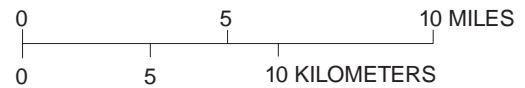
Data collection for this study was designed to measure a period of highly unsteady flow. The study reach was selected for three major reasons: (1) The average slope of the reach was small; thus, sensitive to backwater effects; (2) a data-collection network was available for calibration and could be supplemented for verification; and (3) flow throughout the reach could be controlled by the sluice gates at Stratton Dam. The sluice gates were operated to induce low flow (60–200 ft<sup>3</sup>/s) throughout the reach followed by an abrupt increase in discharge (to about 1,600 ft<sup>3</sup>/s), producing a relatively sharp wave. Stage, discharge, and dye data were collected during an 11-day period (October 31–November 10, 1990) at the 31 sites in the study reach (fig. 1). Locations and types of data collected at each site are shown in table 1. A detailed description of the data-collection synoptic is presented in Turner (1994).

On the mainstem of the Fox River, continuous-stage data were collected using electronic data recorders upstream and downstream from the upstream boundary (Stratton Dam); near Rawson Bridge; upstream and downstream from two of the three uncontrolled overflow dams inside the river reach (the dams at Algonquin and Elgin); at the Huntley Road Bridge in Carpentersville; and upstream and downstream from the downstream boundary, the uncontrolled overflow dam at South Elgin. Other observations of stage were made periodically at nine other locations. The stage data-collection locations were selected to maximize information about the effect of the control structures, such as dams and bridges, on stage-discharge relations including backwater and channel storage.

A total of 132 discharge measurements at 16 locations (of which 24 were made on 7 of the tributaries to the Fox River) were made to define the flow for the river system study reach. The locations and timing of these measurements were determined by preliminary modeling to either define or verify the stage-discharge relations for the unsteady-flow synoptic period or to quantify the discharge through the system for boundary-condition input to the model. The discharge measurements made during the study are considered to be more reliable for the quantification of unsteady flow than discharges computed from ratings, which are developed over time and represent average steady-flow conditions. Thus, the upstream boundary condition was defined by 18 measurements made



Base from U.S. Geological Survey  
 1:100,000 Digital Line Graphs  
 Albers Equal-Area Conic Projection  
 Standard parallels 33° and 45°, central meridian -89°



### EXPLANATION

	BASIN BOUNDARY		MEASURED DISCHARGE
	CONTINUOUS STAGE		RATED DISCHARGE
	DAM		DYE SAMPLE COLLECTION
	SITE NUMBER		PERIODIC STAGE

**Figure 1.** Location of the Fox River study reach and data-collection sites in Illinois. (Site numbers are referenced to table 1.)

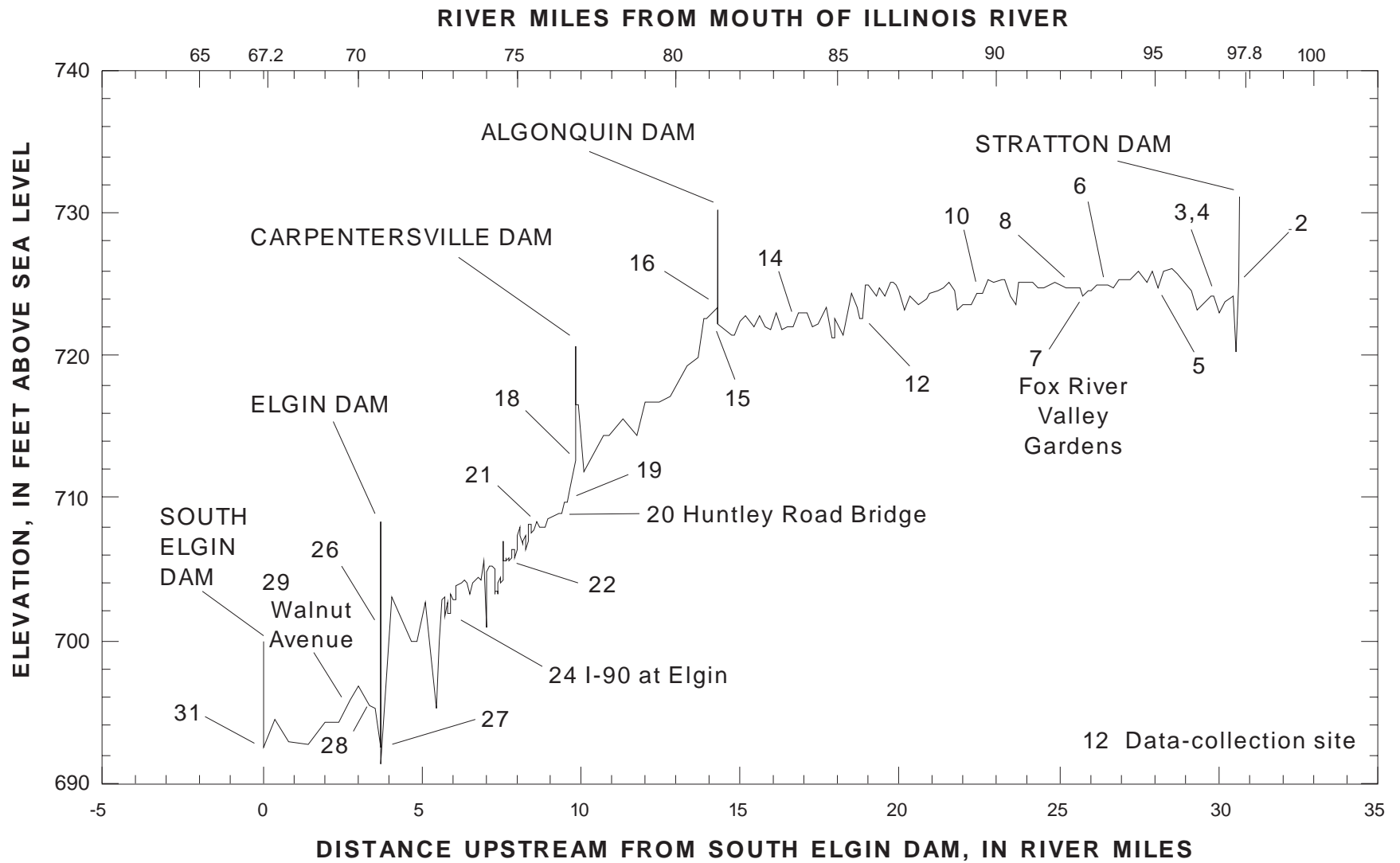


**Figure 2.** Fox River study-reach bottom elevation and data-collection sites in Illinois. (Site numbers are referenced to table 1.)

**Table 1.** Data-collection sites for the Fox River study reach in Illinois

[—, no downstream-order station number; add 67.2 to study-reach mile to obtain approximate Fox River mile (modeled mile may differ slightly)]

Site number	River miles above downstream end of study reach	Downstream-order station number	Station name and U.S. Geological Survey downstream order number	Short name	Type of data collected and location on tributary, if applicable
1	30.6	05549500	Fox River near McHenry	Stratton Dam headwater	Continuous stage, measured discharge.
2	30.6	05549500	...do....	Stratton Dam tailwater	Continuous stage, measured discharge, dye sample collection.
3	29.6	—	Fox River at Ferndale	Ferndale	Dye-sample collection.
4	29.4	—	Fox River at Holiday Hills	Holiday Hills	Do.
5	28.1	05549600	Fox River at Burtons Bridge	Burtons Bridge	Periodic stage, measured discharge, dye-sample collection.
6	26.3	—	Fox River at river mile 93.5 at Burtons Bridge	River reach mile 26.3	Dye-sample collection.
7	25.7	—	Fox River at Fox River Valley Gardens	Fox River Valley Gardens	Periodic stage, measured discharge, dye-sample collection.
8	25.6	05549800	Fox River near Cary	Rawson Bridge	Continuous stage.
9	25.2	05549802	Fox River Tributary at Rawson Bridge	Fox River Tributary	Measured discharge at tributary mouth.
10	22.3	05549815	Fox River at river mile 89.5 above Fox River Grove	River reach mile 22.3	Dye-sample collection.
11	22.2	05549850	Flint Creek near Fox River Grove	Flint Creek	Continuous stage, rated discharge at tributary mile 1.1.
12	18.9	05549865	Fox River at Fox River Grove	Fox River Grove	Periodic stage, measured discharge, dye-sample collection.
13	18.1	05549890	Spring Creek at Fox River Grove	Spring Creek	Measured discharge at tributary mouth.
14	16.8	—	Fox River at Haegers Bend	Haegers Bend	Dye-sample collection.
15	14.4	05550000	Fox River at Algonquin	Algonquin Dam headwater	Continuous stage, rated discharge, dye-sample collection.
16	14.4	05550000	Fox River at Algonquin	Algonquin Dam tailwater	Continuous stage.
17	14.4	05550065	Crystal Creek at Algonquin	Crystal Creek	Measured discharge at tributary mouth.
18	9.8	05550070	Fox River at Carpentersville	Carpentersville Dam	Measured discharge, dye-sample collection.
19	9.5	05550080	Fox River at Chicago Northwestern Railroad Bridge at Carpentersville	Railroad Bridge	Periodic stage.
20	9.3	05550090	Fox River at Huntley Road at Carpentersville	Huntley Road Bridge	Continuous stage, measured discharge, dye-sample collection.

**Table 1.** Data-collection sites for the Fox River study reach in Illinois—Continued

Site number	River miles above downstream end of study reach	Downstream-order station number	Station name and U.S. Geological Survey downstream order number	Short name	Type of data collected and location on tributary, if applicable
21	8.7	05550100	Fox River at East Dundee	East Dundee footbridge	Periodic stage, dye-sample collection.
22	7.6	05550120	Fox River at West Dundee	West Dundee piers	Do.
23	7.4	05550130	Jelkes Creek at West Dundee	Jelkes Creek	Measured discharge at tributary mouth.
24	5.9	05550150	Fox River at I-90 at Elgin	I-90 at Elgin	Periodic stage, dye-sample collection.
25	5.0	05550307	Tyler Creek at State Route 31 at Elgin	Tyler Creek	Measured discharge at tributary mouth.
26	3.7	05550310	Fox River at Lawrence Avenue at Elgin	Elgin Dam headwater	Continuous stage.
27	3.7	05550310	Fox River at Lawrence Avenue at Elgin	Elgin Dam tailwater	Periodic stage.
28	3.4	05550310	Fox River at Lawrence Avenue at Elgin	Elgin bridges	Continuous stage, measured discharge, dye-sample collection.
29	2.7	05550320	Fox River at Elgin	Walnut Avenue Bridge	Periodic stage, dye-sample collection.
30	1.6	05550500	Poplar Creek at Elgin	Poplar Creek	Continuous stage, rated discharge at tributary mile 2.3.
31	0.0	05551000	Fox River at South Elgin	South Elgin Dam	Continuous headwater and tailwater stage, measured and rated discharge, dye-sample collection.

during the study rather than using the published (Fisk, 1988) rating for the sluice gates of Stratton Dam.

Additional determination of discharge for analysis was made by two primary methods. The first method was to use stage-discharge relations. Stage-discharge relations were available for two of the four overflow dams (the dams at Algonquin and South Elgin). A rating also was available for the sluice gates and spillway of Stratton Dam (Fisk, 1988). Discharges determined from these stage-discharge relations were included in the evaluation of the results but not as boundary conditions for the model simulation for verification except for gaged tributary inflow and for sensitivity analysis.

The second method, used only for six minor tributaries with a total area of about 80 mi<sup>2</sup> (26 percent of the total study drainage area), was to estimate the discharge as a percentage of measured discharge on nearby gaged tributaries proportional to the tributary area. The difference between estimating the tributary discharge (either as a proportion of another tributary discharge or as a steady-flow estimate) and simulating it with a rainfall-runoff model was found to be negligible. Discharge measurements were used wherever available with linear interpolation used to define the discharge between consecutive measurements, except for one instantaneous peak flow. That peak flow was defined by the ratio of the tributary area times the peak flow at the nearest gaged tributary because no discharge measurement was available at the site near the probable time of the peak.

A tracer study using fluorescent dye was run simultaneously with the induced flow conditions to obtain transport data for evaluating the total flow field produced in model simulations during the model-verification step. The dye (rhodamine WT20) was injected continuously (except during intermittent intervals of pump failure) at Stratton Dam starting in the low-flow period and continuing through part of the high-flow period (November 2–8, 1990). Water samples were collected manually or automatically at 18 locations at varying time intervals ranging from twice an hour to less than daily throughout the reach to obtain temporal and spatial dye-concentration distributions. Concentrations of the dye were determined as described in Turner (1994).

## DEVELOPMENT OF A ONE-DIMENSIONAL, UNSTEADY-FLOW MODEL

The numerical model used in this study is a one-dimensional, unsteady-flow model based on the integral form of the equations expressing conservation of mass (continuity) and conservation of momentum (motion). For this study, lateral flow was not included, although it is an option in FEQ. The equations represented in the model are based on the de Saint-Venant equations (de Saint-Venant, 1871) and are stated in Cunge and others (1980 p. 13) as follows:

$$\int_{x_1}^{x_2} [(A)_{t_2} - (A)_{t_1}] dx = \int_{t_1}^{t_2} [(uA)_{x_1} - (uA)_{x_2}] dt$$

(conservation of mass) and

$$\begin{aligned} \int_{x_1}^{x_2} [(uA)_{t_2} - (uA)_{t_1}] dx &= \int_{t_1}^{t_2} [(u^2A)_{x_1} - (u^2A)_{x_2}] dt \\ &+ g \int_{t_1}^{t_2} [(I_1)_{x_1} - (I_1)_{x_2}] dt + g \int_{t_1}^{t_2} \int_{x_1}^{x_2} I_2 dx dt \\ &+ g \int_{t_1}^{t_2} \int_{x_1}^{x_2} A(S_o - S_f) dx dt \end{aligned}$$

(conservation of momentum),

where

the independent variables are distance  $x$  and time  $t$ , the subscripts 1 and 2 indicate the direction that the computation proceeds in time and space,

$u$  is the velocity;

$A$  is the cross-sectional area;

$g$  is the acceleration of gravity;

$I_1$  is the hydrostatic pressure exerted on the ends of the control-volume element;

$I_2$  is the component of pressure in the direction of the channel axis because of the nonprismatic channel walls;

$S_o$  is the channel bed slope; and

$S_f$  is the friction slope,  $uA$  times  $/uA/K^2$  where  $K$  is the reach conveyance evaluated using Manning's equation:

$$K = \frac{1.49}{n} AR^{2/3},$$

where

$R$  is the hydraulic radius of the channel cross section (cross-sectional area divided by wetted perimeter).

The value of Manning's roughness coefficient,  $n$ , is related to the channel-boundary friction. Typical values of  $n$  for various channel boundaries can be found in Chow (1959, p. 101–123) and Barnes (1967). It is assumed that the values for Manning's  $n$  determined under steady-flow conditions apply to unsteady flow.

The de Saint-Venant equations are approximated by finite-difference equations. The terms that are dependent on distance are approximated to the second order, and those dependent on time are truncated after the first order. An iterative method, the four-point weighted implicit scheme, is used to solve the finite-difference equations for fixed nodes in the river-reach grid (D.D. Franz, Linsley, Kraeger Assoc., Ltd., oral commun., 1994). Because the de Saint-Venant equations represent, in an approximate form (subject to the limitations described in Cunge and others (1980, p. 8)), all the major forces affecting open-channel flow, the equations also are known as the dynamic or full equations; hence, the model used in this study is referred to as FEQ. An extended-motion equations option is available in the model for simulating the effects of nonuniform flow (through the momentum-flux correction coefficient), channel curvilinearity (through various correction factors for the integrals), wind stress on the water surface, and drag on minor flow-control structures in the river (for example, trash racks). These extended options were not required to simulate the Fox River for the study period considered.

To schematize a river for modeling, it is necessary to split the river conceptually into reaches of gradually varying flow where head loss is relatively constant (for example, losses due to channel friction) and the geometry is relatively prismatic (to avoid losses because of expansion and contraction). Locations where the de Saint-Venant equations for gradually varying flow do not apply include points where tributaries discharge to the mainstem of the river and special hydraulic features, such as bridges, dams, or sudden variations in cross-sectional geometry.

River reaches are represented in FEQ as branches. Each branch has an exterior node at each end of the branch in addition to optional interior nodes, which may be either measured cross sections used to refine the definition of the hydraulic geometry or

roughness of the reach or interpolated cross sections used to improve the convergence characteristics of the model. Flow enters and exits each branch through the exterior nodes. At the junction of each set of exterior nodes, there are two unknowns (discharge or velocity and stage or depth) for each node; therefore, two equations relating the unknown quantities are required. For junctions without special hydraulic features, typical relations are (1) the sum of discharge entering the junction equals zero and (2) water-surface elevations across each pair of nodes at the junction are equal. For junctions where a special hydraulic feature causes a loss in head or controls the stage-discharge relation, other equations must be applied to provide the necessary relations across the junction. These equations are used in FEQUTL routines to compute one-dimensional (flow dependent on head at one of the exterior nodes) or two-dimensional (flow dependent on head at two exterior nodes) function tables, which are accessed as needed during the FEQ simulation. The FEQUTL routines for representing the special hydraulic features, such as bridges, culverts, weirs, and embankments, have been developed from a variety of techniques and other steady-flow models developed by the U.S. Geological Survey and the Federal Highways Administration (Franz and Melching, in press).

## IMPLEMENTATION AND CALIBRATION OF THE FOX RIVER MODEL

The Fox River model was implemented by converting the channel-geometry and hydraulic-structure data from a previously implemented HEC-2 steady-flow model (Hydraulic Engineering Center, 1982) to FEQ format using a utility available in FEQUTL. The main channel of the study reach was modeled as a network of 34 branches. Each branch has two exterior nodes. The number of branches was dictated by the number of structures that affect the flow during certain flow conditions and by the need to incorporate tributary inflows at tributary junctions. Three low-head dams, 19 bridges, and 12 tributaries are represented in the model. Tributary and lateral inflows were represented as point inflows to 12 branches, each of which form a three-way junction with the main-channel network. The model schematic with the model-output locations is shown in figure 3. An oxbow lake is shown connected to branches 11 and 17. The lake is connected only at the downstream end for low flows, and a two-dimensional function table is used at the upstream

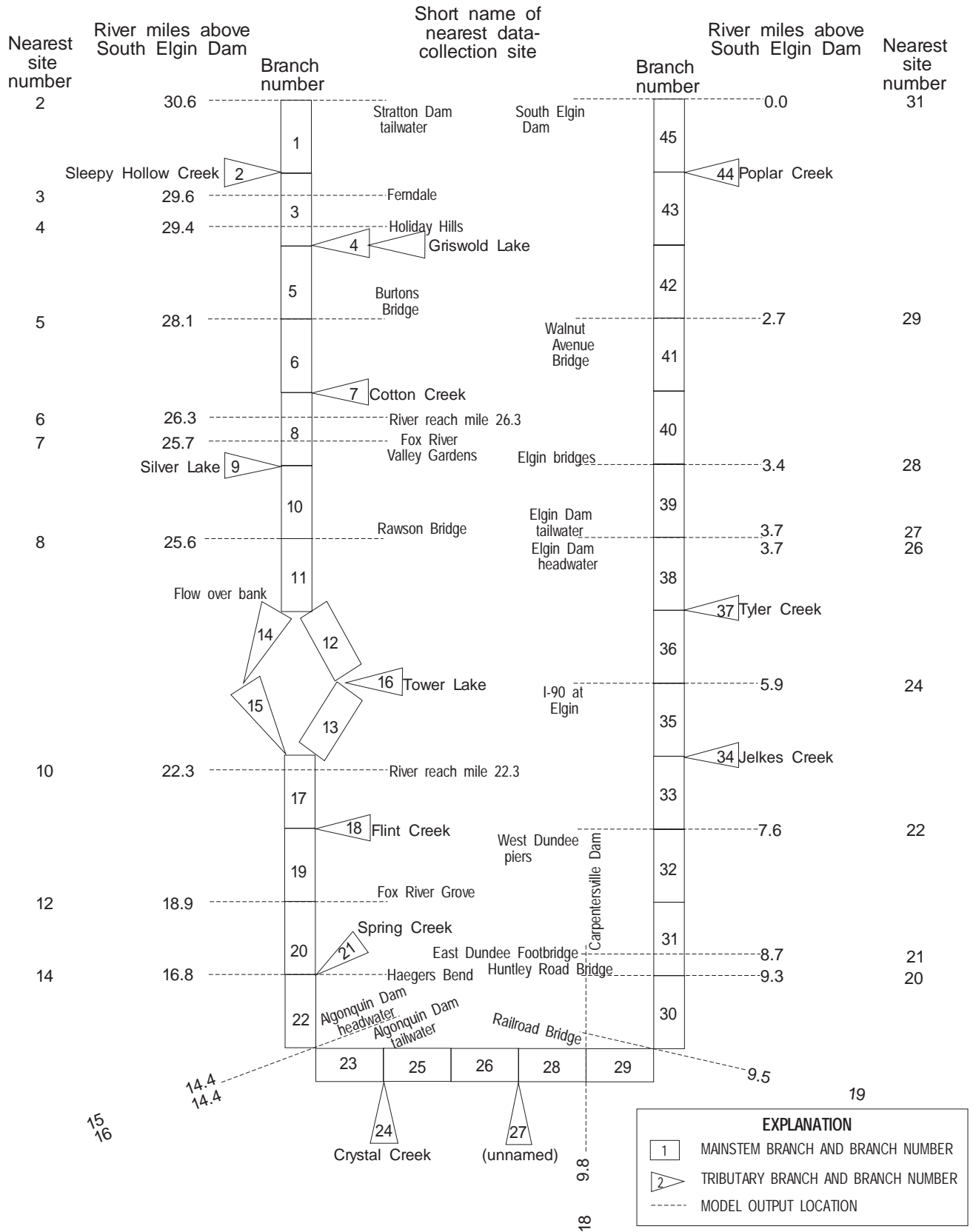


**Figure 3.** Model schematic of the Fox River in Illinois showing output locations. (Site numbers are referenced to table 1.)

end to represent an overland route (weir) for high flows. At normal flows, the network contains no looped junctions.

Model calibration was accomplished in three separate phases. In the first phase, the model was calibrated to include the 18.8-mi reach upstream from the study reach to Wilmot Dam. Rated discharge at Wilmot Dam was the upstream boundary condition for this phase. Stage and discharge at Stratton Dam were used as calibration checks rather than as external boundary conditions. Knapp and Ortel (1992) report on the calibration of the model downstream to Algonquin Dam. Two periods of major flooding (September 1–October 30, 1972 and April 1–June 10, 1973) were used in the calibration, and six additional floods (March 15–April 30, 1960; September 1–October 10, 1972; February 25–April 20, 1974; June 1–September 15, 1978; March 1–May 31, 1979; and March 1–April 30, 1982) were used to validate the calibration. The periods simulated were of 1.5- to 3.5-months duration with peak daily flows ranging from 2,270 to 6,560 ft<sup>3</sup>/s and mean daily low flows ranging from 214 to 2,310 ft<sup>3</sup>/s. Errors in peak stage for the validation periods shown were from 0.2 to 0.5 ft for the Stratton Dam tailwater (site 2), 0 to 0.6 ft for Rawson Bridge (site 8), and 0 to 0.4 ft for the Algonquin Dam headwater (site 15) for depths about 10–12 ft (Knapp and Ortel, 1992, p. 25–37). Simulated peak stages exceeded recorded peak stages for all peaks that were not matched, which may indicate a bias by the modelers to avoid the underprediction of major flood-peak stages. The primary purpose of the model calibration was to provide a tool for comparing various dam-operation schemes and, consequently, an unbiased fit would not be essential.

In the second phase, the model calibration downstream from Algonquin Dam was subsequently refined by personnel at IDNR/OWR with data collected during the two floods used for calibration and four of the six additional floods. (Information downstream from Algonquin Dam was not available for all flood periods.) The full 49.4-mi model reach was used for this step. The primary calibration criterion was the fit of the simulated stage to the limited number of staff-gage readings available at East Dundee footbridge (site 21) and West Dundee piers (site 22) (William R. Rice, Illinois Department of Natural Resources, Office of Water Resources, written commun., 1992).

In the third phase, the calibration was checked by deleting the reach upstream from Stratton Dam and

simulating two additional periods of 2 months each (July 1–August 30, 1990 and May 1–June 30, 1991). This phase was added to check the calibration for lower-flow periods without overbank flow, different upstream and downstream boundary conditions, and different methods of estimating the ungaged tributary inflows. For this phase, stage and rated discharge at Algonquin Dam were the primary criteria for judging the quality of the previous calibration. Further details of the calibration phase of the model implementation are presented in the section “Roughness Coefficient Selection.”

## Channel Geometry

The channel geometry is represented as a series of 321 cross sections. The cross-sectional data were obtained from surveys carried out by the U.S. Army Corps of Engineers (62 cross sections) and by IDNR/OWR (176 cross sections). Supplementary cross sections were determined from topographic maps (43 cross sections), constructed using survey data and topographic maps (5 cross sections), or repeated from adjacent cross sections (35 cross sections) (Illinois Department of Natural Resources, Office of Water Resources, written commun., 1992). Measured channel cross sections of the Fox River at or near the study data-collection sites shown in figures 1 and 2 are shown in figure 4, except river reach mile 22.3, which included a side channel. The cross sections have been truncated so that the same horizontal scale and same vertical scale are shown in all figures. The water-surface elevation is not shown because it varied during the study and was not measured at all sites. The river did not flow overbank during the study period.

The channel is relatively prismatic and has no obvious trend in width from upstream to downstream. The channel is about 400 ft wide upstream from Algonquin Dam. The channel narrows downstream from the dam, then widens to about 400 ft upstream from Carpentersville Dam. Downstream from Carpentersville Dam, the channel narrows to about 200 ft. As the river nears Elgin Dam, it widens again to about 400 feet to the end of the study reach at South Elgin Dam. The study reach is essentially two separate reaches—Stratton Dam to Algonquin Dam headwater and Algonquin Dam tailwater to South Elgin Dam. The channel-bed slope is 0.18 ft/mi for the upstream reach, and 2.06 ft/mi for the downstream reach. For the reach

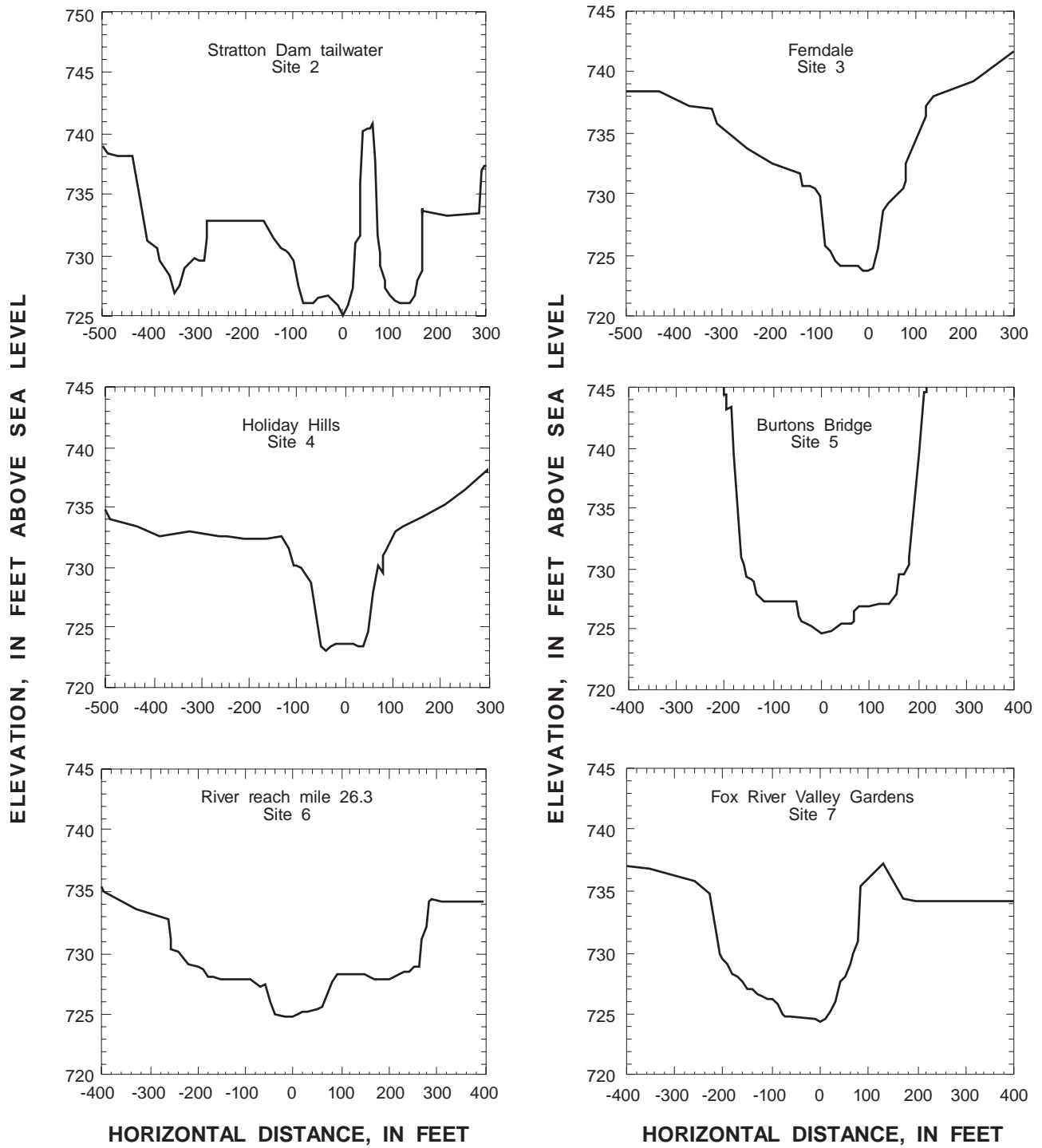


**Figure 4.** Surveyed channel cross section nearest to discharge, stage, and dye data-collection sites for the Fox River study reach in Illinois. (Site numbers are referenced to table 1.)

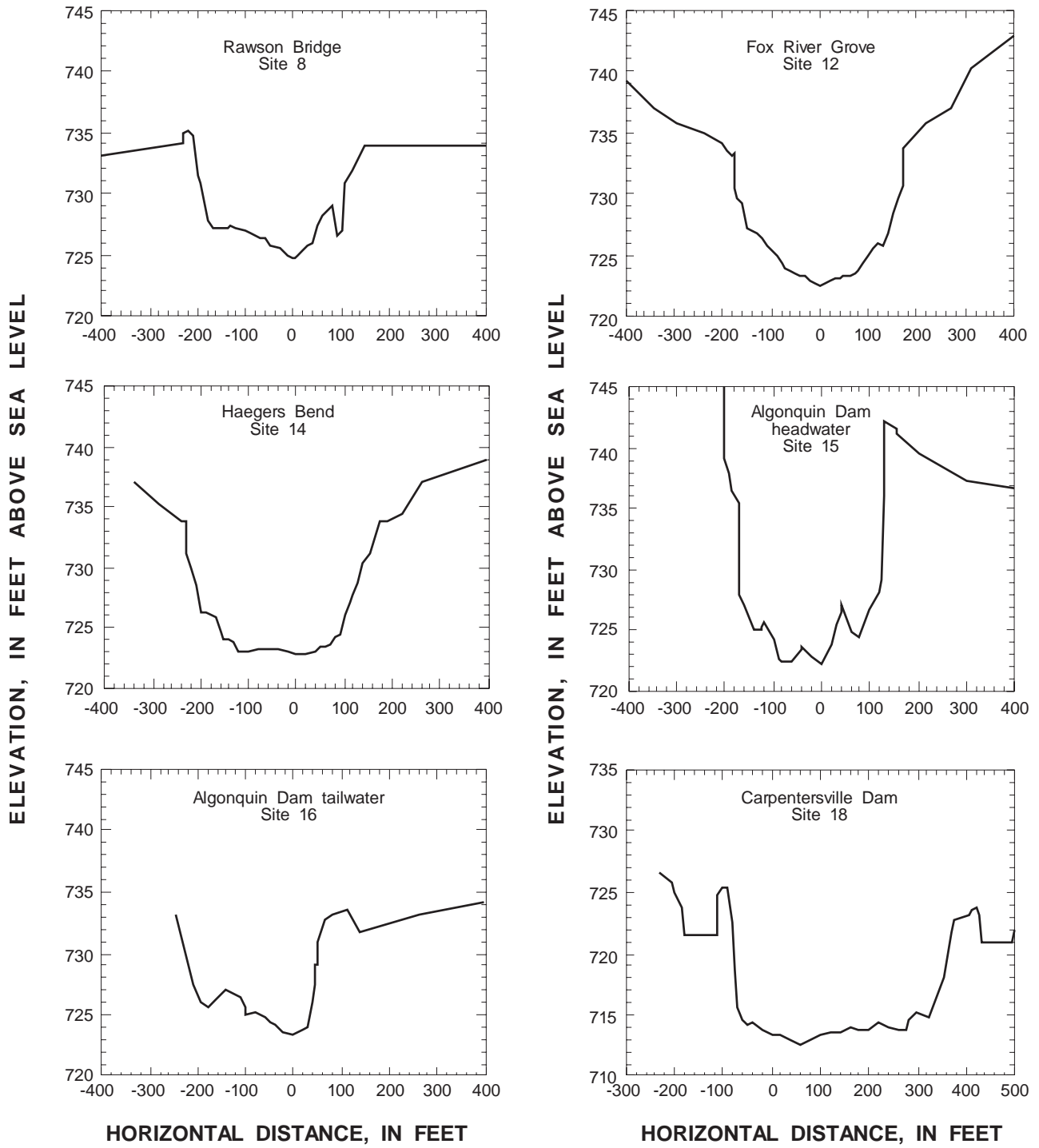


Figure 4. Continued.

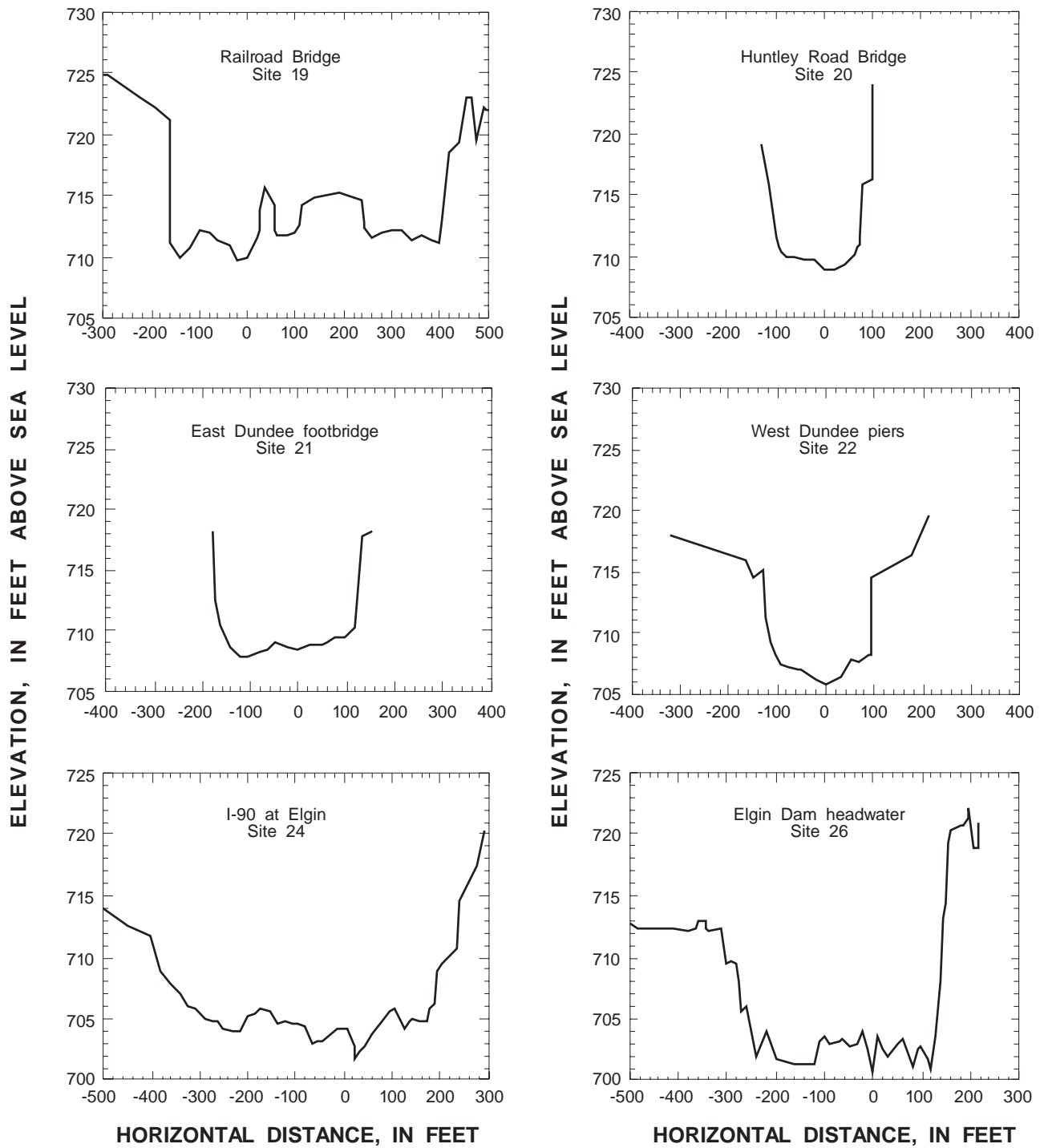


Figure 4. Continued.

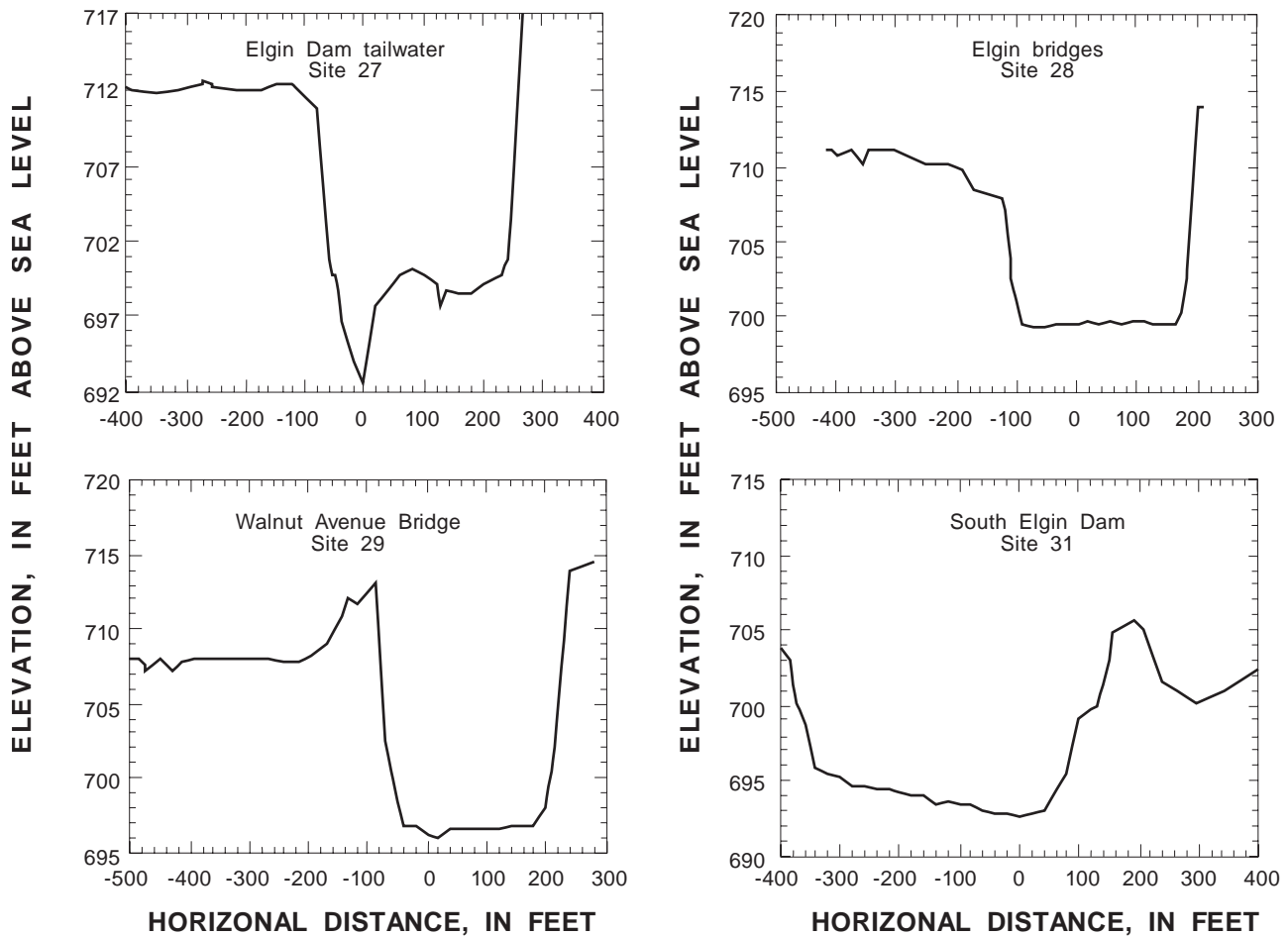


Figure 4. Continued.

upstream from Algonquin Dam, the stage-discharge relation is looped at all locations, even with no controlling structures downstream because the slope is very flat. Downstream from Algonquin Dam, the slope is large enough that the stage-discharge relation has almost no hysteresis for the period of the field study flow, except just upstream from bridges that cause backwater. A zero-inertia option is available in FEQ, which enables simulation without the local and convective acceleration terms. All simulations for this study, however, were done with the full, dynamic equations for unsteady flow.

Because of the very large number of surveyed cross sections, any significant error in the bed-slope representation is unlikely. The surveys were referenced to the level net of the National Coastal and Geodetic Survey, 1929 adjustment.

## Control Structures

Three major interior stage-discharge controls are located in the study reach—overflow dams located at Algonquin, Carpentersville, and Elgin. The water-surface elevation immediately upstream from each dam (sites 15, 18, and 26) is controlled by the stage-discharge relation at the dam, which is determined in FEQUTL by representing the dam as a weir. Stage downstream from each dam is controlled by the channel hydraulic geometry and roughness, and downstream boundary condition. No dam was submerged by the tailwater during the study period. The weir coefficients were modified from Brater and King (1976, p. 5–40) using data for the Stratton Dam spillway (William R. Rice, Illinois Department of Natural Resources, Office of Water Resources, written commun., 1992). The model routines for determining the

stage-discharge relations are adapted from the computational algorithms found in Hulsing (1967).

Nineteen bridges were simulated in the model with the routines provided in FEQUTL after the methodology of the Federal Highway Administration (1970). Head losses for 4 of the 19 bridges were combined with other bridges or neglected. The bridges of particular interest for this study are where data-collection sites were located (sites 5, 8, 12, 15, 19, 20–22, 24, 26, 28, and 29). The bridges at sites 15 and 26 are upstream from low-head dams. Losses for both were simulated in combination with bridges further upstream. The stage recorders or reference points for measuring the water elevation were attached to the bridges at all sites except sites 8 and 28. Because the nearest cross sections to the bridge are the approach and departure sections (usually about one bridge width away), this introduces some possible error because of buildup or drawdown of the water adjacent to the bridge. Site 28 is between two bridges simulated as one bridge. The difference in elevation from the upstream to downstream side of the simulated bridge was less than 0.03 ft for the period simulated.

## Boundary and Initial Conditions

Boundary and initial conditions for the calibration periods were simulated with data collected as part of the streamflow-gaging network operated by the U.S. Geological Survey (USGS). For the calibration simulations, the upstream boundary was rated discharge at Wilmot Dam in Wisconsin. Tributary inflow was estimated using a rainfall-runoff model for all tributaries downstream from Stratton Dam (Knapp and others, 1992). Between Wilmot Dam and Stratton Dam, the rainfall-runoff model was used to generate discharge hydrographs for 50 percent of the incremental area (190 out of 382 mi<sup>2</sup>). Rated-discharge record at a streamflow-gaging station (Nippersink Creek near Spring Grove, downstream-order station number 05548280) was used for inflow hydrographs for the other 192 mi<sup>2</sup>. The downstream boundary was the stage-discharge relation computed with FEQUTL for the South Elgin Dam.

For the calibration check period (the third calibration phase), the upstream boundary for the model was rated discharge at Stratton Dam. Discharge was computed according to the dam relations reported in Fisk (1988). Measurements made during the verification data-collection period indicated that deviation

from the ratings was possible because of inexact setting of the gate openings. The limit of accuracy of the gate-opening measurement is about 0.1 ft. At small gate openings, the rated discharge is highly sensitive to gate-opening differences as small as 0.01 ft. This may cause a bias for specific periods between gate settings, particularly when the gate openings are small.

For the tributary boundary conditions, continuous discharge computed from stage-discharge relations was available for two major tributaries—Flint Creek and Poplar Creek. The discharges computed for these tributaries were scaled to represent the discharge for the remainder of the drainage area by the ratio of the gaged to ungaged areas. Tributary areas, simulated tributary areas (with lateral inflow area added), and the ratios used to scale the known tributary discharges to represent the unknown tributary discharges are shown in table 2. For the study period, measurements were available on all but one tributary downstream from Algonquin Dam (unnamed tributary) and for Spring Creek upstream from Algonquin Dam. Thus, inflows for only six small tributaries (with a total area of 80 mi<sup>2</sup>) were estimated for the verification phase; although, for the calibration phases, no tributary measurements were available. Other minor inflows and outflows were identified as (1) lockages at Stratton Dam, (2) water withdrawals upstream from Elgin Dam, (3) water returns upstream from South Elgin, and (4) ground-water discharge at East Dundee. Inflows were not simulated as their contribution was small in comparison with the unknown tributary inflows. The overall contribution to error, caused by estimating the unmeasured tributary inflows, was checked by comparing different methods of estimation. The effect of scaling the discharge records was almost indistinguishable by using either an estimated steady flow or rainfall-runoff model output on simulated discharge at Algonquin for a major calibration flood period (September–October 1986) for the river reach from Stratton Dam to Algonquin Dam. Total difference in the simulated and rated volume for the October–November 1990 period was 1.92 percent at Algonquin Dam and 5.12 percent at South Elgin Dam, which was insufficient to cause significant errors in the hydraulic routing of the flood wave, and is approximately the limit of accuracy for computed ratings.

The downstream boundary condition was water-surface elevation at the headwater of South Elgin Dam. This boundary condition was selected rather than a stage-discharge relation because the

**Table 2.** Tributary areas and scaling ratios for estimating inflow to the Fox River in Illinois

Fox River tributary	Tributary area <sup>1</sup> , square miles	Tributary used as base	Base tributary area, square miles	Scaling ratio, dimensionless
Sleepy Hollow Creek	20.0	Flint Creek	37.0	0.54
Griswold Lake	7.7	...do....	37.0	.21
Cotton Creek	17.3	...do....	37.0	.47
Silver Lake	8.7	...do....	37.0	.24
Tower Lake	11.5	...do....	37.0	.31
Flint Creek	43.6	...do....	37.0	1.18
Spring Creek	35.0	...do....	37.0	.95
Crystal Creek	34.4	...do....	37.0	.93
Unnamed tributary	14.9	Poplar Creek	35.2	.42
Jelkes Creek	16.3	...do....	35.2	.46
Tyler Creek	45.6	...do....	35.2	1.30
Poplar Creek	51.0	...do....	35.2	1.45

<sup>1</sup>Includes lateral inflow to the Fox River.

stage-discharge relation was based on 9 discharge measurements made over just 2 years. The discharge computed from the rating is used for comparison of the discharge leaving the river system with the simulated discharge; however, the limitation imposed by the uncertainty of the rating is applicable to all discharge computations at the downstream boundary.

## Roughness Coefficient Selection

The initial modified field estimates of Manning's  $n$  were derived from previous steady-flow modeling. In the first phase of calibration, the values were adjusted upstream from Algonquin Dam by personnel at the Illinois State Water Survey (Knapp and Ortel, 1992). In the second phase of the calibration, the values for Manning's  $n$  were adjusted downstream from Algonquin Dam by personnel at IDNR/OWR. A value of 0.030 was selected for the channel downstream from Algonquin Dam. The channel roughness upstream from Algonquin Dam is less uniform and calibrated Manning's  $n$  varied from 0.022 to 0.031.

For the calibration check, the calibrated values for Manning's  $n$  were retained in the model, and two additional calibration periods were simulated to verify the main-channel values for Manning's  $n$  in the main channel. Adjustments to Manning's  $n$  made downstream from Algonquin had no effect on model results upstream from Algonquin Dam, but adjustments to Manning's  $n$  upstream from Algonquin affected dis-

charges and stages both upstream and downstream from Algonquin. This is because the flow conditions downstream from Algonquin Dam do not affect flow upstream from the dam, but the discharges from upstream from Algonquin Dam are routed downstream. Tributary discharge was estimated as discussed in the previous section.

Model calibration includes the comparison of measured stage and discharge at an internal location with the simulation results. Data were available for the Fox River at the Algonquin Dam headwater, which is midway between the two exterior boundaries in terms of drainage area. The discharge and elevation simulation results for the two calibration check periods—July–August 1990 and May–June 1991—at Algonquin Dam are shown in figures 5 and 6. These results indicate that discharge estimates were adequate and that the routing of discharge was well timed. The elevation results are less significant because they are dependent on the quality of the calculated and the simulated ratings of the dam. The error in stage was very small for all but the peak of August 20, 1990, where a 6.6-percent error in discharge resulted in a 0.3-ft error in stage (from a total depth of 9.8 ft). Not enough measured data were available elsewhere in the study reach for the calibration-check periods to justify changing the calibrated values for the study reach. The errors found in this third phase of calibration were comparable to the errors shown in Knapp and Ortel (1992, p. 25–37) for the first calibration phase using other flood periods.

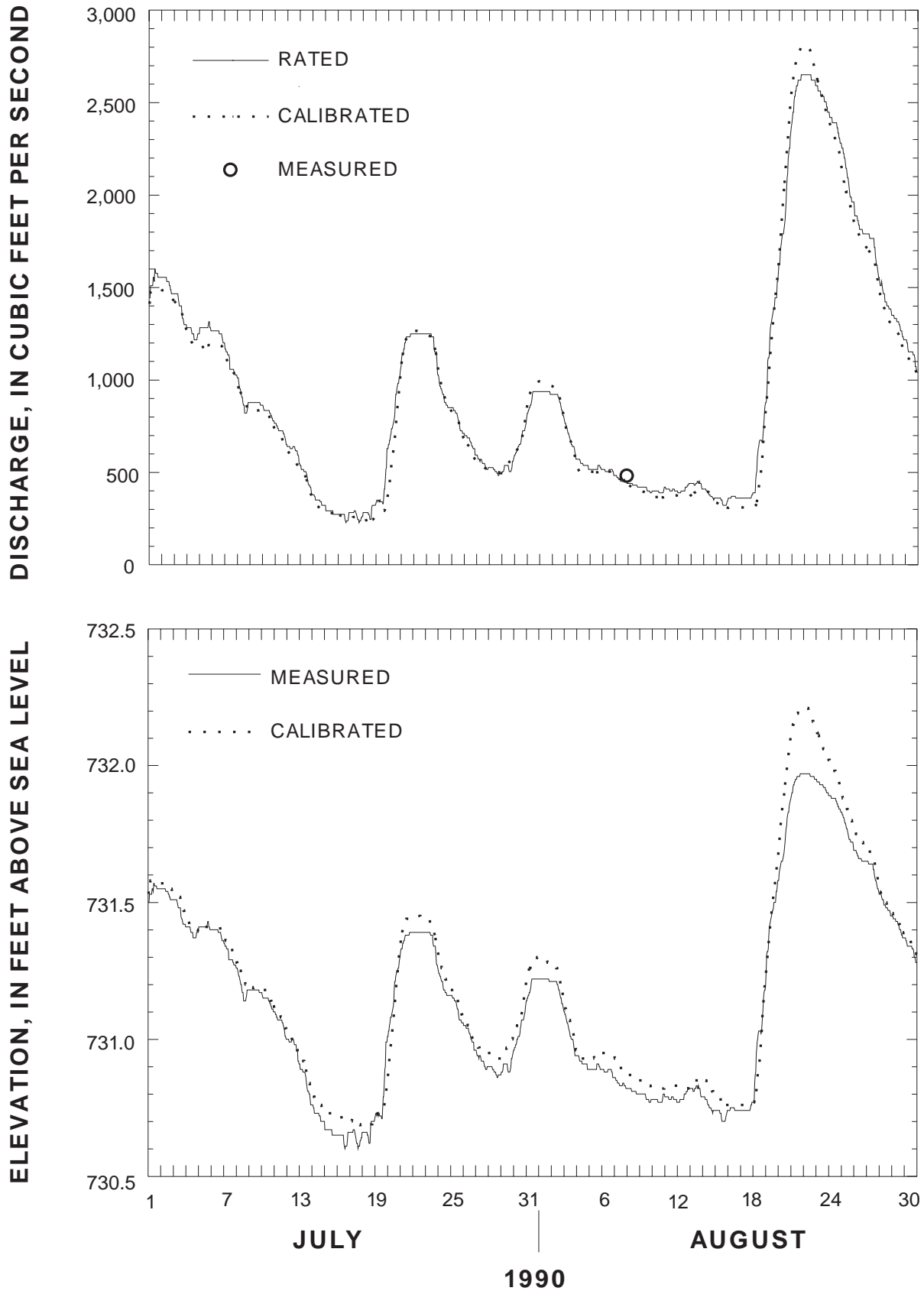


**Figure 5.** Measured or rated and calibrated discharge and stage for the July–August 1990 calibration-check period for the Algonquin Dam headwater on the Fox River in Illinois.

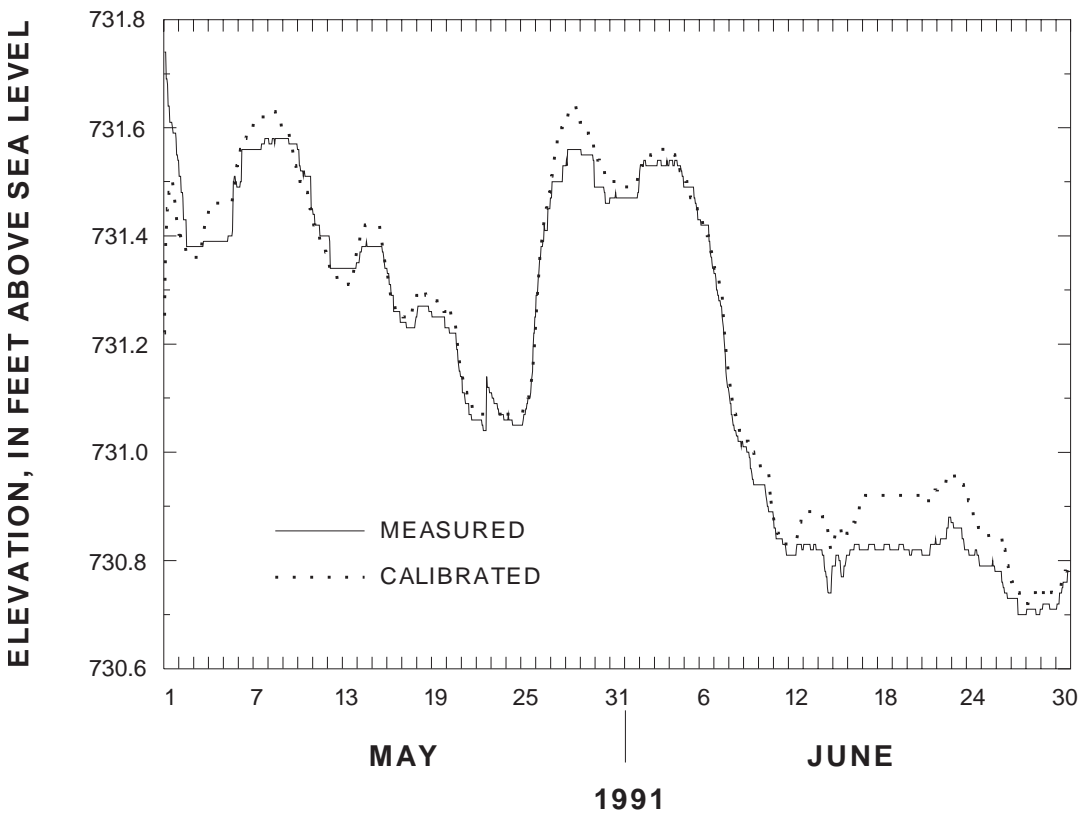
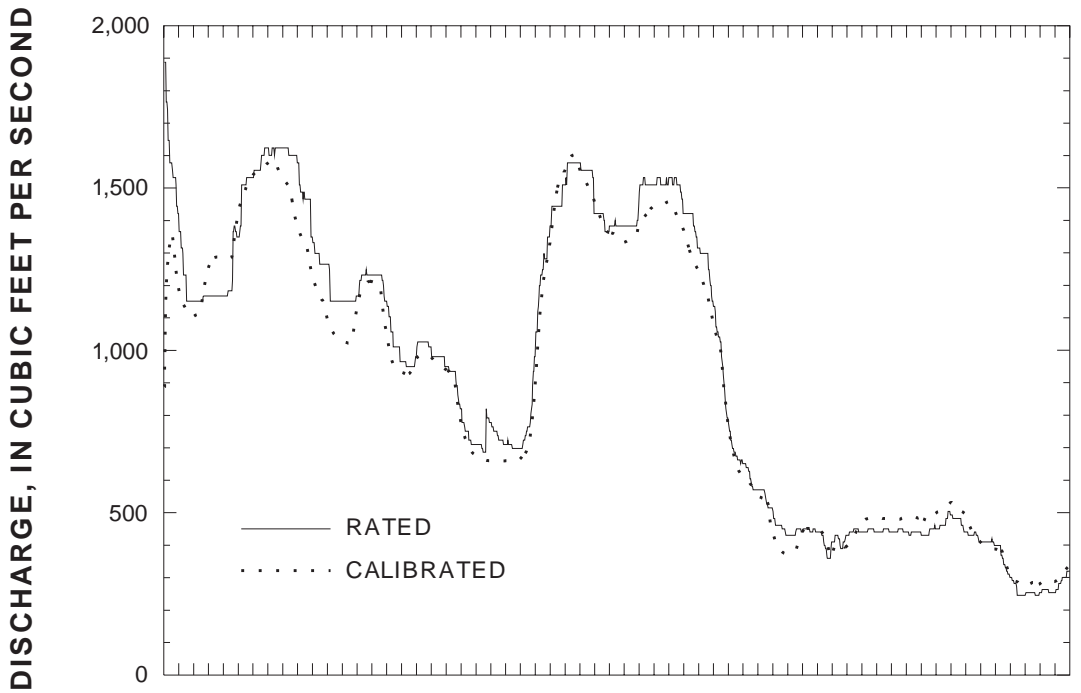


**Figure 6.** Measured or rated and calibrated discharge and stage for the May–June 1991 calibration-check period at the Algonquin Dam headwater on the Fox River in Illinois.

## Transport-Model Description

The FEQ simulation results were formatted for input to the BLTM (Jobson and Schoellhamer, 1987). BLTM was selected because of the wide range of applications verifying the model (Schaffranek, 1989). The convection-dispersion equation is solved in the model using a Lagrangian reference frame. This reference frame is such that the computational nodes move with the flow and is advantageous only when dynamic conditions are important (McCutcheon, 1989, p. 45). The solution scheme begins with a series of fluid parcels that are assumed to be completely mixed. The convection-dispersion equation is applied to each parcel. As the solution proceeds, a new parcel is added at the upstream boundary during each time step. The volume of the parcel is changed only by tributary inflows.

The convection-dispersion equation in the Lagrangian reference frame is

$$\frac{\partial C}{\partial t} = \frac{\partial}{\partial \xi} \left( D \frac{\partial C}{\partial \xi} \right) + \Phi ,$$

where

$C$  is concentration;

$t$  is time;

$D$  is longitudinal-dispersion coefficient;

$\Phi$  is the rate of change of concentration because of tributary inflow; and

$\xi$  is the Lagrangian distance coordinate given by

$$\xi = x - x_0 - \int_{t_0}^t u dt ,$$

where

$x$  is the Eulerian (stationary) distance coordinate along the river;

$u$  is the cross-sectional mean stream velocity; and

$x_0$  is the location of the parcel at time  $t_0$ .

The longitudinal-dispersion coefficient is

$$D = D_f |u| \Delta x ,$$

where

$D_f$  is the dimensionless dispersion factor; and  $\Delta x$  is the parcel length.

$D_f$  is the ratio of interparcel mixing rate to the channel discharge and is equivalent to the inverse of the Peclet number. A commonly accepted value of 0.3 (Jobson, 1987, p. 173) was used as the dispersion factor for this study.

The BLTM requires input of initial conditions—a series of parcels with the initial constituent concentration in the river and boundary conditions—time-ordered parcels with constituent concentrations at each external boundary node that flows into the system. The only simulated constituent for this study is rhodamine WT20, a fluorescent dye. The dye was chosen because it is water soluble, easily detectable, relatively conservative, and harmless in low concentrations. The boundary-condition dye concentrations were calculated from the injection-solution concentration, the injection rate, and the discharge of the river at the injection point.

The boundary conditions of flow are supplied from the output of FEQ. The output is reformatted to provide the flow conditions at each node throughout the reach for each hourly time step. Four hydraulic values are required by BLTM at each node: discharge, cross-sectional area, top width, and tributary inflow. Top width is utilized for decay coefficient subroutines and is not used in this study.

## VERIFICATION OF THE FOX RIVER MODEL

For open-channel flow models, verification is accomplished by comparing measured and simulated stage, and discharge at locations intermediate to the boundaries without further adjustment of the calibrated parameters, such as Manning's  $n$  and weir coefficients. For dynamic-wave models, such as FEQ, the comparison of stage and discharge is extended to include the potentially hysteretic stage-discharge relations at several points in the river reach and the celerity of the flood wave. The flood-wave celerity, which also is known as the absolute-wave velocity, is the sum of the water velocity and the dynamic-wave celerity (Chow, 1959, p. 540). The dynamic-wave celerity is given for a rectangular channel as the square root of the acceleration because of gravity times the depth of flow (Chow and others, 1988, p. 286). The dynamic-wave celerity is not measured directly in the field; however, as the water velocity and the flood-wave celerity can be

measured, the accuracy of this term can be inferred. By extracting the simulated total flow field in time and space from the hydraulic-model output and inputting it to a transport model, the accuracy of the simulated storage and water velocity can be determined from a comparison of the transport simulation results with measured dye-concentration data. The accuracy of the simulated dynamic momentum and channel storage, as reflected in the width of the looped stage-discharge relation, is a criterion of model accuracy along with differences in the measured and simulated values of stage and discharge.

To determine an accurate picture of the model performance, it is important that the distinction between model calibration and verification phases of the study be maintained. For this study, the calibration phase was completed before the verification data set was compiled. Model verification was investigated by comparing the calibrated model results with the data collected during unsteady flow induced by Stratton Dam operations from October 31–November 5, 1990. Stage and (or) discharge measurements were made at 18 locations on the mainstem during an 11-day period from October 31–November 10. To diminish the effects of inaccuracies in the initial conditions, the model simulation was begun on October 25. Because no measurements (except continuously recorded stage at Stratton Dam, Algonquin Dam, and South Elgin Dam) were available before about October 30, the upstream discharge boundary condition was uncertain. Therefore, results are shown beginning on October 30. The effects of channel storage and the capability of the model to route a rapid change in discharge through a river containing a large number of controlling features (bridges and overflow dams) were tested by comparing the field data with the calibrated-model output.

Several sources of error are possible that are unrelated to the dynamic-wave equation solution routines. These sources include the inaccurate determination of the volume and timing of the inflow discharges, including the upstream boundary condition; incorrect values for the calibrated roughness coefficients; the model representations and routines selected for calculating the head losses through bridges and over weirs (and any other structure not described by the de Saint-Venant equations); errors in gage (including boundary conditions) or weir-crest datums; and the placement of gages within the transition region between the structure and the approach or departure section of hydraulic structures, where model output is not possible. Some or

all of these difficulties are always present in field studies because of the impossibility of achieving complete knowledge of large-scale physical flow systems and constraints, such as accessibility and budget, on data acquisition in the field. Despite these difficulties, information on the robustness of the hydraulic model can be gained by comparing the simulation results with the measured data; the adequacy of simulated results, despite imperfect inputs, can be demonstrated.

A comparison of the time- and distance-integrated flow field was made possible by simulating the transport of a conservative dye using the injection time series recorded in the field and comparing the simulated temporal and spatial concentration distributions to the measured concentration distributions. By comparing the quality of the transport-simulation results with the quality of the hydraulic-simulation results, valuable knowledge about the capability of the model to simulate the water velocity, the flood-wave celerity, and indirectly, the dynamic-wave celerity can be obtained.

## Hydraulic Simulation Results

Data were collected at a total of 16 stage and (or) discharge locations throughout the study reach in addition to the two boundary data-collection sites. Of these sites, only the Algonquin Dam headwater had a continuous record available for calibration. Four other sites—Rawson Bridge (8), Fox River Grove (12), East Dundee footbridge (21), and West Dundee piers (22)—had few data available for use in calibration (periodic measurements of water-surface elevation). All other data used in the verification are independent in time and separate in space from the calibration data set. The results are plotted in upstream to downstream order in figure 7. The locations used for model output nodes are those with surveyed or constructed (not interpolated) cross sections nearest the data-collection site, usually the end of a model branch. The cross sections are shown in figure 4, and the locations within the model are shown in figure 3. A graphical presentation of the simulation results is the most comprehensive because both relative and absolute errors in the stage, discharge, wave shape and timing, and bias are readily apparent. Because the absolute depth varies with the wave location in time, relative or percent errors are variable, and relative errors determined during the wave trough are not applicable to wave peaks.

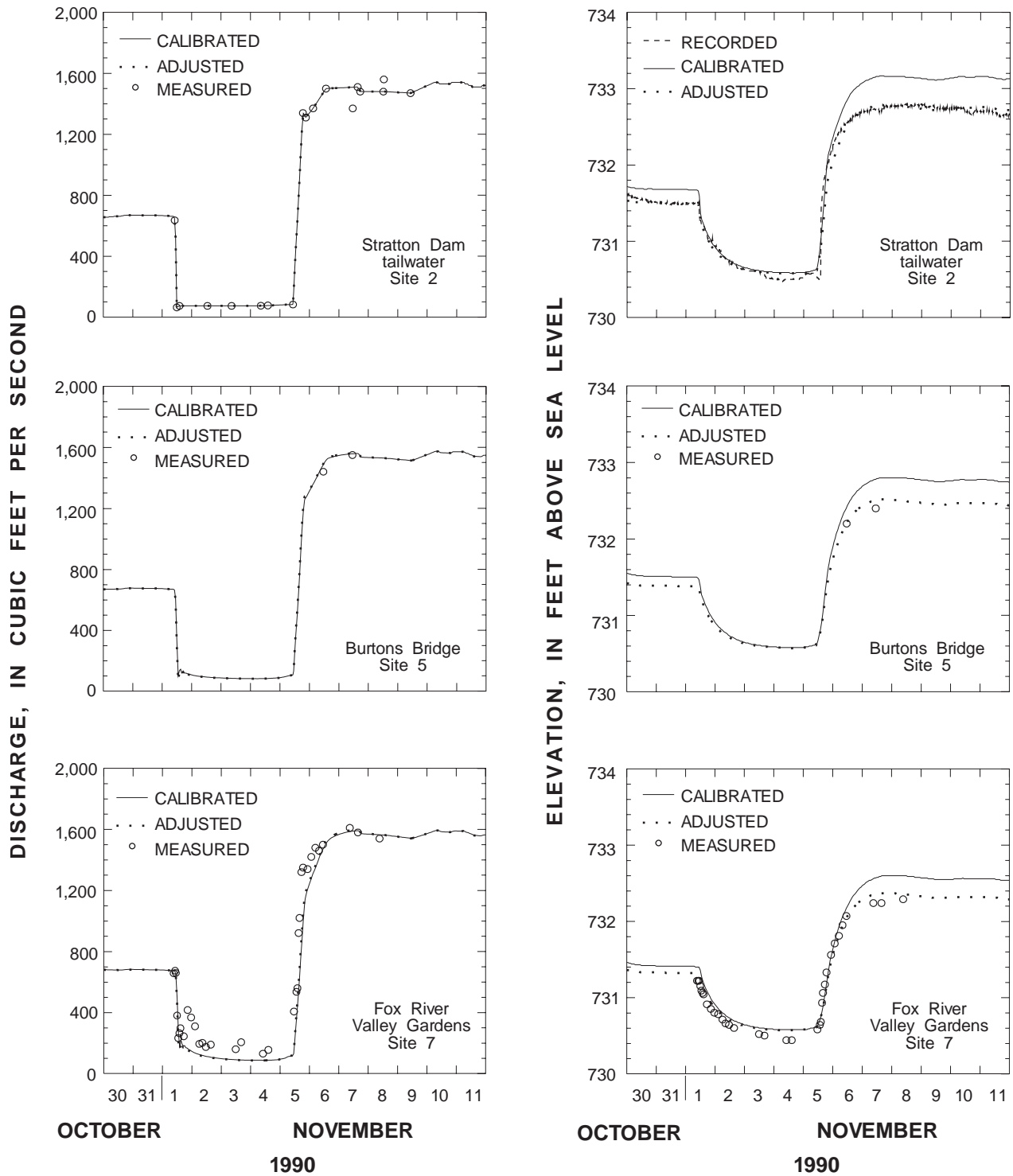


**Figure 7.** Measured or rated and simulated discharge and stage at data-collection sites on the Fox River in Illinois. (Site numbers are referenced to table 1.)

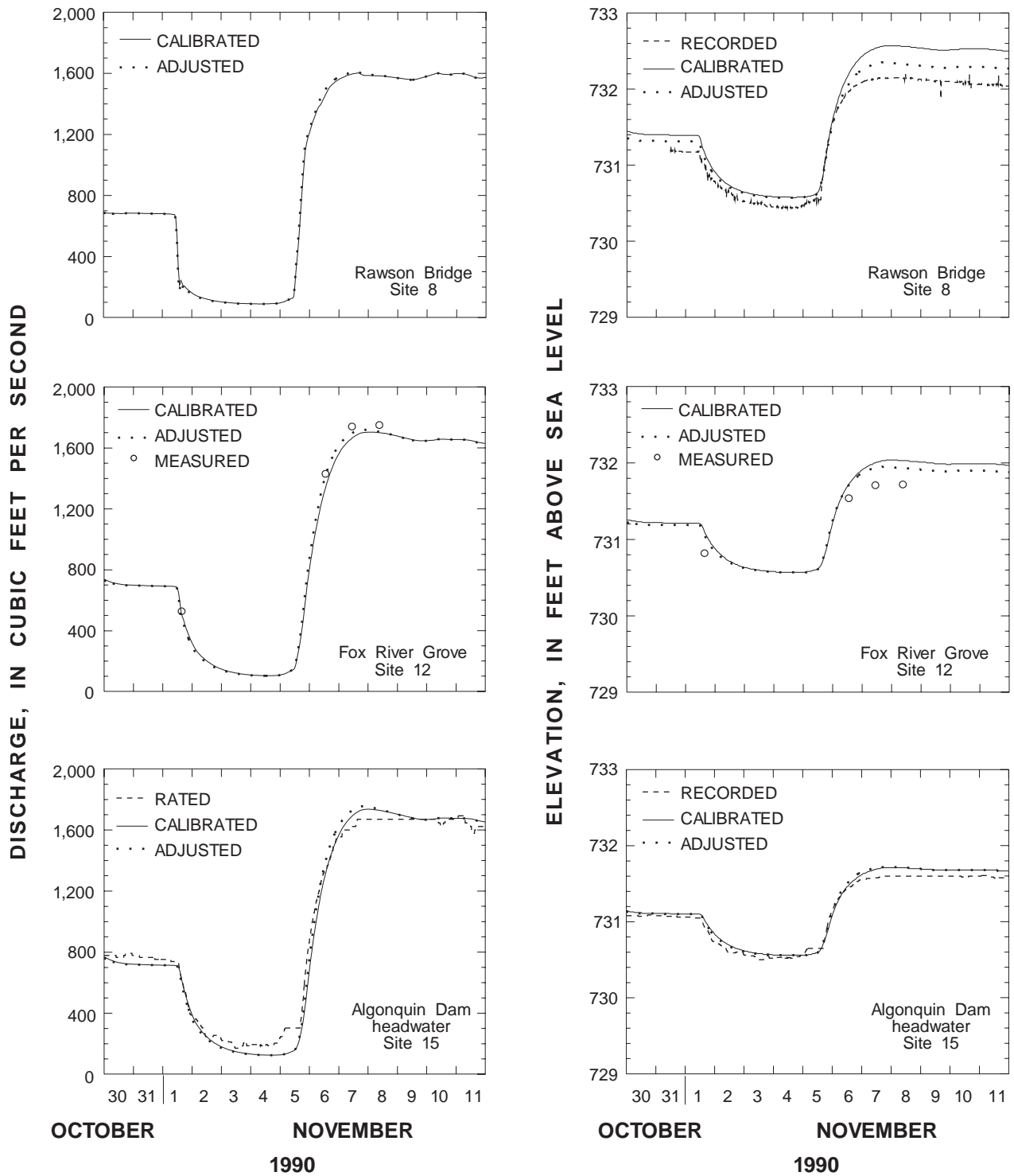


Figure 7. Continued.

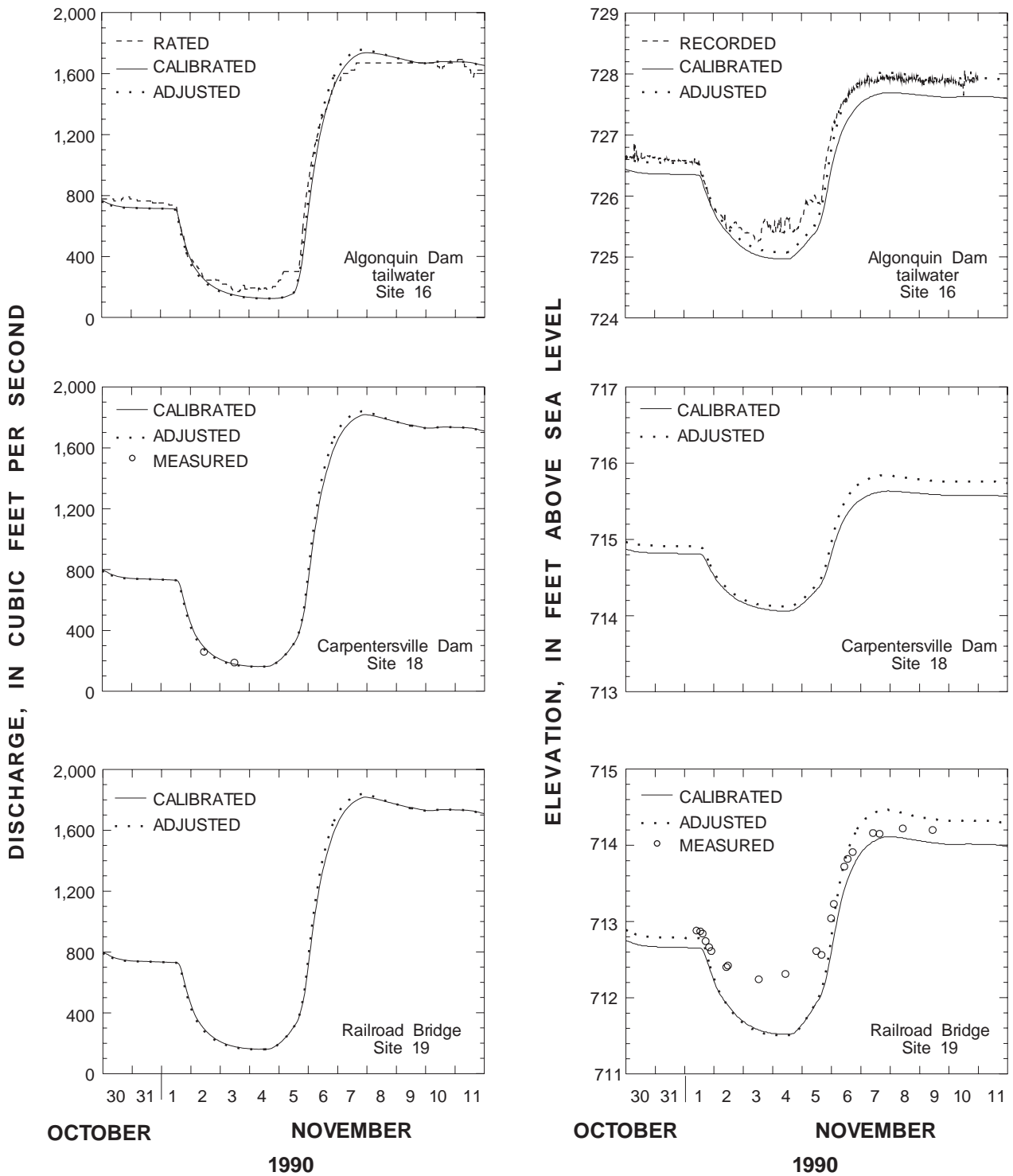


Figure 7. Continued.

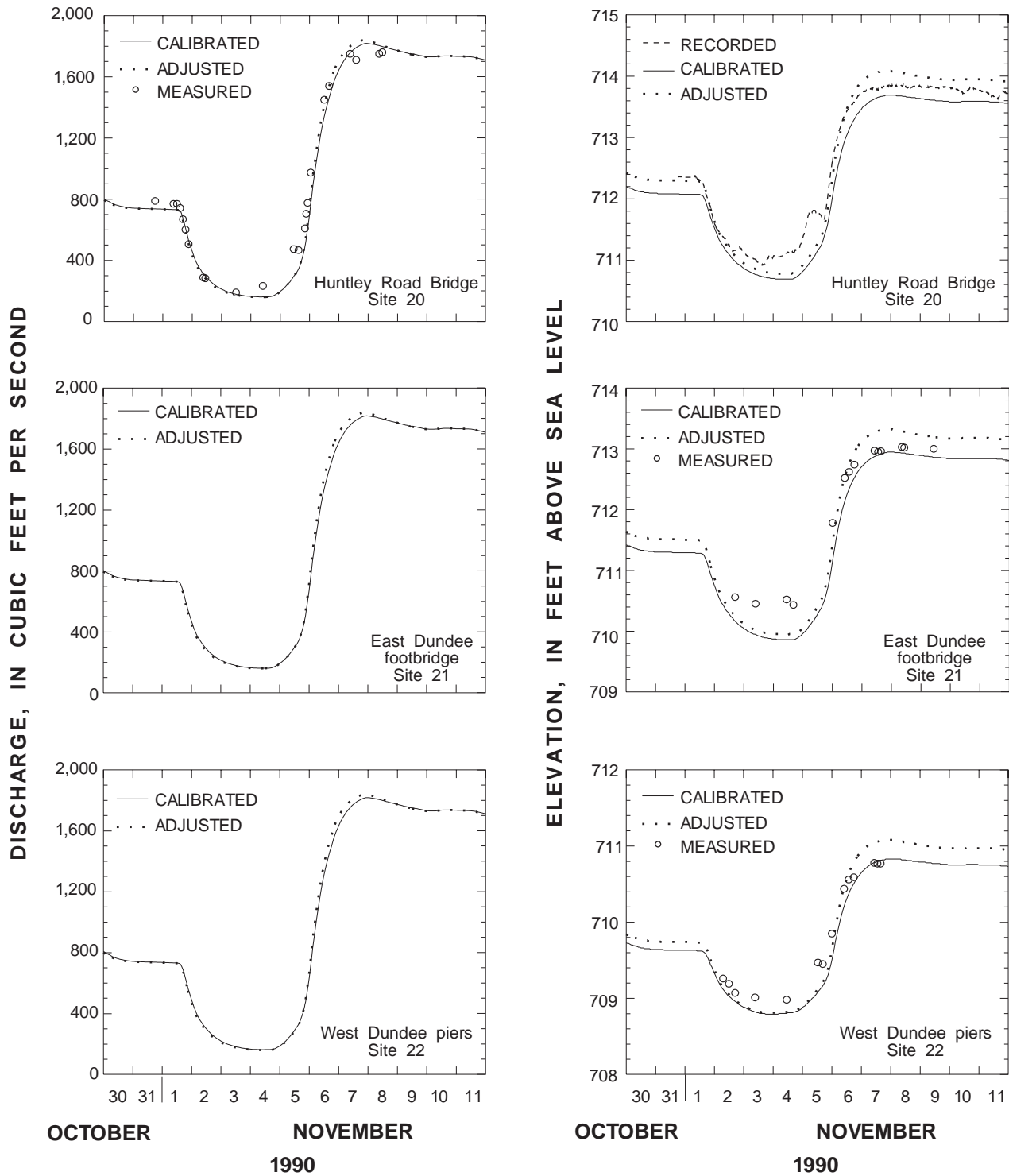


Figure 7. Continued.

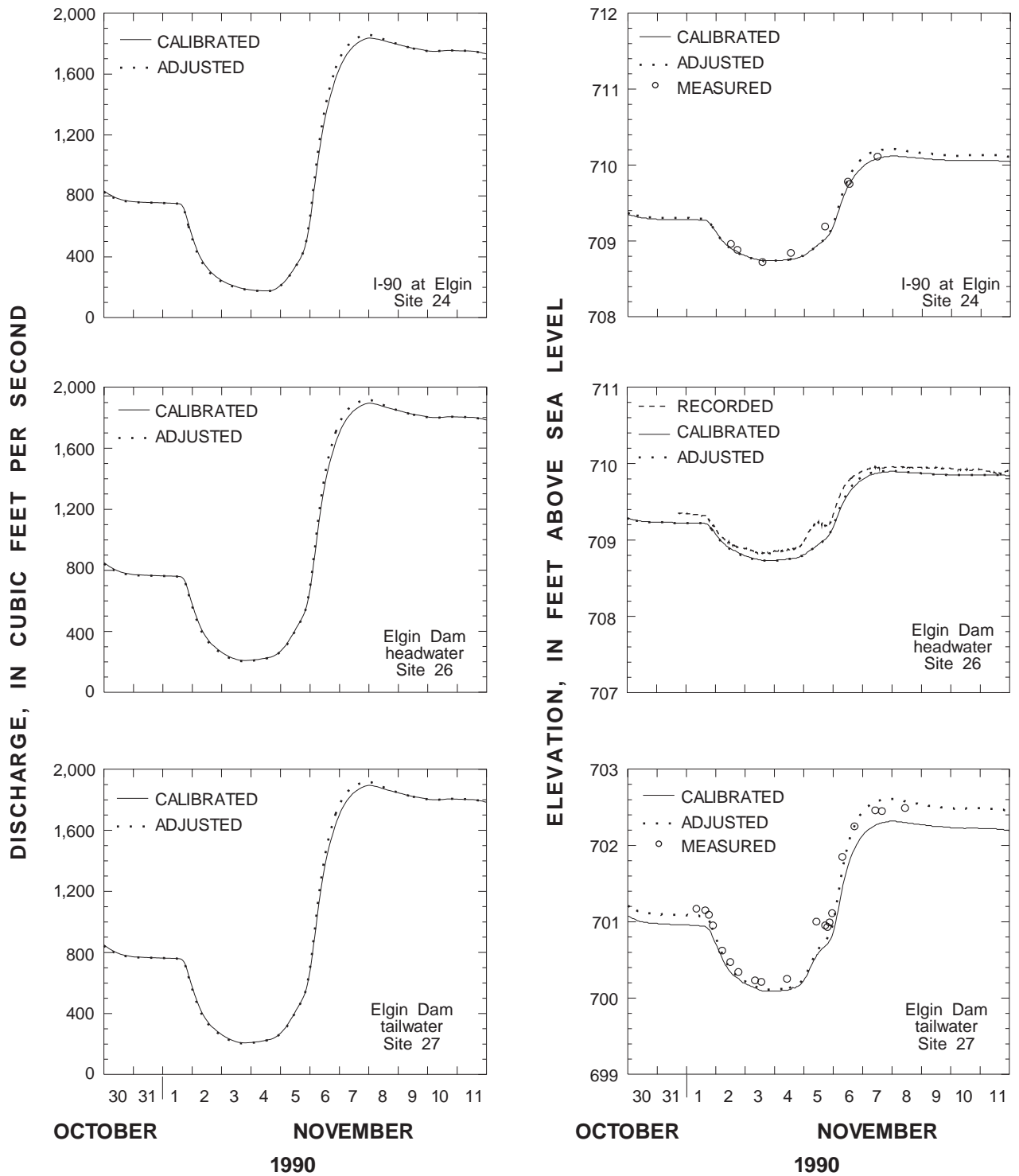


Figure 7. Continued.

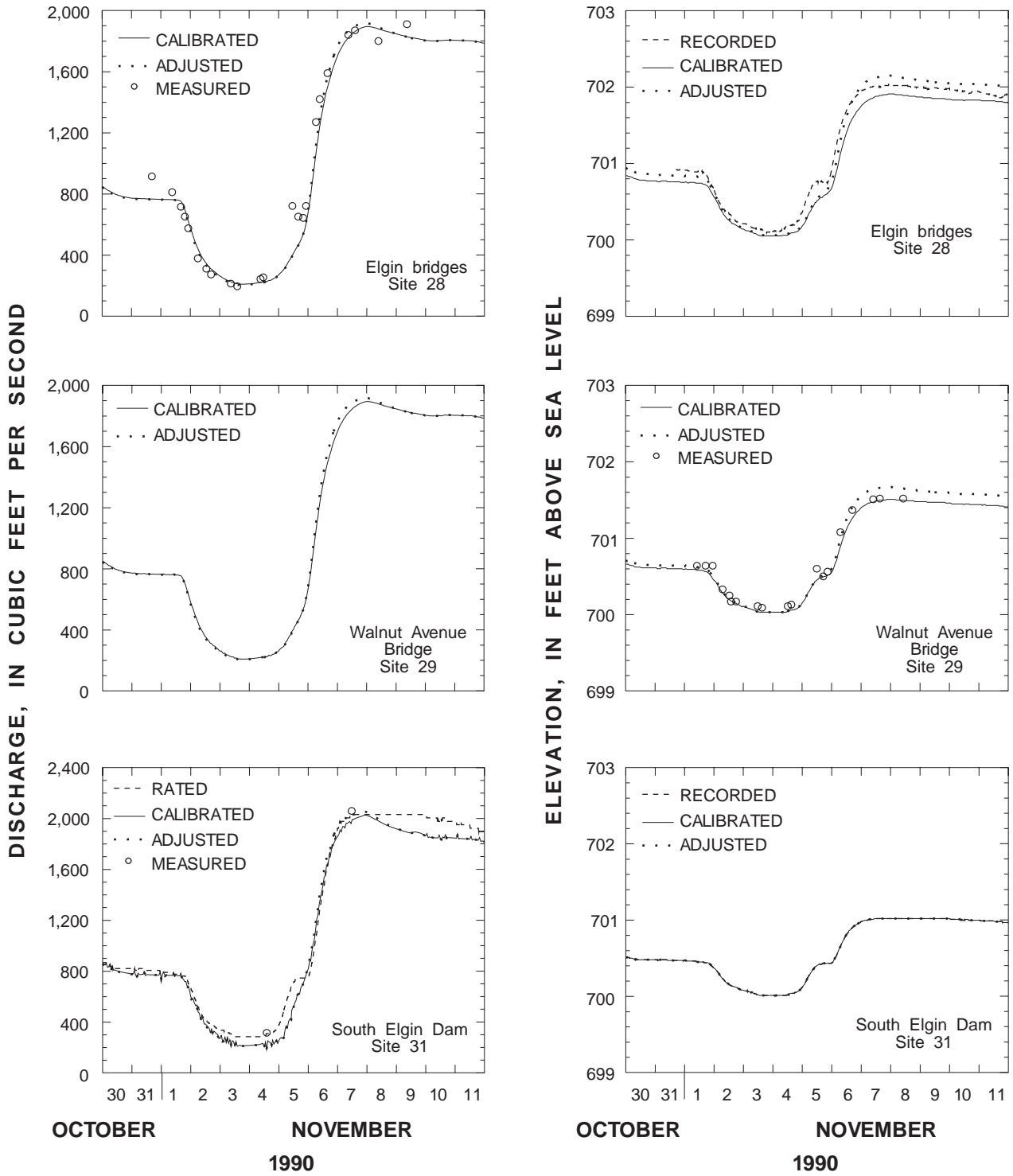


Figure 7. Continued.

In addition to the verification model output, an additional calibration step is shown in figure 7. A 0.006 decrease in Manning's  $n$  upstream from Algonquin Dam and a 0.005 increase in Manning's  $n$  downstream from Algonquin Dam generally improved the results throughout the entire study reach. The results of this additional calibration step are identified in figure 7 as the adjusted curve. This adjusted calibration is shown for illustration only and was not used elsewhere in this report, except as base value for sensitivity analysis of the computational parameters. Because no record was available for periods other than the study period, recalibration could not be justified. The results appear to indicate however, that the new values may be more appropriate for within-bank flow. The possible bias toward a more conservative (higher) value for Manning's  $n$  in the reach upstream from Algonquin Dam was discussed in the section "Implementation and Calibration of the Fox River Model." The resulting lower discharge for a given value of stage upstream from the dam would result in the selection of lower values of Manning's  $n$  for the reach downstream from the dam. Because the model was first calibrated for the upstream reach and secondly for the downstream reach, this may explain the apparent need for opposite and approximately equal adjustments to the calibration.

Several observations may be made concerning the simulation results. First, the flood-wave celerity (the absolute-wave velocity, which, in this case, is a wave trough rather than peak) has been accurately reproduced throughout the entire reach for either value of Manning's  $n$ . Dams and bridges, even when not ideally represented, do not alter the basic applicability of the dynamic-wave routing routines for the study reach. The effect of the change in Manning's  $n$  from the calibrated to the adjusted values on the flood-wave celerity was not appreciable. The average traveltime of the flood wave through the entire reach was about 12 hours. For the reach upstream from Algonquin Dam, the traveltime was about 3 hours and was about 9 hours for the reach downstream from the dam. Although the channel-bottom slope is steeper for the downstream reach than for the upstream reach, two intervening dams in the downstream reach result in a lower dynamic-wave celerity. Because the lower reach is steeper, less area is required to convey the same volume of discharge. As the Fox River channel is essentially prismatic, the depth is shallower in the lower reach. Because the dynamic-wave celerity is

proportional to the square root of the depth, a shallower depth results in a lower celerity for the dynamic wave.

Second, the inflow hydrographs were estimated by relatively crude methods. The upstream boundary condition of discharge at Stratton Dam was based on the 18 discharge measurements made at the site. Each discharge measurement at Stratton Dam has a potentially disproportionate effect on the shape of the simulated hydrographs because of the time between successive measurements. The lack of greater temporal resolution for the upstream boundary condition at Stratton Dam resulted in two outlying measurements causing notches in the simulated stage and discharge results, which were apparent, though progressively damped out down to the Algonquin Dam headwater (site 15). It appeared that the flow values were in error by about 9 percent for the first measurement and 5 percent for the second measurement. There was no evidence to support the possibility that the differences between measurements were due to anything other than measurement error, either in stage measurements or other measurements made before and afterwards. Consequently, the measurements were removed from the boundary condition hydrograph shown in figure 7 (site 2). The measurements are shown as the points not connected to the discharge hydrograph.

Discharge measurements were made on all but one of the simulated tributary streams downstream from Algonquin Dam and on Spring Creek upstream from the dam, and are listed in Turner (1994, table 3). These measurements were used as model inputs instead of proportioning discharge for the ungaged tributaries relative to the gaged tributary streams as discussed in the "Implementation and Calibration of the Fox River Model" section. Turner (1994, table 3) indicates that no measurement was made on November 5 on Jelkes Creek, so a proportion of Poplar Creek was substituted for that day. The rainfall that fell on November 4 and 5 resulted in an increase in discharge on November 5, which is not adequately captured in the discharge measurements. A hydrologic model was not used to generate tributary hydrographs for this study to maintain the emphasis on the dynamic-wave routing routines of FEQ and to avoid the uncertainty of additional model parameters. The difference between the simulated and rated flow volume at Algonquin was only 1.92 percent of the flow and at South Elgin 5.12 percent of the total flow. A large proportion of this difference is due to infrequency of measurements on the larger tributaries. The total difference is small

enough, particularly in that the observed discharge volume is derived from ratings, to investigate the hydraulic-model characteristics.

The discharge measurements at Fox River Valley Gardens (site 7) and the recorded stage at Algonquin Dam tailwater (site 16) require specific discussion. Measurement conditions at Fox River Valley Gardens during low-flow conditions of the study period (November 1–5, 1990) were particularly poor because of wind, and measurements were made from a boat with some measurement subsections having very low velocities. It is possible that these conditions caused the measurements to be higher than the actual discharge, or the assumed direction of the meter may have been incorrect. This cannot be verified or disproven as there were no other discharge measurements made during that time period in the vicinity of the section.

A variable-resistance potentiometer was used at the Algonquin Dam tailwater (site 16) to transform the stage registered by the float wheel to the data recorder. The potentiometer apparently malfunctioned both before and after the study period. It is not clear whether some fluctuations registered during the study period were due to malfunction or the inflow from Crystal Creek, which enters the Fox River about 15 ft downstream from the tailwater gage. Crystal Creek drains an upstream lake that was drawn down starting at 0800 hours, November 5, 1990. The drawdown was not designed to exceed approximately  $26 \text{ ft}^3/\text{s}$ . However, rain began falling on November 3 and peaked at about 0200 hours November 5 contributing additional flow. Discharge measurements to define the inflow were made several times during the study period, and the largest discharge measurement of  $110 \text{ ft}^3/\text{s}$  at 1400 hours November 5 was probably close to the peak discharge.

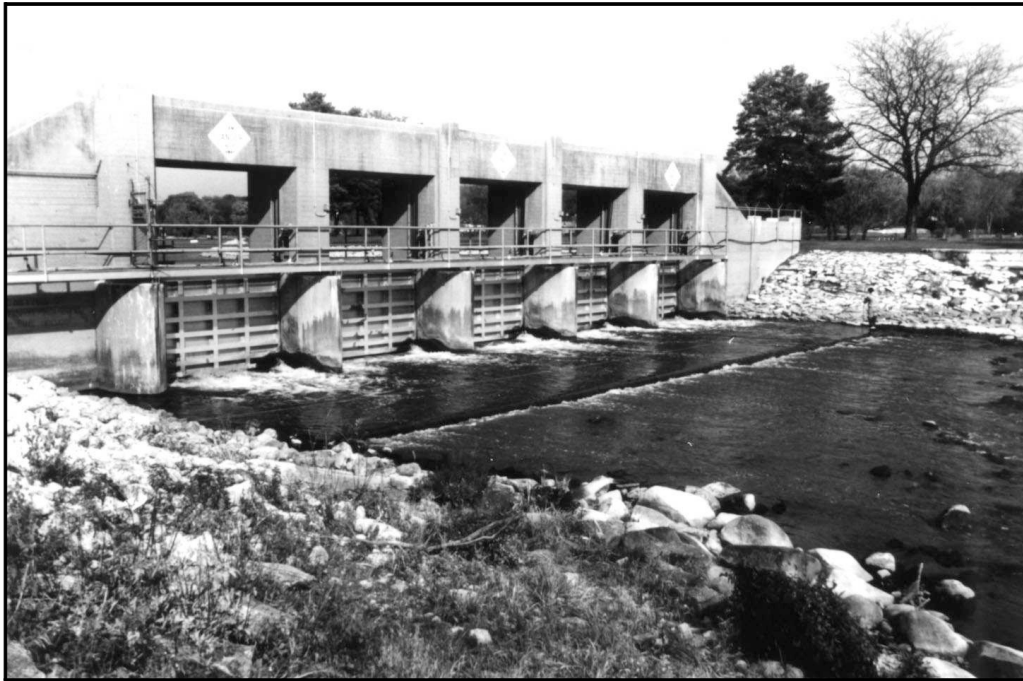
Third, the fit of the simulated to the measured stage throughout the reach generally was accurate—within 0.2 ft at most sites during the low-flow conditions. Exceptions were sites 16 and 19–21; the wave trough was more pronounced for the simulated than for the measured hydrographs. One possible reason for this exception was the difficulty of simulating the stage in the immediate vicinity of the bridges. The gages were attached to the upstream side of the bridges at sites 19, 21, and 22, and to the downstream side of the bridge at site 20. The largest difference between the simulated and measured stage was at Railroad Bridge (site 19), where the difference was about 0.8 ft for the wave trough. The fall in the water surface through the bridge

was too large to attach a staff gage, so all stage measurements were made with a tape and weight from the upstream side of the bridge.

A second possible reason for the error in simulating the wave trough is the inadequate determination of head-loss coefficients through the bridge. Photographs of selected Fox River data-collection sites, including the upstream boundary, Stratton Dam tailwater (site 2) at low flow; the measuring site at Fox River Valley Gardens (site 7); a dam typical of the low-head overflow dams in the reach; and Elgin Dam headwater (site 26) are shown in figure 8. The Railroad Bridge (site 19) has a large number of wood pilings that create a non-standard opening for representation with the Federal Highway Administration (1970) bridge routines.

A third possible reason for the differences noted at sites 19–22 is the very shallow depths that were present during the wave trough. The differences between the minimum measured stage and the minimum cross-section elevation were 2.44 ft at the Railroad Bridge (site 19), 2.6 ft at Huntley Road Bridge (site 20), 2.53 ft at East Dundee footbridge (site 21), and 3.28 ft at West Dundee piers (site 22). The analogous depths at the other sites ranged from 4.2 ft to 8.22 ft. Because many stage measurements were made infrequently by tape and weight, the minimum measured depth is not necessarily the minimum depth reached during the study period. It is possible that because of the decrease in hydraulic radius and increase in relative roughness at very shallow depths, the effective value of Manning's  $n$  is higher than it is at greater depths (Chow, 1959, p. 104). An option is available in FEQU TL for varying the value of Manning's  $n$  with depth, which may potentially improve the low-flow simulation results; however, evaluating a physically reasonable value for the variation with depth was outside the scope of this study.

The effect of poor representations of bridges or channel roughness at shallow depths apparently does not appreciably change the flood-wave celerity and that only localized effects result on the shape of the stage hydrograph. The excessively deep trough is damped out as the wave continues downstream, for example, the simulated trough is deep at Algonquin Dam tailwater (site 16); shallow at Carpentersville Dam (site 18); deep at the Railroad Bridge, Huntley Road Bridge, and East Dundee footbridge (sites 19–21); and shallow at West Dundee piers (site 22). The shape of the discharge hydrograph is almost constant throughout the reach. Stage was reproduced accurately with



A



B

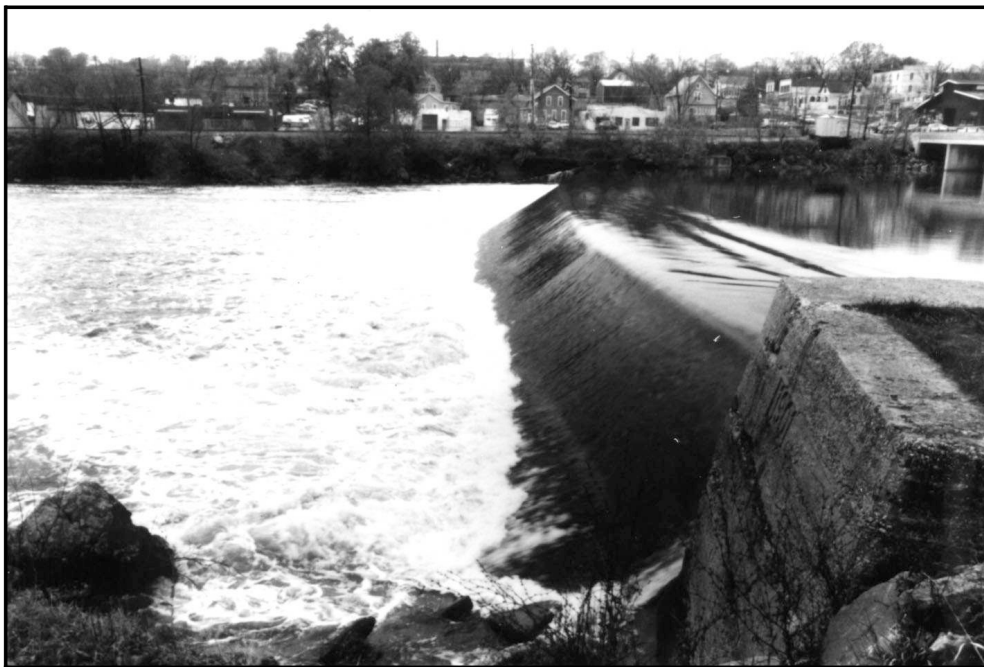
**Figure 8.** Selected data-collection sites on the Fox River in Illinois. (Site numbers are referenced to table 1.) A, Stratton Dam tailwater, Site 2 (view looking upstream); B, Fox River Valley Gardens, Site 7 (view looking upstream); C, Railroad Bridge, Site 19 (view looking upstream); D, Elgin Dam headwater, Site 26.

the modified Manning's  $n$  at other bridges in the model (see sites 5, 8, 12, 28, and 29). These bridges were located in deeper reaches of the river, and head losses through these reaches were apparently represented adequately.

According to Cunge and others (1980, p. 198), a channel with a bed slope of less than 0.0001 will usually have a looped stage-discharge relation (which indicates hysteresis due to channel storage and variable momentum slope), whereas, channels with slopes



C



D

**Figure 8.** Continued.

greater than 0.001 will almost always have a single-valued stage-discharge relation if there is little backwater effect from dams, tributaries, and other hydraulic structures. The stage-discharge relation upstream from an unsubmerged weir is essentially single-valued because no downstream effect can be felt upstream

from the weir. The bed slope upstream from Algonquin Dam is 0.000034; hence, hysteresis in the stage-discharge relation is expected at all locations. Downstream from Algonquin Dam, the bed slope is 0.00039, so hysteresis is possible depending on the backwater effect of control structures and the rate of change in

stage (Fread, 1975). Hysteresis is a function of the dynamic nature of the flood wave; therefore, the greater the change in the velocity and depth of the wave the greater the hysteresis (Faye and Cherry, 1980). The stage-discharge relations for selected data-collection sites in the reach for the study period are shown in figure 9. Several sites have no discharge measurements, so only the simulated relations are shown.

Model simulations made during the planning of the study identified Fox River Valley Gardens (site 7) as a location of significant hysteresis in the stage-discharge relation (Turner, 1994). There was apparent difficulty in matching the measurements made during the low-flow condition (figures 7 and 9). The quality of the measurements, particularly at low velocities is poor because of the operating characteristics of the current meters at low velocity and the uncertain direction of the velocity at depths of zero visibility. The observed and simulated ratings determined for the site are to be very similar in shape and width (fig. 9), though the stage datum appears displaced by about 0.1 ft.

The stage-discharge relation for Algonquin Dam and the other dams (Carpentersville and Elgin) is determined in FEQ from the tables generated in FEQUTL to represent the dams as weirs. No calibration of the weir coefficients was attempted prior to the verification because of the lack of measured data. The rated and simulated stage-discharge relations at Algonquin Dam headwater (site 15) are shown in figure 9. The maximum difference in the stage-discharge relation is about 0.10 ft. If there is any error in the elevation of the dam crest, this error will affect depths slightly for a short distance upstream or to the next upstream control structure. The effect of possible datum errors is reported in the "Sensitivity Analysis" section.

The gage for the Huntley Road Bridge (site 20) was located on the downstream side of the bridge, and the channel was the controlling factor for the stage-discharge relation at the site. Because of the lack of backwater influence from structures downstream from the bridge, there was only slight hysteresis in the stage-discharge relation. The simulation results were in good agreement with the measured data for the adjusted roughness coefficient.

The results at Elgin Bridges (site 28) are affected by the difference in stage shown in figure 7. This error may be due to the relatively shallow depth at this site or an inadequate representation of the bridges, which are located on both sides of the gage, as discussed earlier. The head losses at the bridges were represented in the

model by one bridge; however, the difference in stage from upstream to downstream from the bridge was 0.03 ft or less indicating that the bridge was probably not represented as sufficiently constricting, particularly as the streamflow increases. The simulated stage-discharge relation at Walnut Avenue Bridge (site 29), just downstream from Elgin Bridges is good, which demonstrates the ability of the model to damp out errors as better representations of hydraulic geometry and (or) roughness are obtained downstream.

## Transport Simulation Results

Dye studies are used to measure traveltime of solutes and dispersion characteristics and discharge in streams. For this study, simulated dye transport is compared with measured transport to evaluate the flow field supplied to the transport model. The velocity at which the water and dissolved dye are traveling is determined from the flow field. Accurate velocities must be simulated in the flow model for the simulated peak to arrive at the dye-collection site at the correct time. The dispersion factor affects the attenuation of the dye-concentration peak, but for this study, the results, especially for the high flow, are not sensitive to changes in the assumed dispersion factor. Jobson (1987) reports that applying a dispersion factor of 0.2–0.4 is within the optimum range for numerical accuracy; therefore, a dispersion factor of 0.3 was assumed in the model.

The dye was injected continuously for 6 days starting at 1432 hours on November 2, 1990, and continuing until 1400 hours, November 8, 1990. The concentration and injection rates of the dye solution were measured. The concentration at the upstream boundary, the point of injection, is a function of the injection concentration, injection rate, and the discharge during the period of injection. The concentration at the boundary decreased as the discharge increased when the gates at Stratton Dam were opened at 1400 hours, November 5. Samples were taken periodically throughout the injection period and until November 11 at 18 locations throughout the study reach to determine the spatial and temporal distribution of the dye (Turner, 1994).

The frequency of dye sample collection varied at the 18 sites. At Burtons Bridge (site 5), River reach mile 26.3 (site 6), River reach mile 22.3 (site 10), and Fox River Grove (site 12) automated samplers collected samples every half hour to every 2 hours.

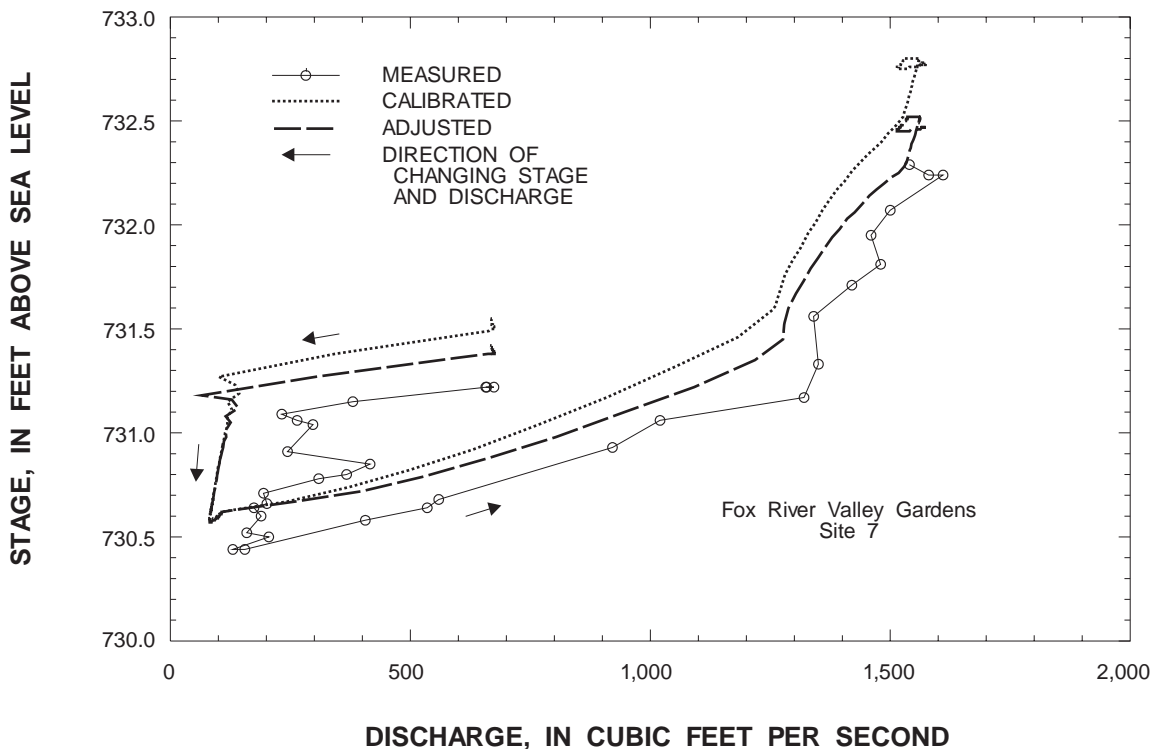
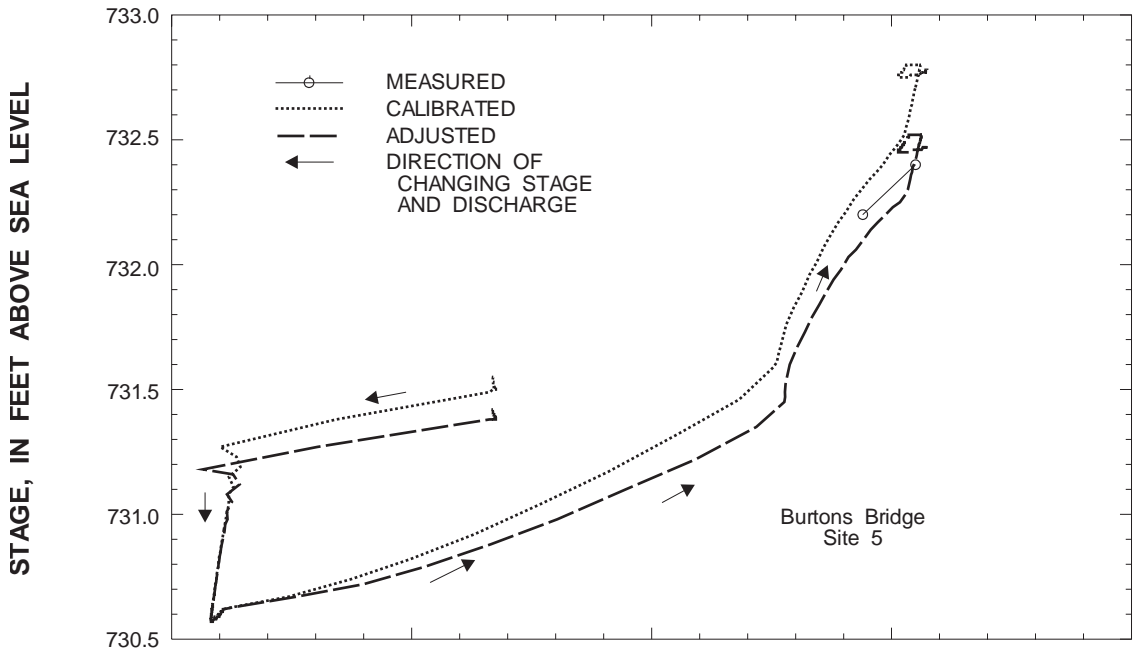


**Figure 9.** Measured or rated and simulated stage-discharge relations at data-collection sites on the Fox River in Illinois for the October 30–November 11, 1990, study period. (Site numbers are referenced to table1.)

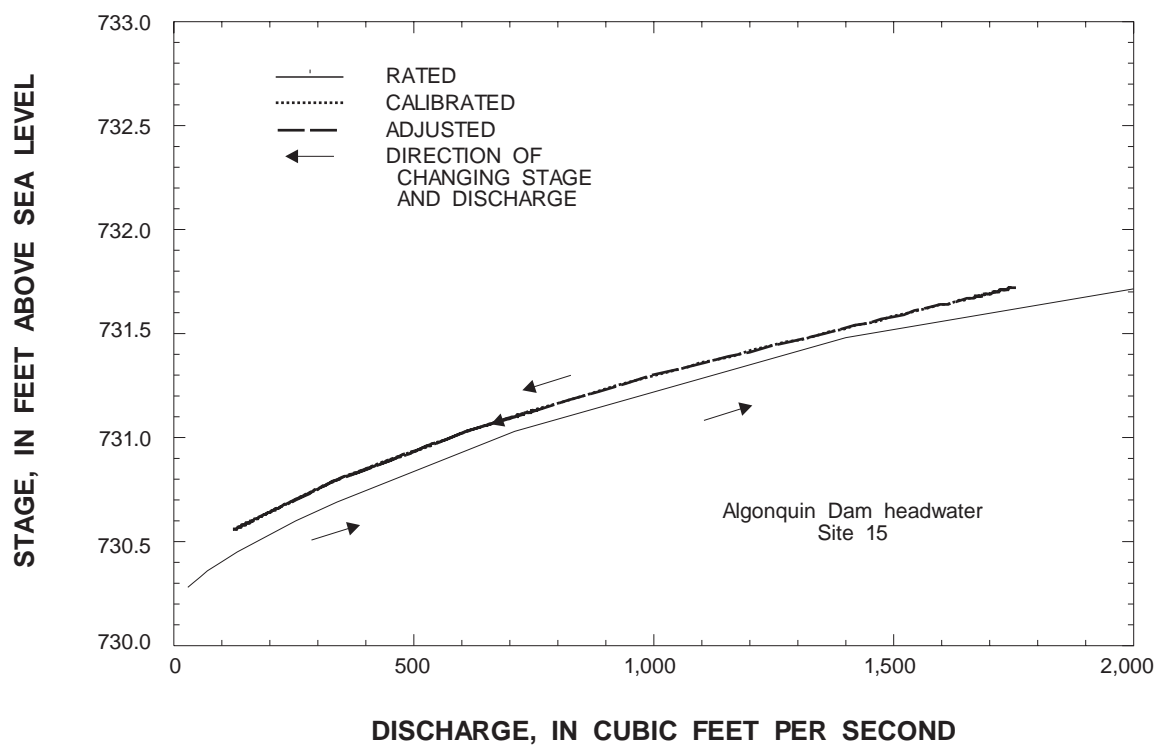
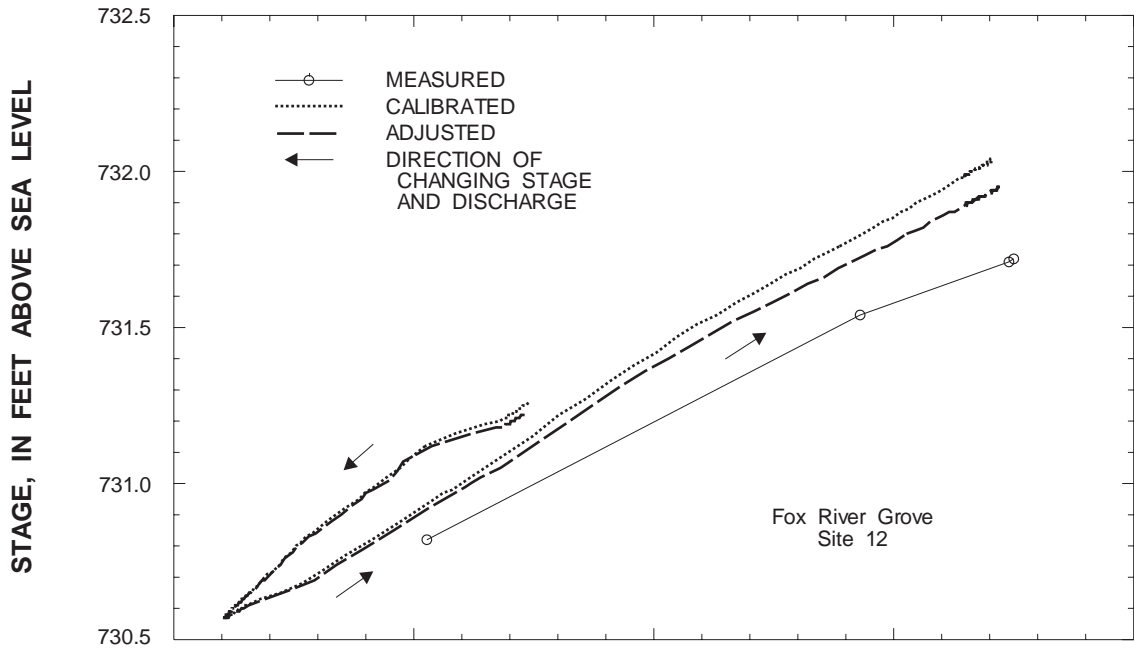


Figure 9. Continued.

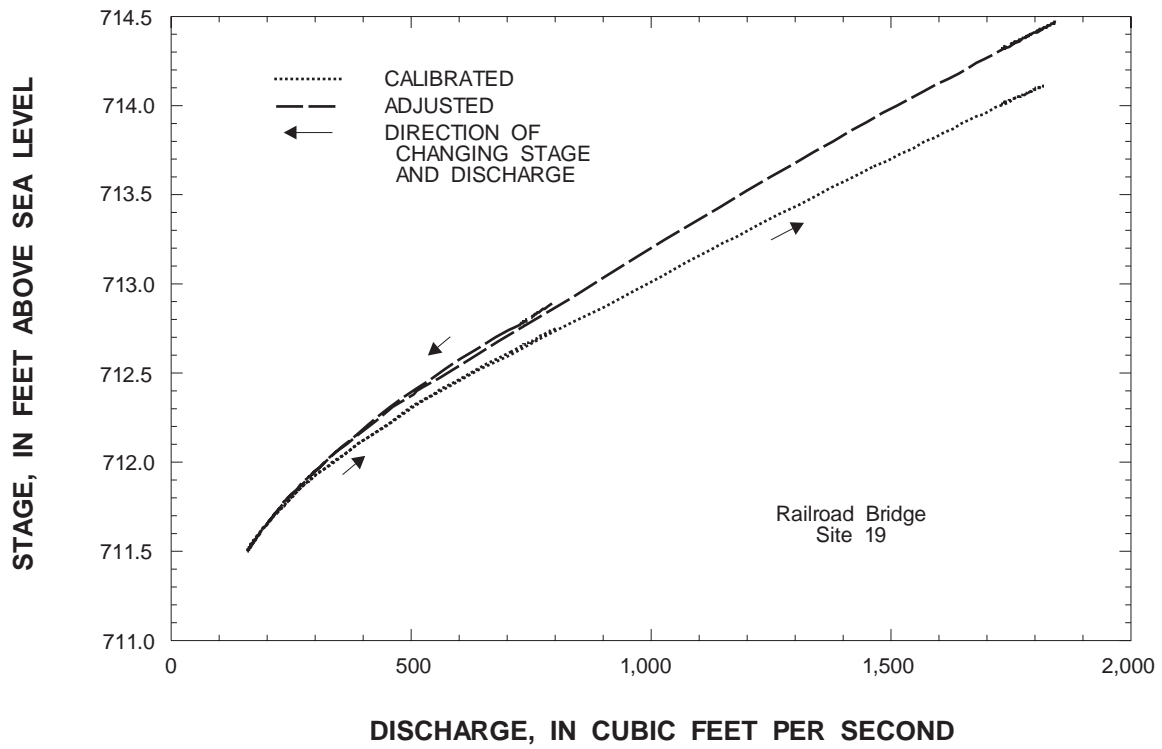
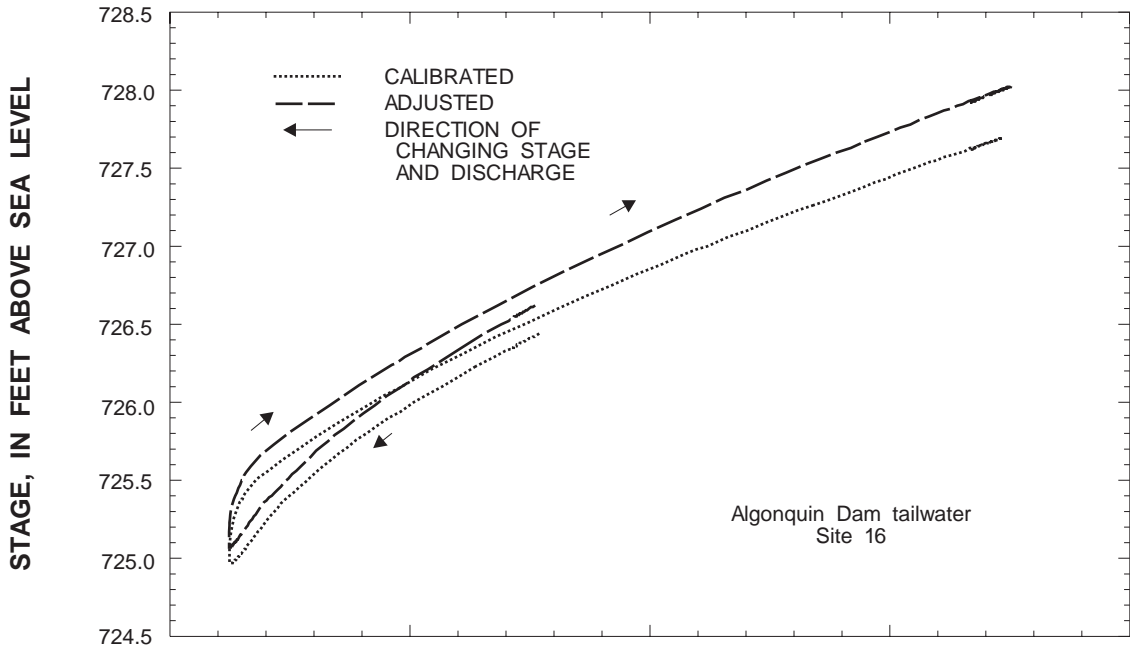


Figure 9. Continued.

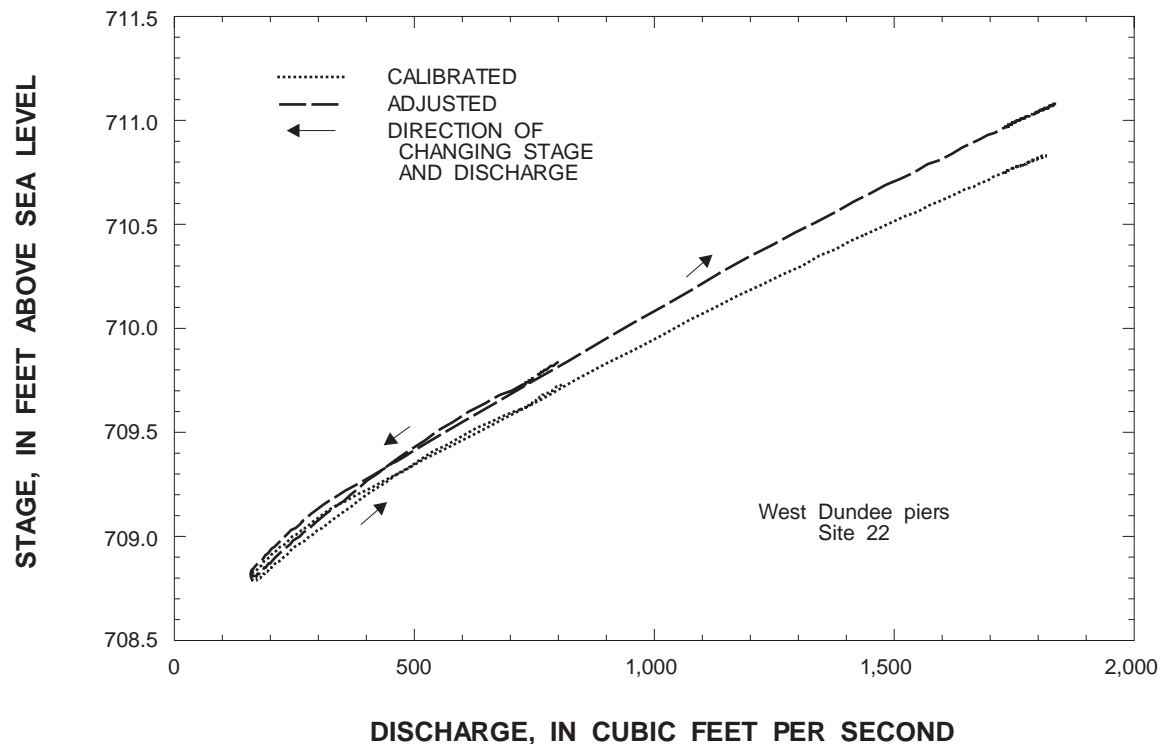
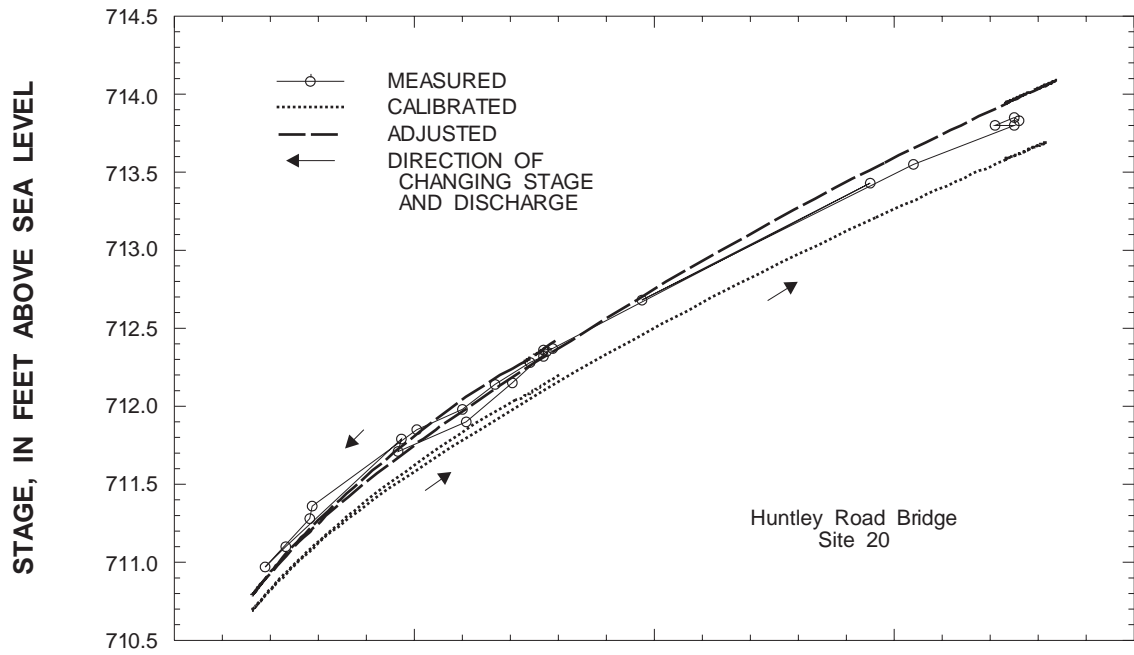


Figure 9. Continued.

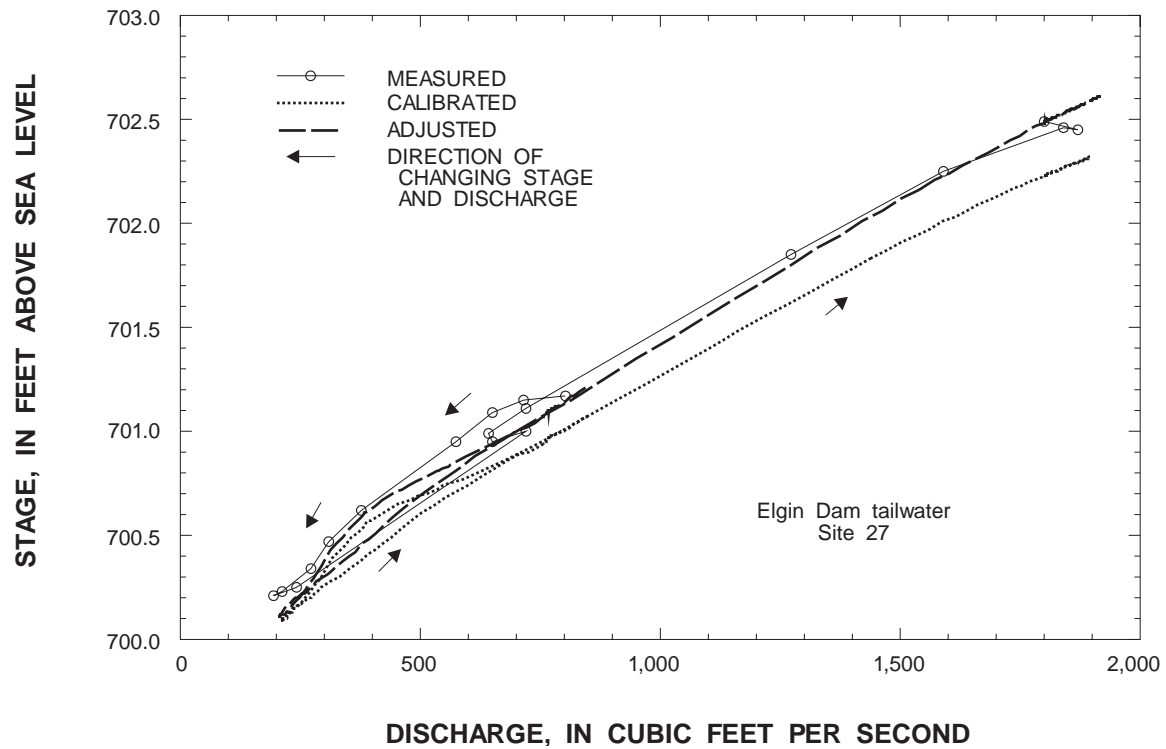
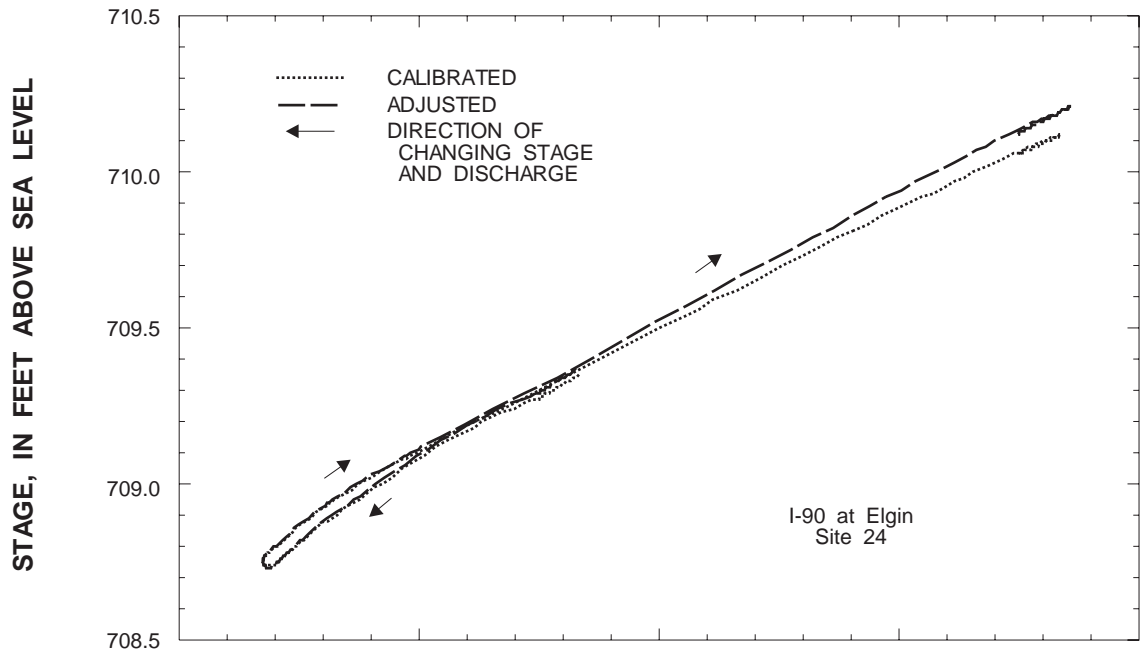


Figure 9. Continued.

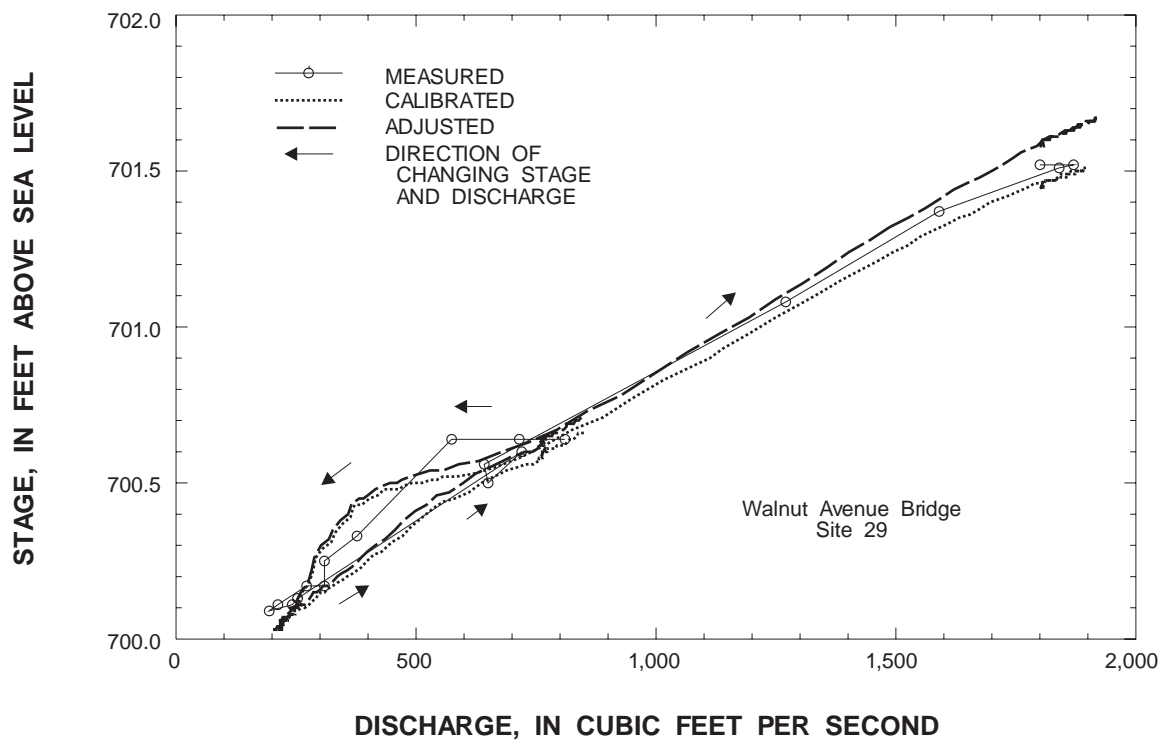
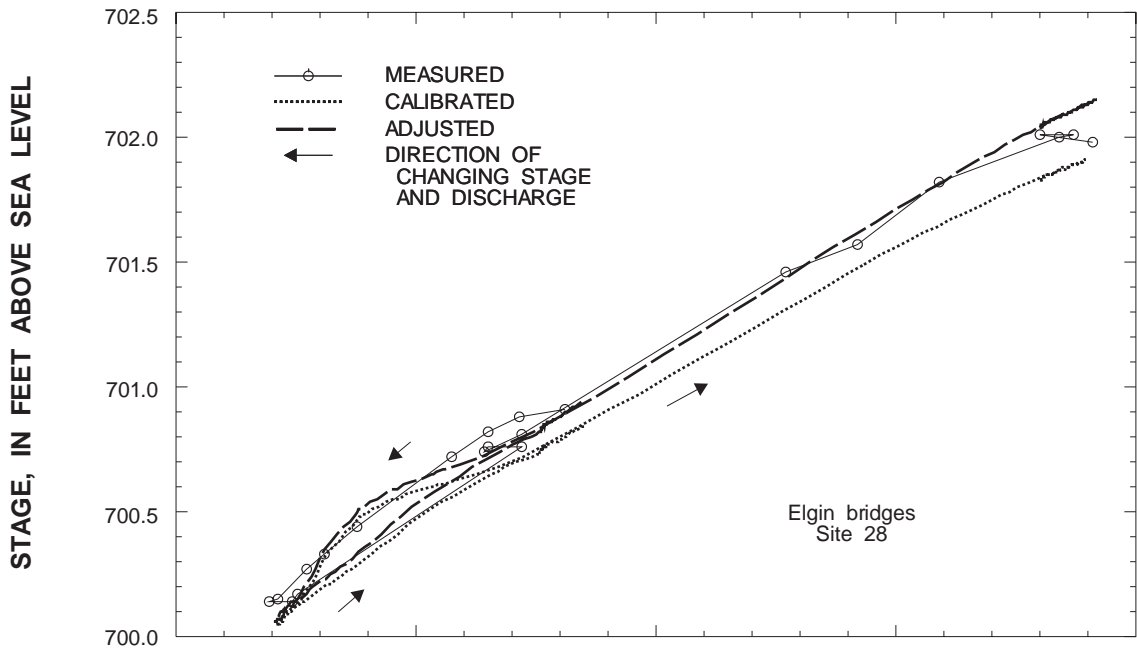


Figure 9. Continued.

Samples from the automated samplers at sites 6 and 10 from the afternoon of November 3 through the morning of November 5 were lost. Measured dye samples during that period were collected manually at those two locations. On November 6–7, the sampler failed and samples were not collected at site 10. At the remaining 14 sites, dye samples were collected manually as often as feasible.

The simulated and measured dye concentrations at all but 1 of the 18 sites are presented in figure 10 together with simulated and (or) measured discharge. The first plot in the figure is the dye-concentration boundary condition input to the model for simulation. The simulation began at 0100 hours on October 25, 1990, and was run with a time increment of 1 hour. The dye-concentration results are not shown at Stratton Dam tailwater because the sampling site is too close to the injection site for the dye to be satisfactorily mixed. The initial peak in the dye concentration at all sites is that observed during low flow, and the secondary peak represents the peak concentration during high flow. As the high flow begins, the volume of water is greatly increased; thus, the dye is diluted and the dye concentration decreases. The concentration decrease to 0  $\mu\text{g/L}$  between the low- and high-flow peaks is because the dye injection ceased for approximately 15 hours late on November 5 because of dye-injection-pump failure.

The timing and attenuation of the dye during the simulation are similar to that measured, especially at the upstream sites. As the wave proceeds downstream, increase in timing error is visible at Elgin bridges, site 28, 27.2 mi downstream from the injection. It appears that as the solution proceeds downstream, the simulated peaks may be slightly later than those measured. At Elgin bridges, the low-flow simulated dye-concentration peak appears somewhat later than the measured dye-concentration peak, but the high-flow dye-concentration peaks match well. It is difficult to say if the simulated velocities are transporting the dye too quickly or if the measured dye curve is misinterpreted because of the infrequent measured dye-concentration samples. For the same reason, the calculation of the total mass of dye at the downstream point could not be determined. The decay of dye was assumed to be zero because the decay was difficult or impossible to distinguish significantly from zero.

At Fox River Grove (site 12), the low-flow dye concentration measured and simulated peaks do not compare well. During the study, it was noted that

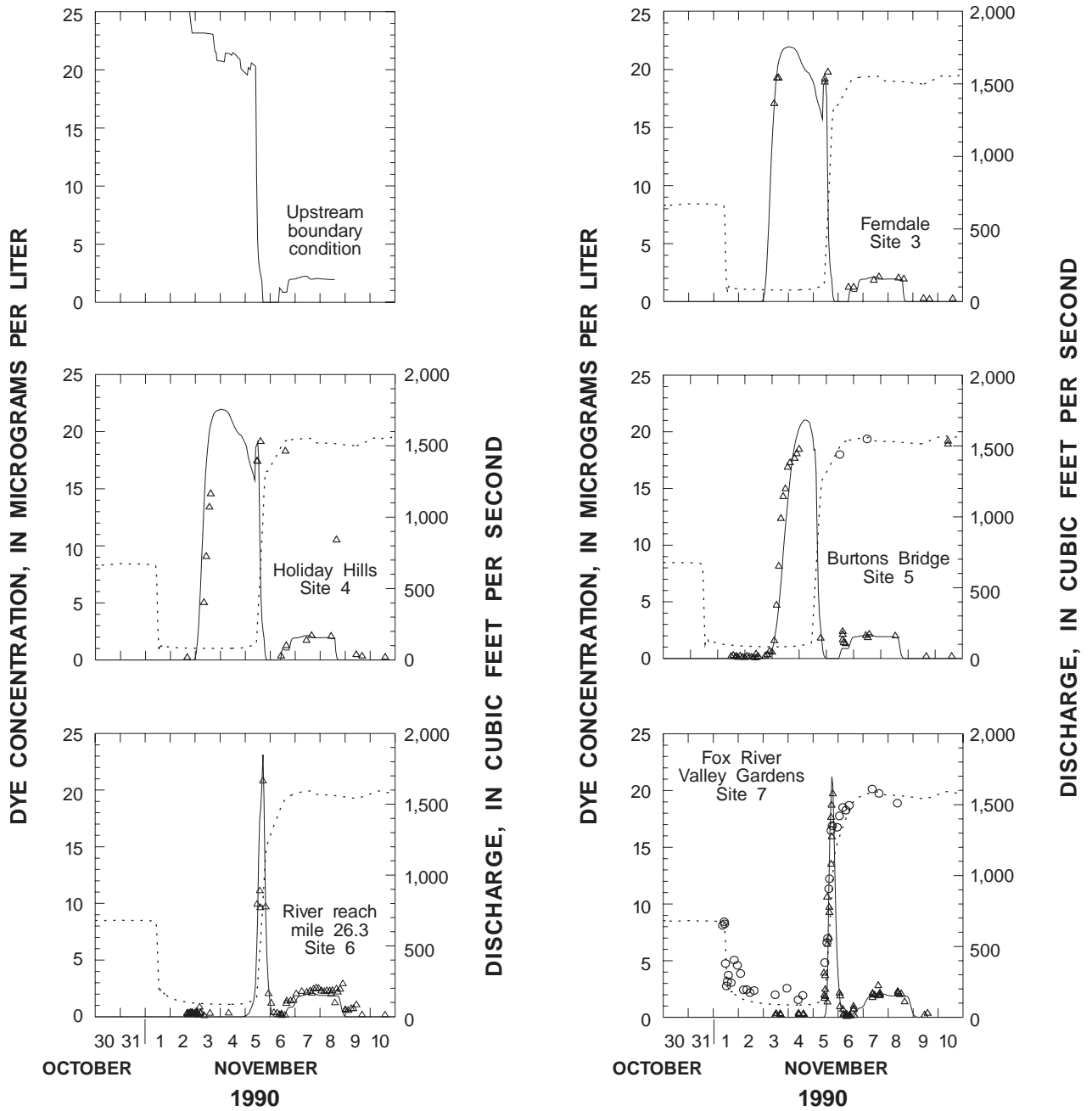
samples collected from the automated sampler at that site were cross-contaminated from November 5 at 1800 hours to November 6 at 2000 hours. The sampler at the site was swamped allowing for the samples to intermix and be diluted. This explains the low measured concentrations during the November 5–6 period. Some measured dye points appeared to be outliers, such as those on November 6 and 8 at Holiday Hills (site 4). These values may be due to contamination of the sample or to an error in noting a scaling factor during the fluorometric analysis of the sample.

Dye sampling at most of the sites is not detailed enough to allow a strict definition of the low-flow peak. The peak of the dye concentration might easily have been missed because of the rapid rise and fall of the dye concentration, thus, making it difficult to define differences in the measured and simulated dye concentration accurately. Graphical presentation of simulated and measured dye concentrations, however, indicate that the flow field simulated in FEQ was accurate as errors over time and space in the routing routines would be reflected in the dye-transport simulation results. The dye-transport simulation results are especially encouraging in the overall calibration because velocity may be the most difficult parameter (of discharge, stage, and velocity) to simulate in unsteady-flow modeling (Xia, 1991, p. 200).

## SENSITIVITY ANALYSIS

Model sensitivity analysis is performed to identify how changes in input parameters affect the simulation results. For flow modeling, the input parameters may be classified in three groups: (1) the computational parameters, (2) those based on physical measurements, and (3) those subject to calibration from the interpretation of physical data and modeling results. The first category includes the convergence criteria, the number of iterations allowed, the temporal and spatial discretization, and the temporal-integration weighting factor. In the second category, the parameters most likely to affect the results include the channel geometry and the boundary and initial conditions, including datum errors. The third category primarily consists of the roughness coefficient, although weir or bridge head-loss coefficients also can be included.

Convergence testing, which is the sensitivity of the model results to various computational control parameters, is an essential prerequisite to any modeling effort. The various computational parameters interact



**EXPLANATION**

- SIMULATED DYE
- ..... SIMULATED DISCHARGE
- △ MEASURED DYE
- MEASURED DISCHARGE

**Figure 10.** Measured and simulated dye concentrations and discharge at data-collection sites on the Fox River in Illinois. (Site numbers are referenced to table 1.)

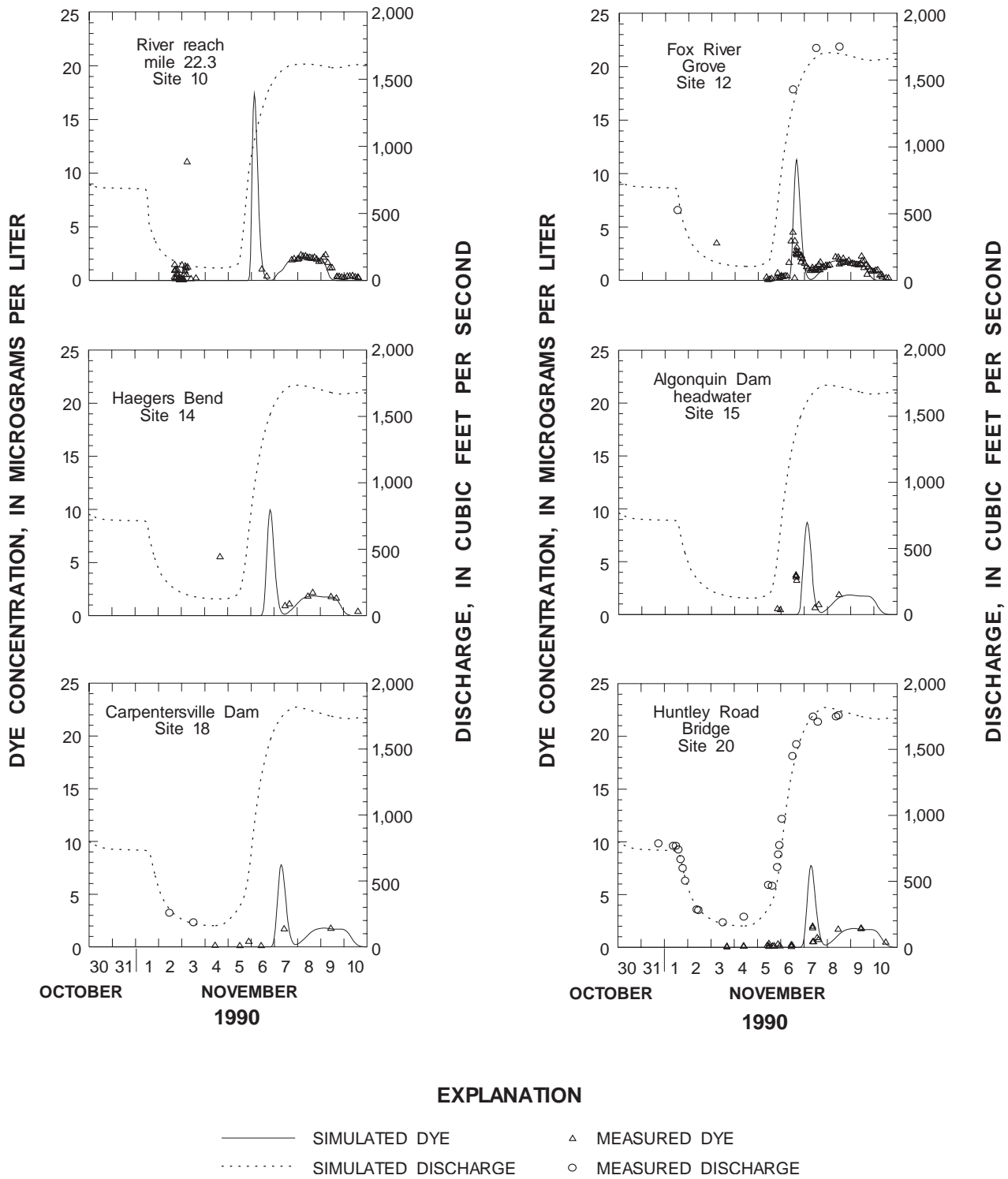
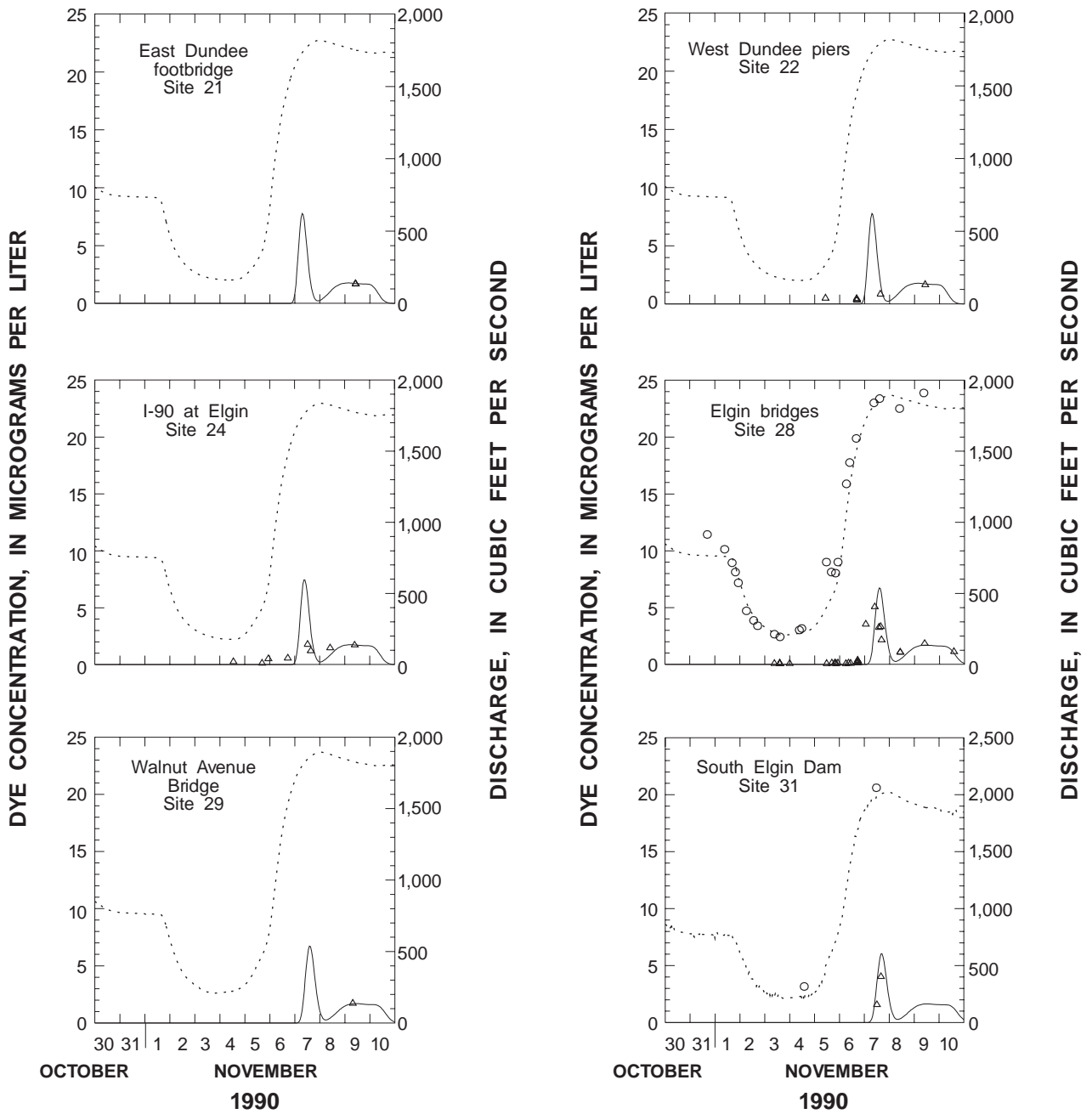


Figure 10. Continued.



**EXPLANATION**

- SIMULATED DYE
- △ MEASURED DYE
- - - - - SIMULATED DISCHARGE
- MEASURED DISCHARGE

Figure 10. Continued.

and holding all but one computational parameter constant to examine the sensitivity of the one parameter is often not feasible; however, the effect of each parameter on model convergence can be qualitatively illustrated. For the base simulation for model sensitivity to the computational parameters, the upstream boundary condition was computed discharge from the stage-discharge relation (rating) at Algonquin Dam. The downstream boundary condition was the water-surface elevation at South Elgin Dam. The tributary discharge was estimated as the scaled inflows shown in table 2. The roughness coefficient used was the adjusted value except where the calibrated value is indicated.

## Convergence

Convergence testing is done to ensure that the time step, distance step, and convergence criterion are small enough that additional steps or iterations do not significantly alter the results; thus, the discrete solutions to the flow equations are approaching the exact solution to the continuous equations. There are two forms of convergence criteria available. The relative criterion compares the size of the change in each unknown for each iteration to some quantity, and the ratio is compared to the specified criterion. The absolute criterion compares the size of the difference directly to the specified criterion. Other user-specified computational parameters include the number of iterations allowed per time step, the number of nodes allowed a secondary tolerance, and the temporal-integration weighting factor. Convergence is declared when all unknowns satisfy the convergence criterion simultaneously. If the convergence criteria are not met within the number of iterations allowed per time step, the time step is reduced, the temporal-integration weighting factor is incremented by the user-supplied factor, and a solution is computed again. This process continues until the convergence criteria are met or the time step is less than the minimum allowed. Computational robustness can be increased by allowing a specified number of nodes a secondary tolerance (Franz and Melching, U.S. Geological Survey, in press).

For this study, the convergence criterion is set by inputting an acceptable tolerance for the relative difference in the unknown flow or depth from consecutive corrections using Newton's method in FEQ. The effect of convergence criteria set to 0.005, 0.05,

and 0.5 on discharge and stage results at Huntley Road Bridge (site 20) is shown in figure 11. The maximum difference is less than the rounded off error of 0.01 ft. If the time to complete the simulation with a relative tolerance of 0.05 is considered to be 1.0, then the time for a relative tolerance of 0.005 is 3.05, and the time for a relative tolerance of 0.5 is 0.82. Therefore, the best balance between accuracy and computational time was determined to be at a relative tolerance of 0.05, as there is a potentially 10-times improvement in accuracy at a cost of only a 22-percent increase in computational time.

For linear equations, a temporal-integration weighting factor of 0.5 provides the greatest theoretical accuracy because the application of the integration method then reduces to the trapezoidal method. However, instabilities may develop because of nonlinearities in the physical flow conditions. The resulting oscillations may be damped out by using a larger value for the temporal-integration weighting factor. A value of 0.6 is often considered a good compromise between accuracy and stability (Schaffranek and others, 1981, p. 18). The convergence of the model solution to the most theoretically accurate value is shown in figure 12. Although no evidence of instability appeared in this particular simulation, oscillations did develop in other simulations; therefore, a value of 0.6 was used for all verification simulations.

The selection of the appropriate computational and input-data time intervals depends on the temporal resolution of the flow features of interest, the availability of data for boundary conditions and calibration, the availability of computational resources, and the convergence characteristics of the model. The finite-difference approximations for the continuous flow equations will fail to converge to the specified relative tolerance within the specified limit of iterations if the time step is too large. Even when the model has converged, a smaller time step ( $\Delta t$ ) may change the solution obtained. Time steps in FEQ are adjusted automatically to a minimum specified time step to converge to a solution within the specified limit of iterations. After convergence has been achieved, the time step is increased in a stepwise fashion to the maximum size allowed by the input statement unless the number of iterations approaches the limit too closely. Increasing the time step adds apparent robustness to the model simulations, as manually reducing the time step for the entire simulation period is not required. A log of all reductions in time step is printed in the output. For the

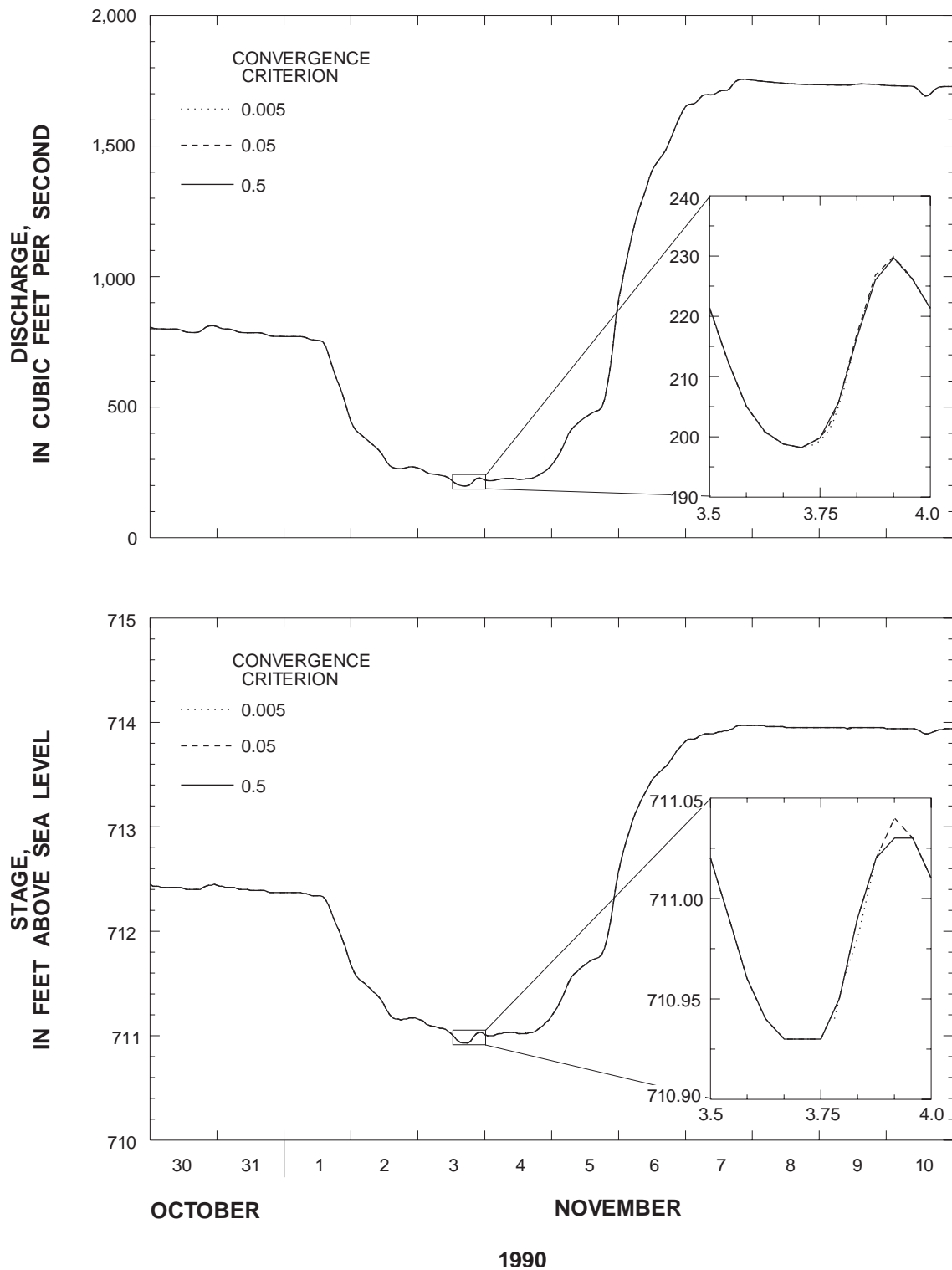


**Figure 11.** Effect of varying the convergence criterion on simulated discharge and stage at Huntley Road Bridge at Carpentersville, Ill.

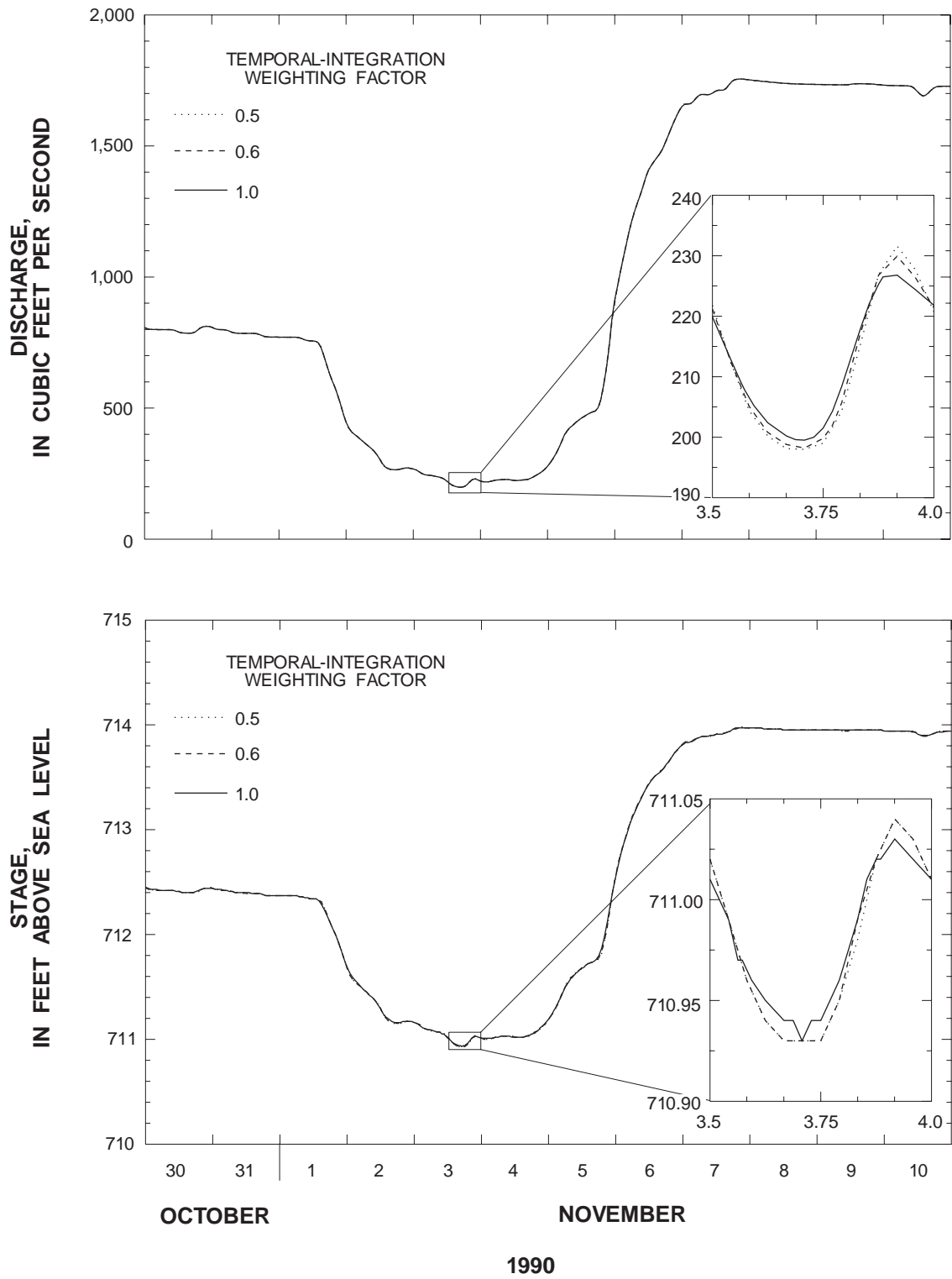


**Figure 12.** Effect of varying the temporal-integration weighting factor on simulated discharge and stage at Huntley Road Bridge at Carpentersville, Ill.

simulations done in the next example, a minimum time step of 5 minutes was allowed for all simulations; however, the time step was reduced in simulation to no less than 30 minutes for only 32 of 470 hourly time steps and not at all for the other time-step simulations.

To test the effect of time-step size, the model was run from Algonquin Dam to South Elgin Dam. This reach was selected because continuous data are available for both stage and rated discharge at the upstream and downstream boundaries. The rated discharge is based on measurements made above the two low-head dams, which function as free weirs making the stage-discharge relation essentially single-valued. The results for 5-minute, 15-minute, and 1-hour time steps using hourly boundary data are shown in figure 13. Hourly data were used for this test to restrict the cause for any difference to the selection of time step rather than the effective data resolution. For example, the comparison of a simulation time step of 5 minutes with a simulation time step of 1 hour using 5-minute data would result in differences because boundary condition data of greater resolution than 1 hour would not be used as the hourly step in simulation. For the effective resolution required here, a maximum time step of one hour appears to be sufficient. The effect of using different input-data time intervals is discussed in the “Boundary and Initial Conditions” section. The stepped appearance of the enlarged water-surface elevation segment is because of the minimum change of 0.01 ft in the model output. The vertical scale is greatly exaggerated to show the detail.

The finite-difference approximations for the continuous equations governing the flow at each node must be solved simultaneously for each time step. The finite-difference approximations of the equations may fail to converge to a solution if the distance between the nodes is too large, in which case, computational nodes must be added. The nodes are in the form of additional cross sections, which may be obtained from measured data, linearly interpolated, or repeated from available cross sections. Even when the model converges to within the specified relative tolerance, the solution may differ from that obtained with additional computational nodes. The convergence characteristics of the model were tested by decreasing the distance,  $\Delta x$ , between nodes. The results for three representative sites are shown in figure 14. The results indicate that the model converges adequately for the base run because the addition of 132 more nodes, which reduces  $\Delta x$  from an average of 473 ft to an average of 259 ft, does not

effectively change the results at any location. The 56 computational nodes included in the base model run, which reduced  $\Delta x$  from an average of 731 ft to an average of 473 ft, have a small effect on the results (about 0.05 ft at Huntley Road Bridge and less at other sites) indicating that the reduction in  $\Delta x$  does slightly affect convergence. The removal of all cross sections interior to the branch ends, which increases  $\Delta x$  to an average of 4,181 ft, has a large effect on stage but none on the discharge. This simulation combines the effect of the larger  $\Delta x$  with the effect of much less geometric information. The flood-wave celerity is unaffected because the depth of the channel is relatively constant. The importance of geometric information to the model results is discussed in the next section.

The importance of the computational parameters in damping or preventing numerical oscillation is illustrated in figure 15. A very small oscillation developed during a sensitivity test of the effect of decreasing the calibrated value of Manning’s  $n$  by 30 percent. The water-surface elevation approached zero at some locations in the river channel. The unrealistic dry-bed situation put a large demand on the model computationally. Several different computational parameters were varied to determine their effect on the model output. The most effective approach was to add an interpolated cross section. The resulting decrease in  $\Delta x$  was sufficient to prevent the computational difficulty from occurring. The second most effective approach was to increase the temporal-integration weighting factor by 0.15 to a value of 0.75. The initial oscillation was reduced and did not propagate in time. Decreasing the weighting factor to the theoretically most accurate value of 0.50 also reduced the initial oscillation but it continued for almost 1 day. Allowing additional iterations per time step prior to convergence reduced the initial instability but allowed slight oscillations thereafter, whereas reducing the size of the maximum and minimum values for the time step increased the steepness of the initial oscillation, but reduced the propagation of it thereafter. Therefore, reducing  $\Delta x$  was the most effective means of improving the computational characteristics of the model in this case.

## Hydraulic Geometry

The hydraulic geometry of a stream includes both the channel cross-sectional and channel-slope data, which are measured in the field or from maps, and the measured dimensions of the bridges, dams,

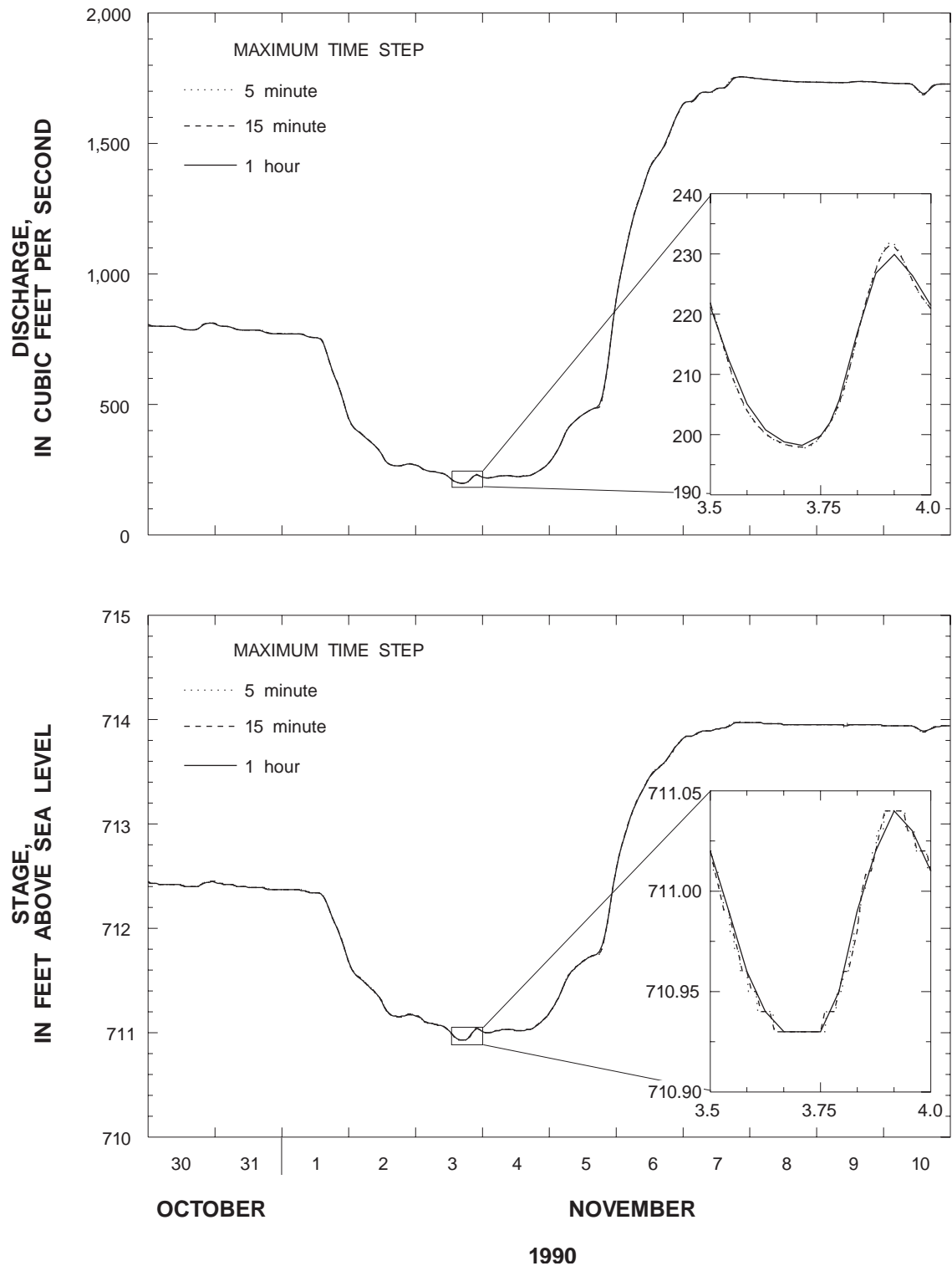


**Figure 13.** Simulated discharge and stage for maximum computational intervals of 5 minutes, 15 minutes, and 1 hour at Huntley Road Bridge at Carpentersville, Ill.

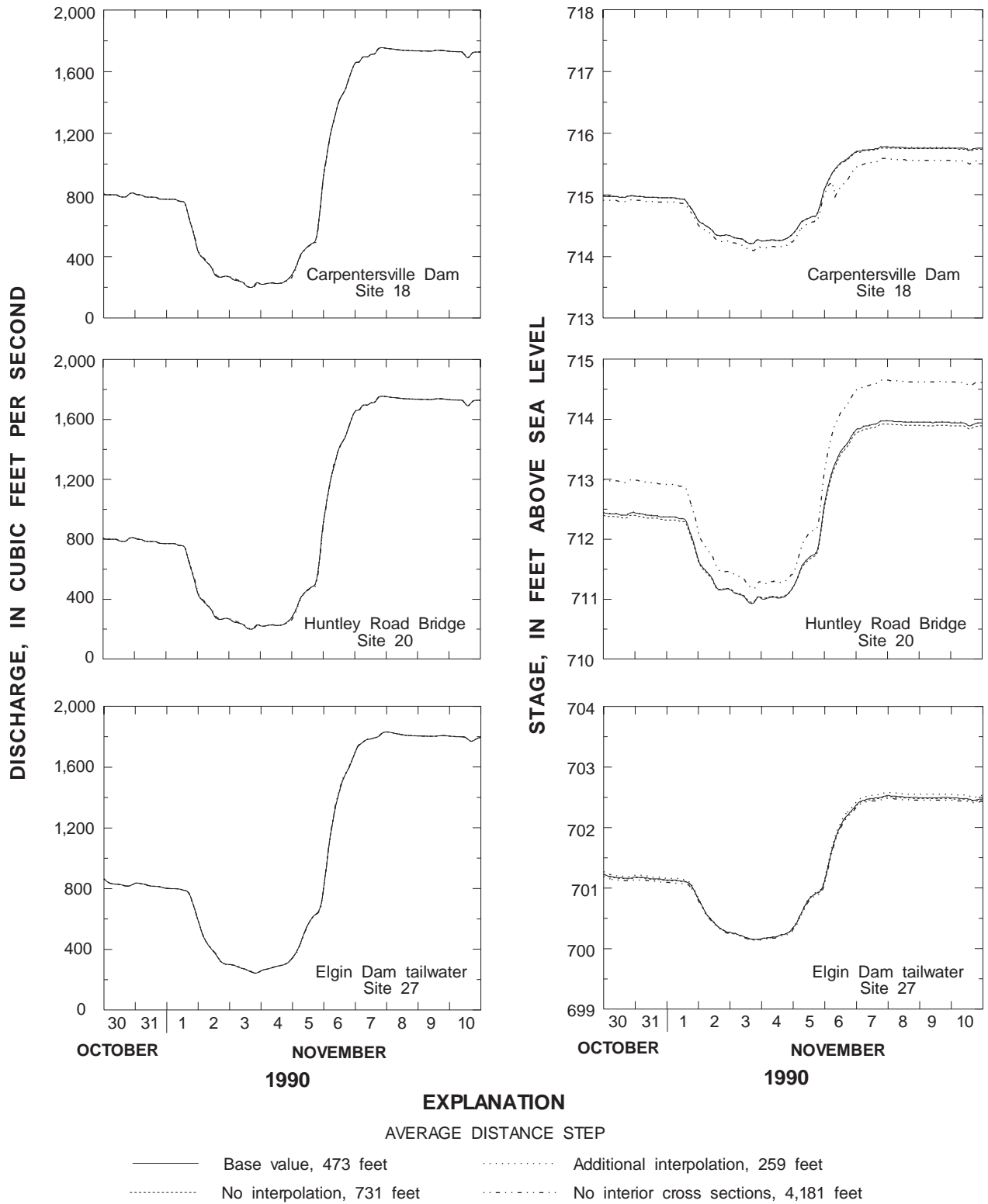
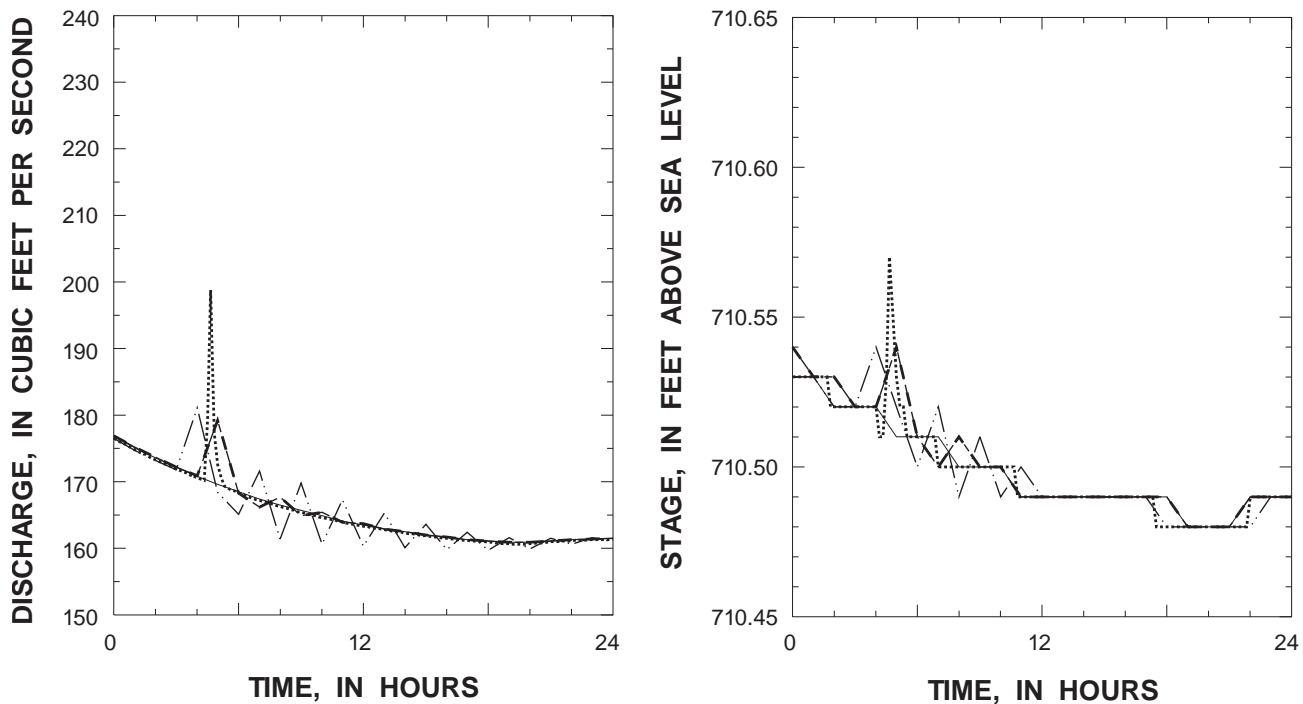


**Figure 14.** Effect of varying computational distance step on simulated discharge and stage at selected sites on the Fox River in Illinois.



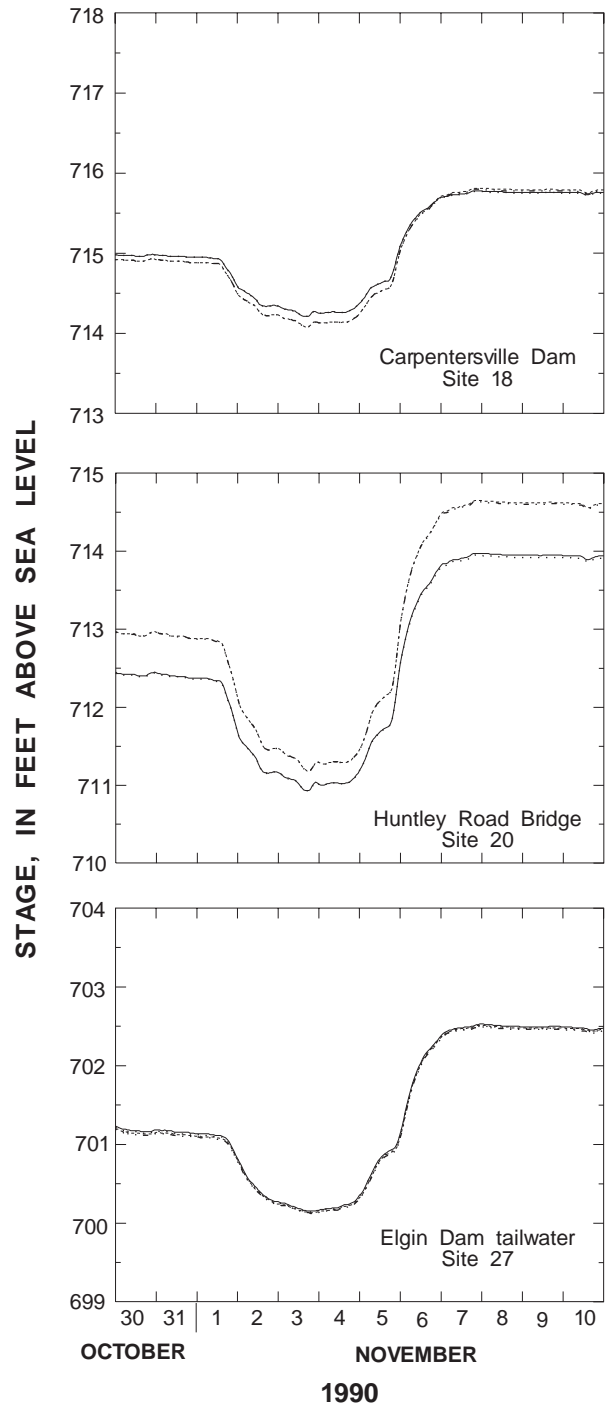
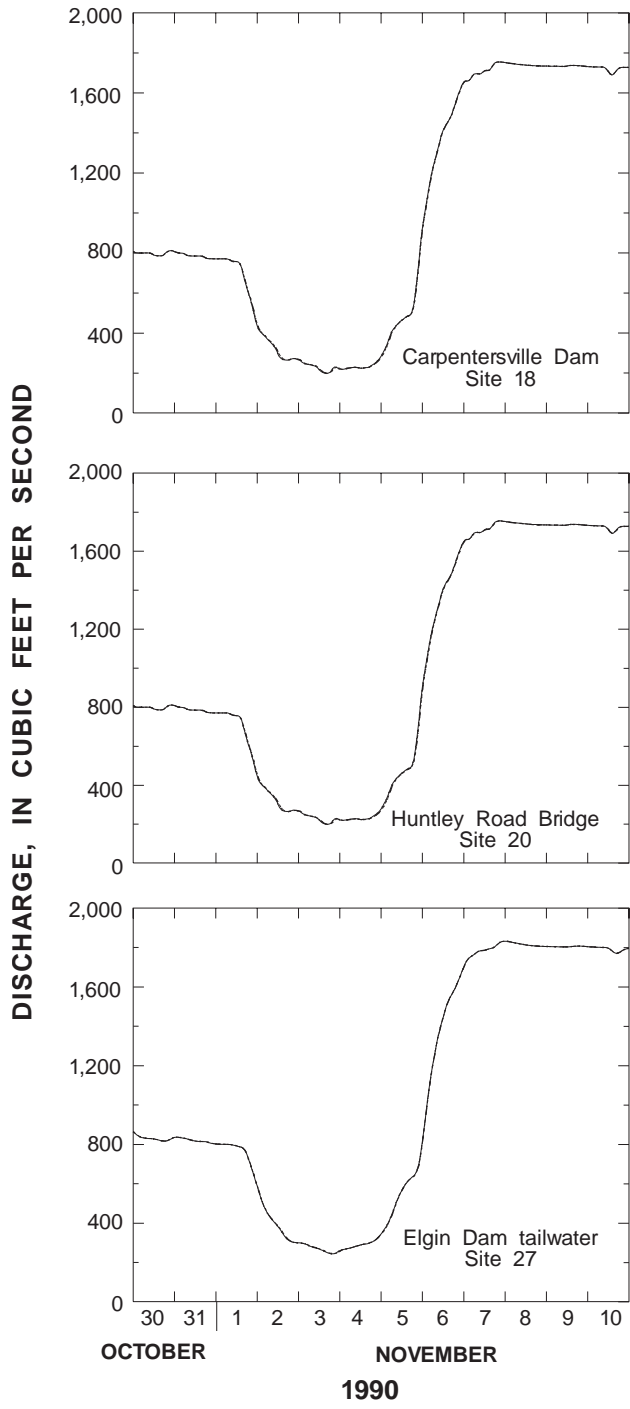
#### EXPLANATION

- BASE VALUES
- ..... TIME STEP REDUCED BY 3,000 SECONDS, MINIMUM TIME STEP REDUCED BY 0.9 SECONDS
- INTERPOLATED CROSS SECTION ADDED UPSTREAM
- · - · - · - WEIGHTING FACTOR DECREASED BY 0.10
- - - - - ITERATIONS ALLOWED INCREASED BY 2

**Figure 15.** Effect of varying computational parameters on model error.

and other hydraulic structures. The relative importance of cross-sectional geometry to producing reliable and accurate simulation results was tested by replacing measured cross sections with interpolated cross sections. The effect of removing all cross sections interior to the exterior nodes (locations where bridges, dams, or tributaries require internal boundary conditions) at three representative sites is shown in figure 16. Dynamic-wave celerity depends primarily on the depth of flow, and the relatively prismatic shape of the Fox River is indicated by the good timing of the simulated hydrographs; however, local errors in stage are caused by incomplete or insufficient channel-geometry information. The stage simulation results at Carpentersville

Dam (site 18) are low because the channel downstream from the dam is assumed to be wider than it is. The opposite effect is apparent at Huntley Road Bridge (site 20) where stage is high in the absence of measured cross-sectional data because of the narrow cross section included in the model just downstream from the bridge. Comparison of figure 16 with figure 14 for the no-interior-cross-sections simulations indicates that the lack of geometric data is the major cause of the error in stage and not the increase in the computational distance between nodes ( $\Delta x$ ) because the missing measured cross sections of figure 14 are replaced with interpolated cross sections in figure 16, yet the results are similar. At Carpentersville Dam (site 18), however,



**EXPLANATION**  
GEOMETRIC DATA

- |       |  |       |  |
|-------|--|-------|--|
| —     | All cross sections   | ..... | All cross sections, no bridges   |
| ..... | Interior reach cross sections replaced with interpolated nodes | ..... | Interior reach cross sections replaced with interpolated nodes, no bridges |

the larger computational distance step used for the no-interior-cross-sections simulation in figure 14 results in nonconvergence as indicated by the difference in the stage results between figures 14 and 16 where no measured interior cross sections are used.

The effect of removing all the bridge geometric data also is shown in figure 16. The approach and departure cross sections were left in the model to represent the branch ends and to provide data for the linear interpolation of computational cross sections. Bridges generally were not constricting for the simulated flows investigated in this study but did, however, have a local effect on stage. The calibrated result from figure 6 for the Railroad Bridge as well as the effect of multiplying the computed headloss by 3.5 and the effect of removing the bridge completely from the model simulation is

shown in figure 17. (The simulations shown in fig. 17 were run using boundary conditions for the full model, from Stratton Dam to South Elgin Dam.) The effect of completely removing the bridge is very minimal. The constricting effect of the bridge on stage is somewhat approximated by multiplying the computed head loss by a factor of 3.5. The bridge is nonstandard with large numbers of irregular wood pilings (see fig. 8) and was apparently not represented adequately by the available bridge routines (Federal Highway Administration, 1970). Nevertheless, these apparent effects are localized and may be partly because of the placement of the stage recorders on bridge piers. This result is given to show these effects and was not applied to other simulations. Further investigations of bridge modeling representations, particularly with newer routines, such as

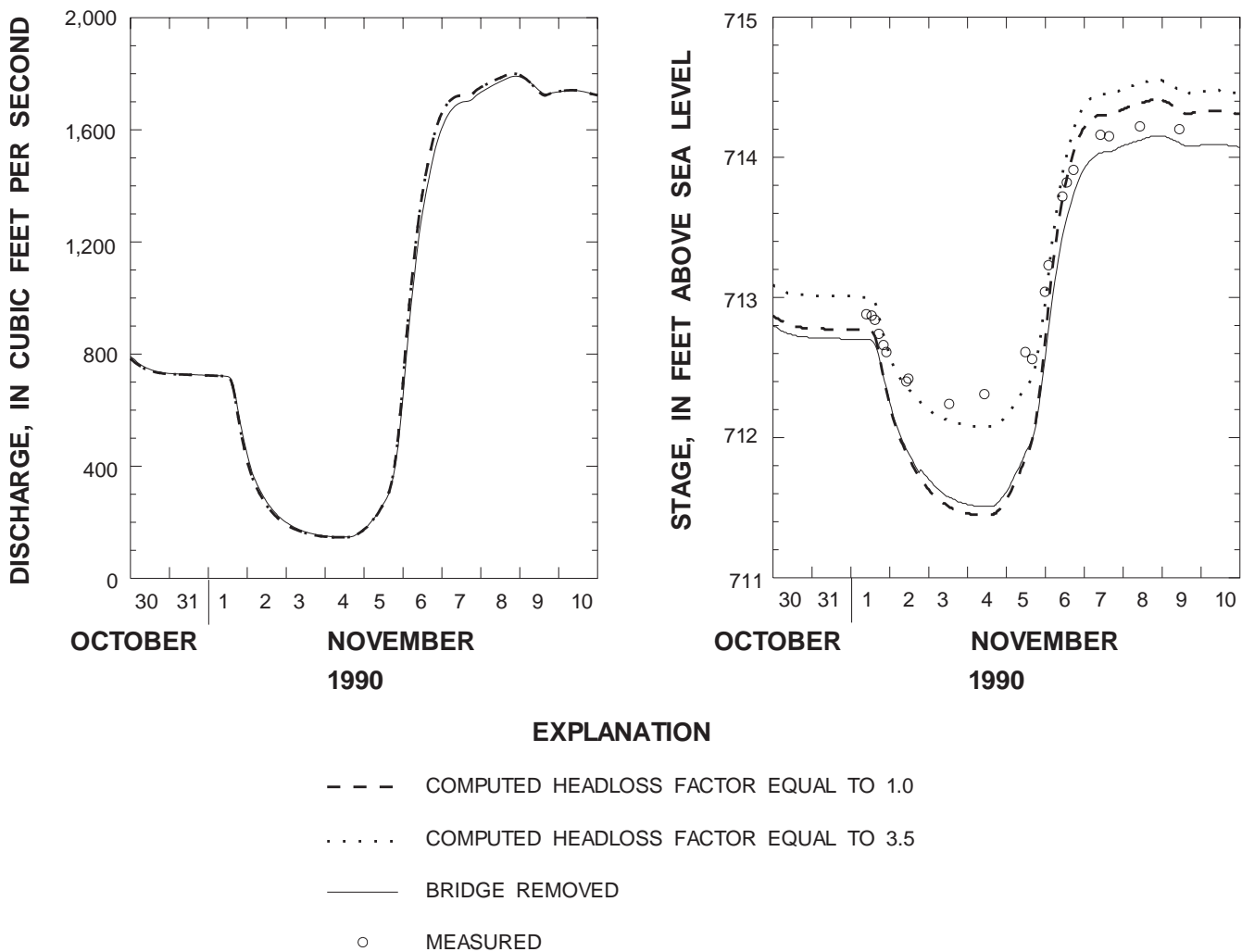


**Figure 17.** Effect of bridge head-loss coefficients on simulated discharge and stage at the Railroad Bridge at Carpentersville, Ill.

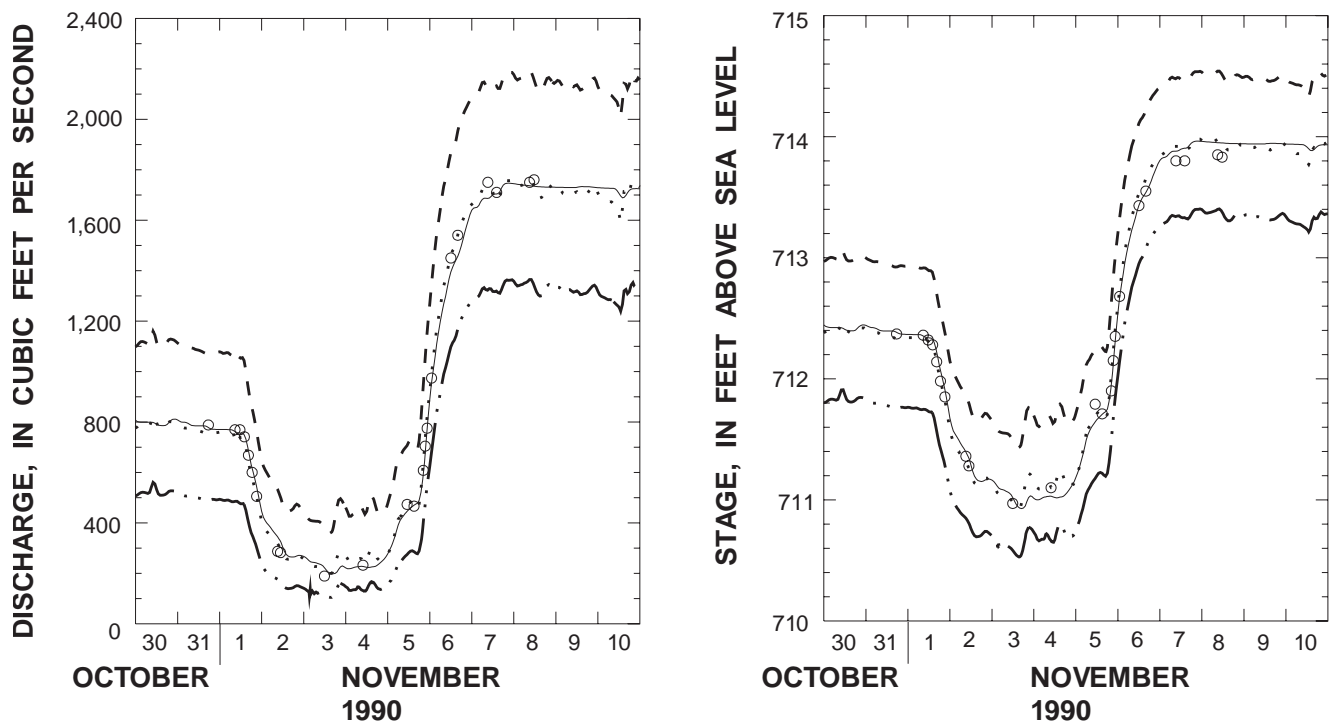
the Water Surface PROfile (WSPRO) (Federal Highway Administration, 1986), may be warranted. These routines have been incorporated into the latest version of FEQUTL.

### Boundary and Initial Conditions

A degree of uncertainty in the boundary conditions is present in hydraulic model simulation because the flow of every tributary is not measured; lateral flow is not measured, and even measured discharges and stages have associated errors. In addition, if datums at the upstream and downstream boundaries have an inherent error, it can lead to a systematic error in the

boundary-condition data where stage is used. An error in datum also may affect one or more cross-sectional-area determinations. The possible effects of these errors were examined by using different combinations of boundary conditions and by varying the gage datums or dam-crest elevations by specified amounts.

The effect of error in the gage datum was found to be significant throughout the study reach only for the upstream boundary and only when stage is used for the upstream boundary condition. This is shown at the Huntley Road Bridge (site 20) in figure 18, where the displacement in upstream boundary gage datum of 0.5 ft is reflected exactly in the stage results when stage is the upstream boundary condition. This relatively



#### EXPLANATION

BOUNDARY CONDITIONS AND  
UPSTREAM ELEVATION

- Q-Z, Actual elevation
- ..... Z-Z, Actual elevation
- Z-Z, Increased 0.5 feet
- · - · - Z-Z, Decreased 0.5 feet
- Measured

**Figure 18.** Effect of boundary-datum error on simulated discharge and stage at Huntley Road Bridge at Carpentersville, Ill., for discharge-stage (Q-Z) and stage-stage (Z-Z) boundary conditions.

large value was selected to have clearly visible results. The effect of boundary gage-datum error on stage results was linearly related to the size of the error. Consequently, discharge results are in error by the amount required by the stage-discharge relation at this site. Huntley Road Bridge is located downstream from the second overflow dam (Carpentersville Dam) from Algonquin Dam, which is the upstream boundary for this simulation.

The effect of a displacement in the downstream-boundary gage datum was not visually discernible upstream from the next upstream dam. No effect from downstream resulted upstream from the dams because the discharge is a single-valued function of the dam-headwater stage at each dam.

The effect of an error in the dam-crest elevation is shown in figure 19. The elevation of the dam crest at the Elgin Dam headwater (site 26) was reduced by 0.4 ft, and the simulation results are shown for Huntley Road Bridge (site 20) and I-90 at Elgin (site 24). Both locations are between Elgin Dam and the next dam upstream, Carpentersville Dam (site 18). Huntley Road Bridge is 5.6 mi upstream from Elgin Dam, whereas I-90 at Elgin is only 2.2 mi upstream from Elgin Dam. The effect of the error in dam-crest elevation is clearly discernible for the stage results at I-90 at Elgin, but cannot be discerned at Huntley Road Bridge. The effect on stage diminished with distance between Elgin Dam and Huntley Road Bridge. Downstream from Elgin Dam, the error in dam-crest elevation had no effect nor was discharge affected at any location.

Other model experiments compared the effect of using various boundary conditions with the river reach between the tailwater of Algonquin Dam and the headwater of South Elgin Dam. The results are discussed in Ishii and Wilder (1993). The experiments on the full model are not reported because of the poor quality of the low-flow discharge measurements made in the upstream reach.

Another aspect of boundary-condition data concerns the temporal resolution of the data. The temporal resolution required depends on the time scale of the hydraulic conditions of interest for the particular problem being modeled. The time scale required depends on the control conditions and the size of the river. Clearly, the accuracy of the simulation results cannot exceed the accuracy of the input boundary-condition data. The effect of only the computational time-step size was shown earlier in the "Convergence" section. For figure 13, hourly boundary data were used

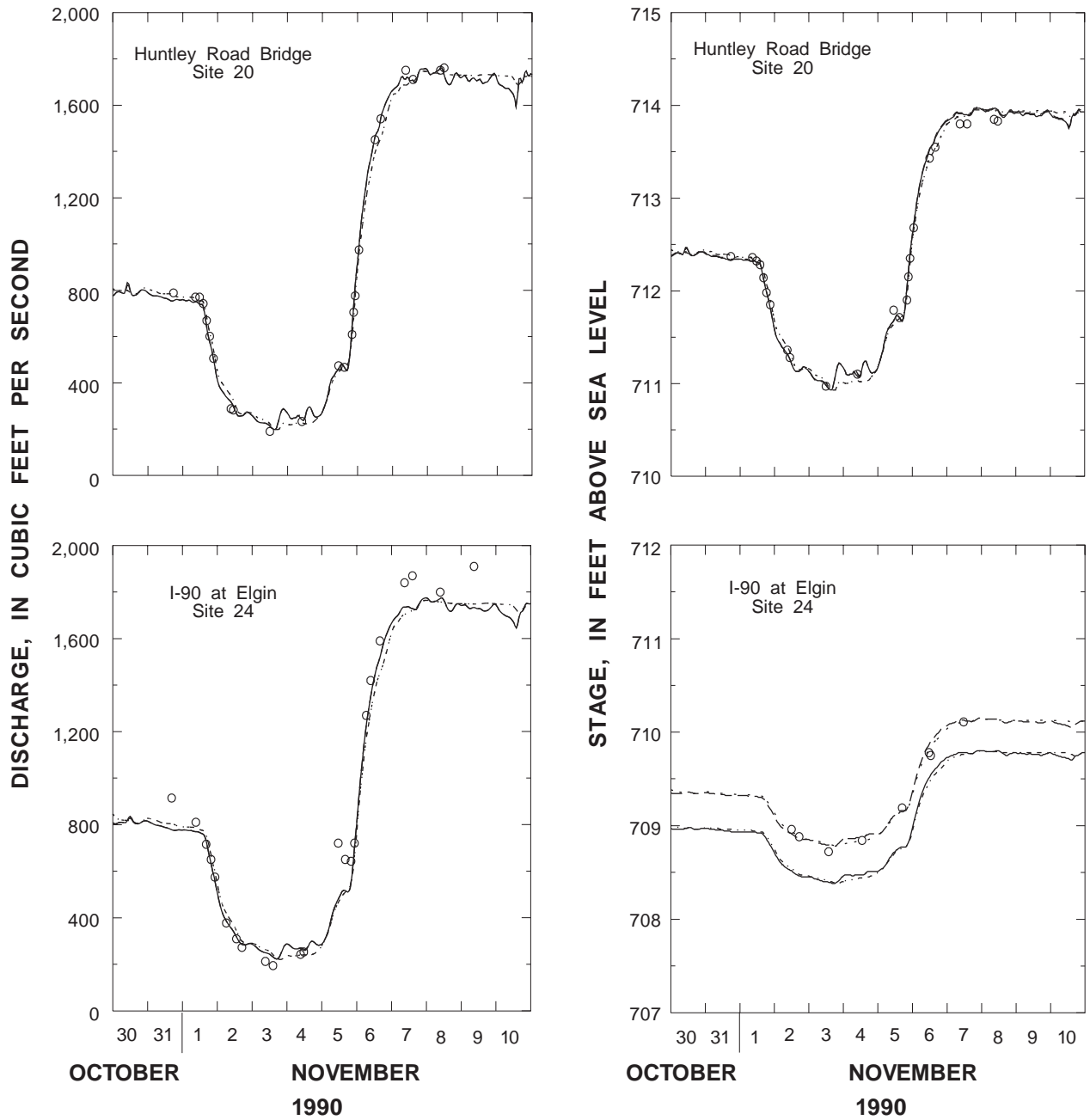
and the time-step size was varied. To separate the effect of the temporal resolution of the boundary-condition data from the effect of time-step size, model simulations using a constant time-step size of 5 minutes were made. The temporal resolution of the boundary data varied from 5 minutes to 24 hours. The difference between the use of 5-minute and hourly data is virtually undetectable, but the use of 6-hour data resulted in routed flows mistiming by about 2 1/2 hours for the example shown. The use of 24-hour data reduced the accuracy of the timing by as much as a day and resulted in inaccurate flows (fig. 20). The simulation results reflect the quality of the temporal resolution of the boundary-condition data as shown in figure 21. Comparing figures 13 and 20, most of the difference is due to the time-step size rather than the data resolution. The boundary-condition data between intervals is linearly interpolated in FEQ when the computational time step requires greater data resolution.

The effect of time-step size and boundary-condition data temporal resolution are not normally completely separable during model simulation because the time step is automatically reduced in the model to reach convergence requirements. The results of using a maximum time-step size that is the same value as the effective boundary-condition temporal resolution is shown in figure 22. The difference between results using 5-minute and hourly boundary-condition data and time-step size is small, though the effects of the two types of temporal information are combined.

Initial conditions have been found relatively unimportant in ensuring that the computed flow converges to the correct solution provided that the simulation has proceeded long enough for channel friction to dissipate the error in the initial estimate (Lai, 1982, p. 288). This was verified by comparing the results using an estimate, and 50 percent and 150 percent of the estimate for the initial flows. The model converged for all simulations to the same solution within 12 hours corresponding to 12 time steps as shown in figure 23.

## Roughness Coefficient

The channel-boundary friction is represented by the roughness coefficient, Manning's  $n$ . The value for Manning's  $n$  should be initially selected based on engineering judgment by reference to the physical conditions of the river channels and other flow paths. The value for Manning's  $n$  should be subject to modification in subsequent calibration only within a



**EXPLANATION**

**BOUNDARY CONDITIONS AND DAM CREST ELEVATION**

- ..... Q-Z, Actual elevation
- Z-Z, Actual elevation
- . - . - . Q-Z, Decreased 0.4 feet
- Z-Z, Decreased 0.4 feet
- Measured

**Figure 19.** Effect of boundary-datum error at the Elgin Dam crest on simulated discharge and stage upstream and downstream from the dam for discharge-stage (Q–Z) and stage-stage (Z–Z) boundary conditions on the Fox River in Illinois. (Site numbers are referenced to table 1.)

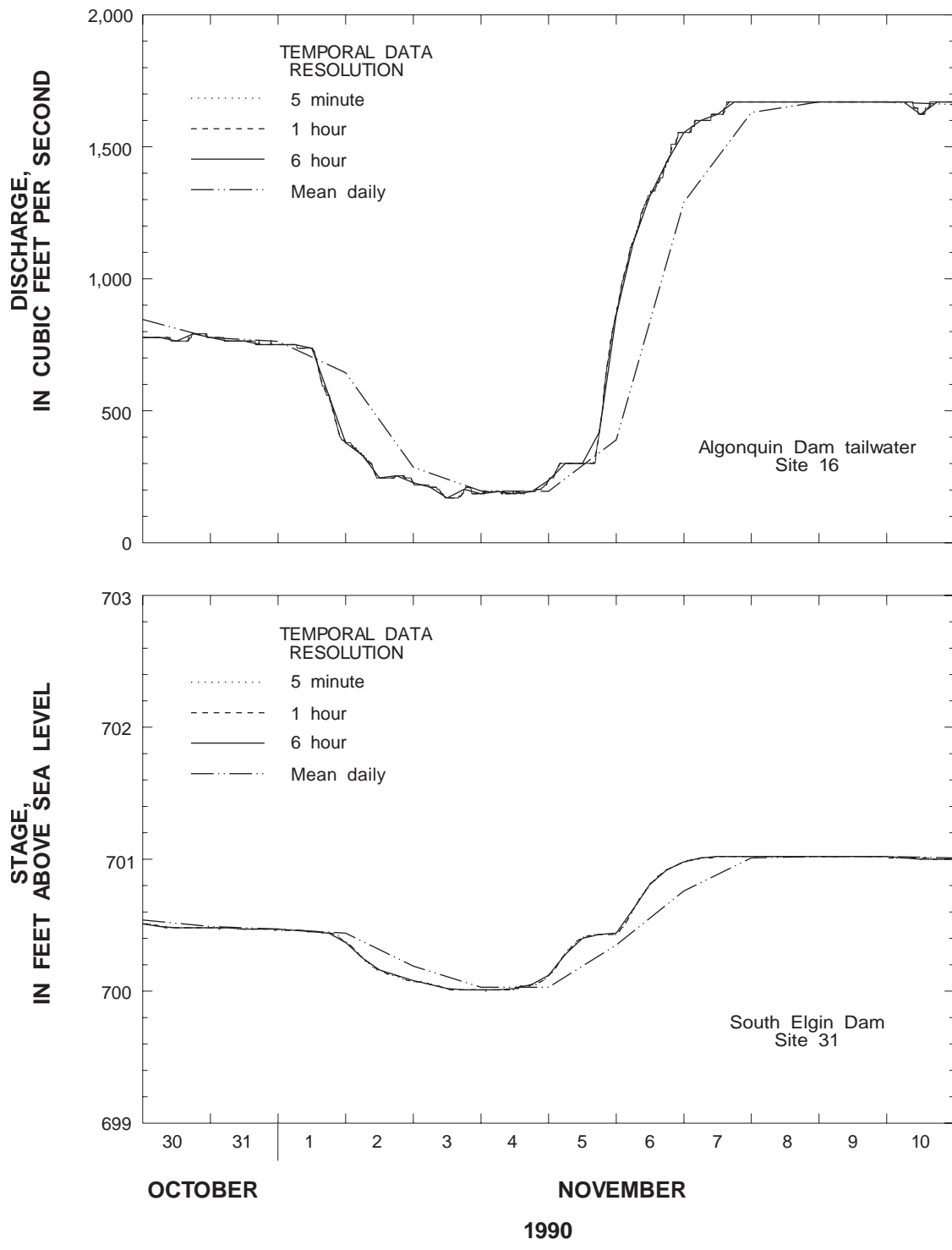


**Figure 20.** Upstream and downstream boundary conditions for 5-minute, 1-hour, 6-hour, and mean daily time intervals for the Fox River study reach in Illinois. (Site numbers are referenced to table 1.)

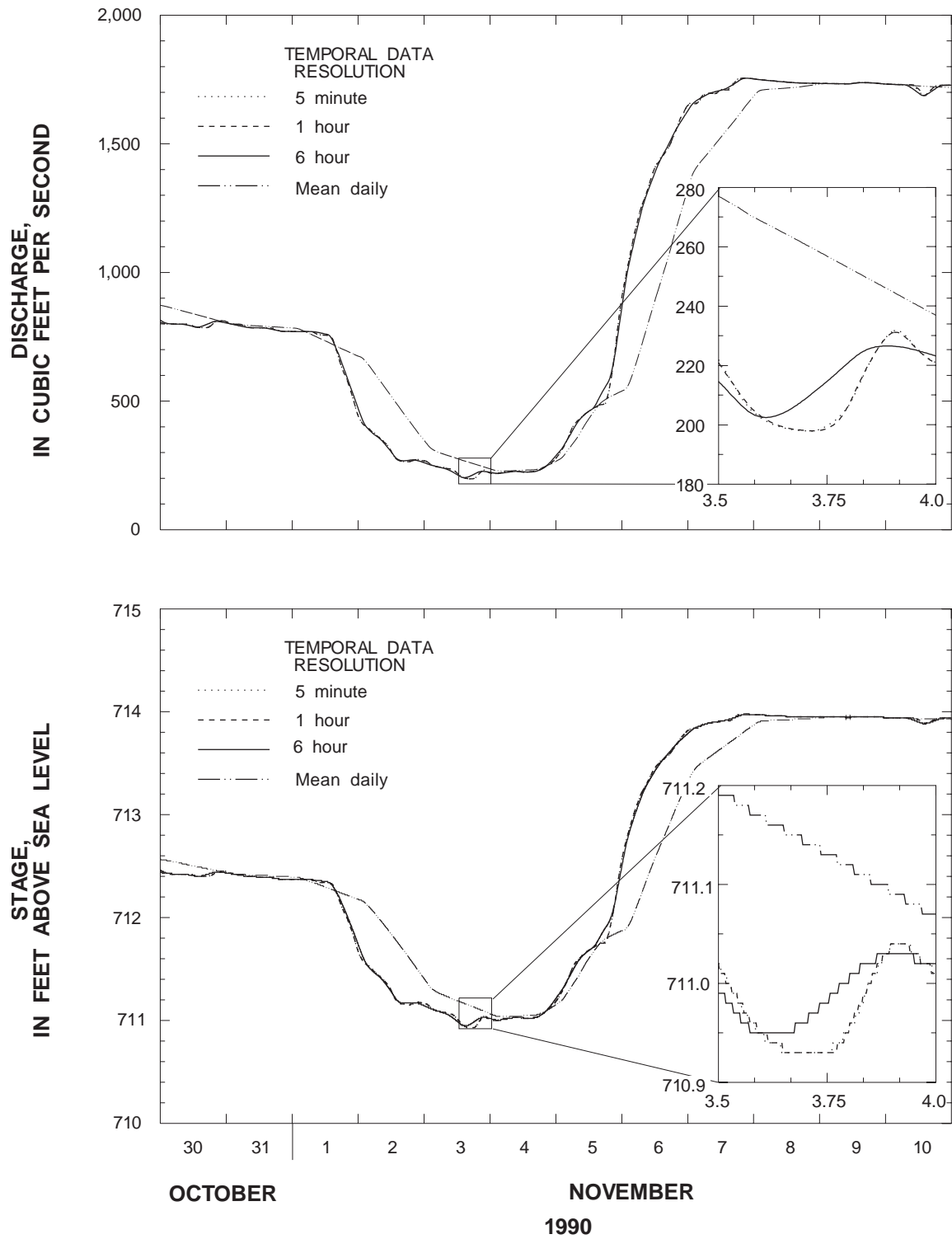


**Figure 21.** Effect of boundary-condition data time resolution on simulated discharge and stage at Huntley Road Bridge at Carpentersville, Ill.

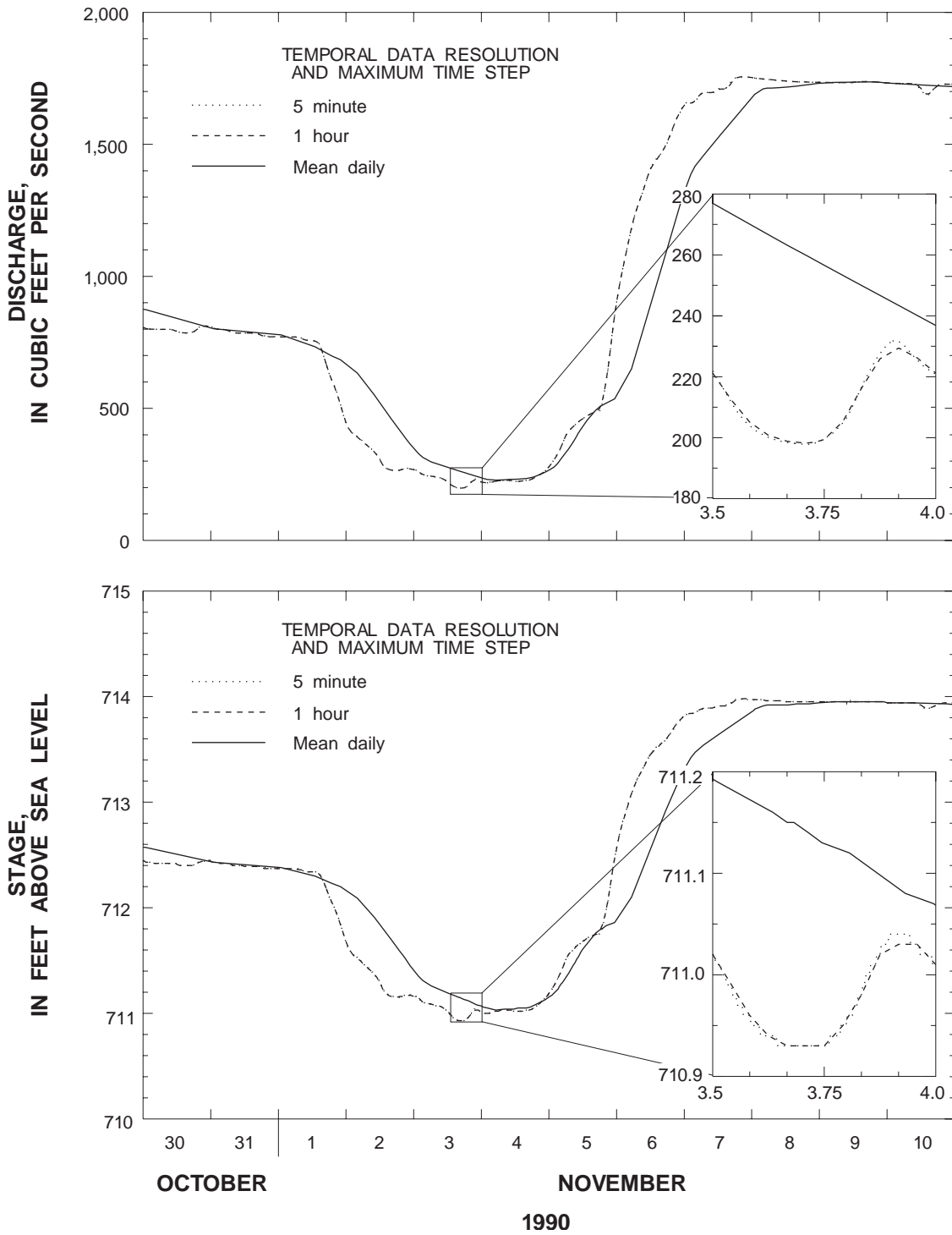
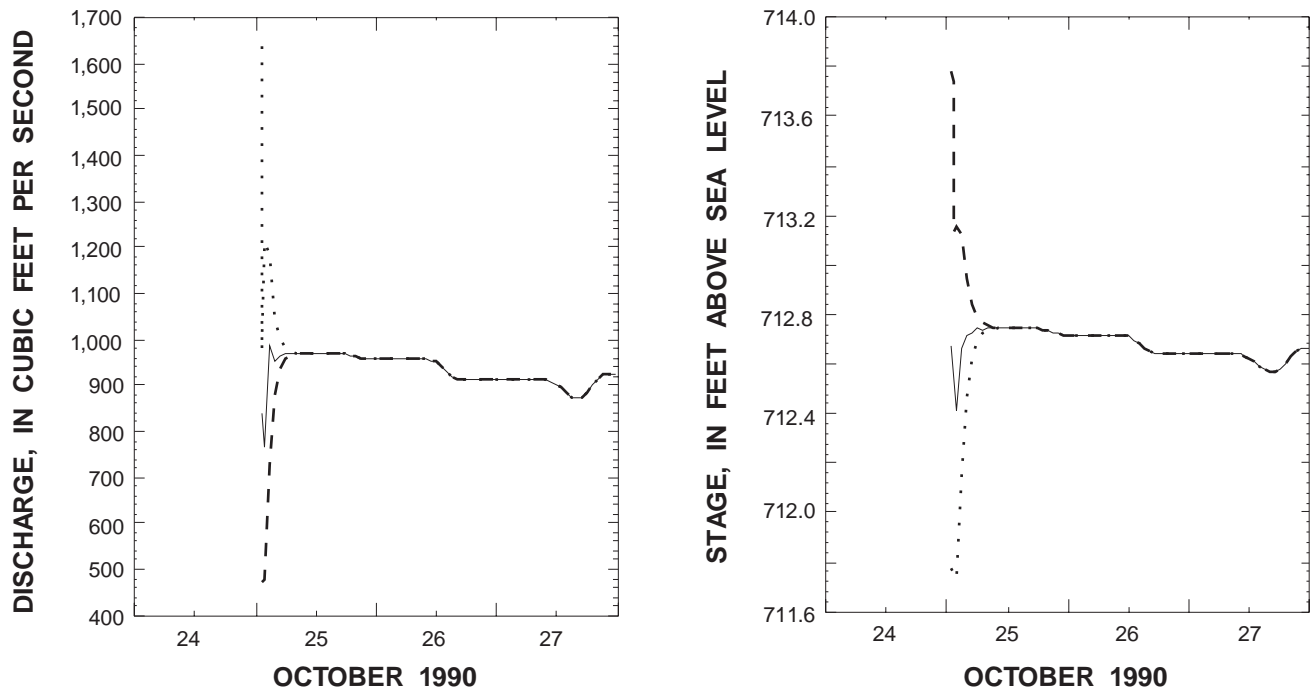


**Figure 22.** Effect of input-data time resolution and maximum computational interval on simulated discharge and stage at Huntley Road Bridge at Carpentersville, Ill.



**EXPLANATION**

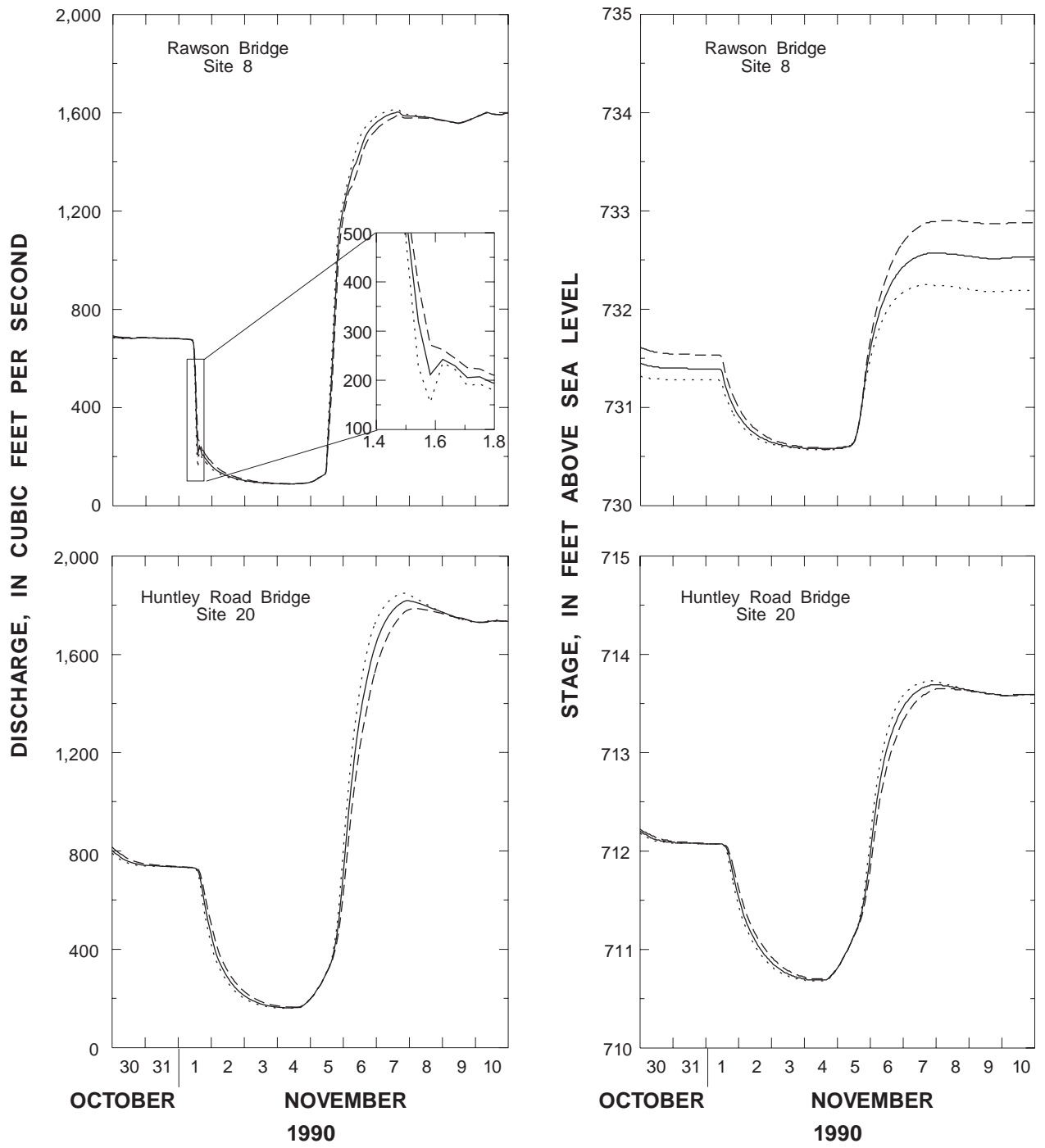
- ..... INITIAL DISCHARGE  
150 percent of base
- Base
- 50 percent of base

**Figure 23.** Effect of varying initial conditions on simulated discharge and stage at Huntley Road Bridge at Carpentersville, Ill.

physically reasonable range. It is assumed that the ranges described in standard references, such as Chow (1959, p. 101–123), for steady flows are applicable to unsteady-flow modeling. Localized changes in Manning’s *n* should not be made without physical justification, as this could result in the roughness coefficient replacing the effect of hydraulic features (bridges, channel geometry, and other features) other than the reachwise resistance because of channel-boundary friction and bedform. This would result in a poor calibration, as the measured flows and stages may be reproduced for one period but may not even approximate the correct values for flows other than the calibration period.

The effect of the roughness coefficients on model results is observed during the calibration phase of modeling. For the verification phase, the roughness

coefficient, Manning’s *n*, is not adjusted. The effect of increasing and decreasing the value of Manning’s *n* by 30 percent from the calibrated value upstream and downstream from Algonquin Dam, respectively, is shown in figures 24 and 25. Because the study reach may be divided into two distinct subreaches based on channel slopes and the internal-boundary control between them, the effect of adjusting Manning’s *n* on one reach may or may not affect the flows and stages simulated in the other reach. For example, figure 24 shows that the increase and decrease in Manning’s *n* for the reach upstream from Algonquin Dam results in a corresponding decrease and increase in flows at Huntley Road Bridge, which is in the reach downstream from Algonquin Dam. This result indicates that a miscalibration on the upstream reach of the river may result in a miscalibration of the downstream reach as

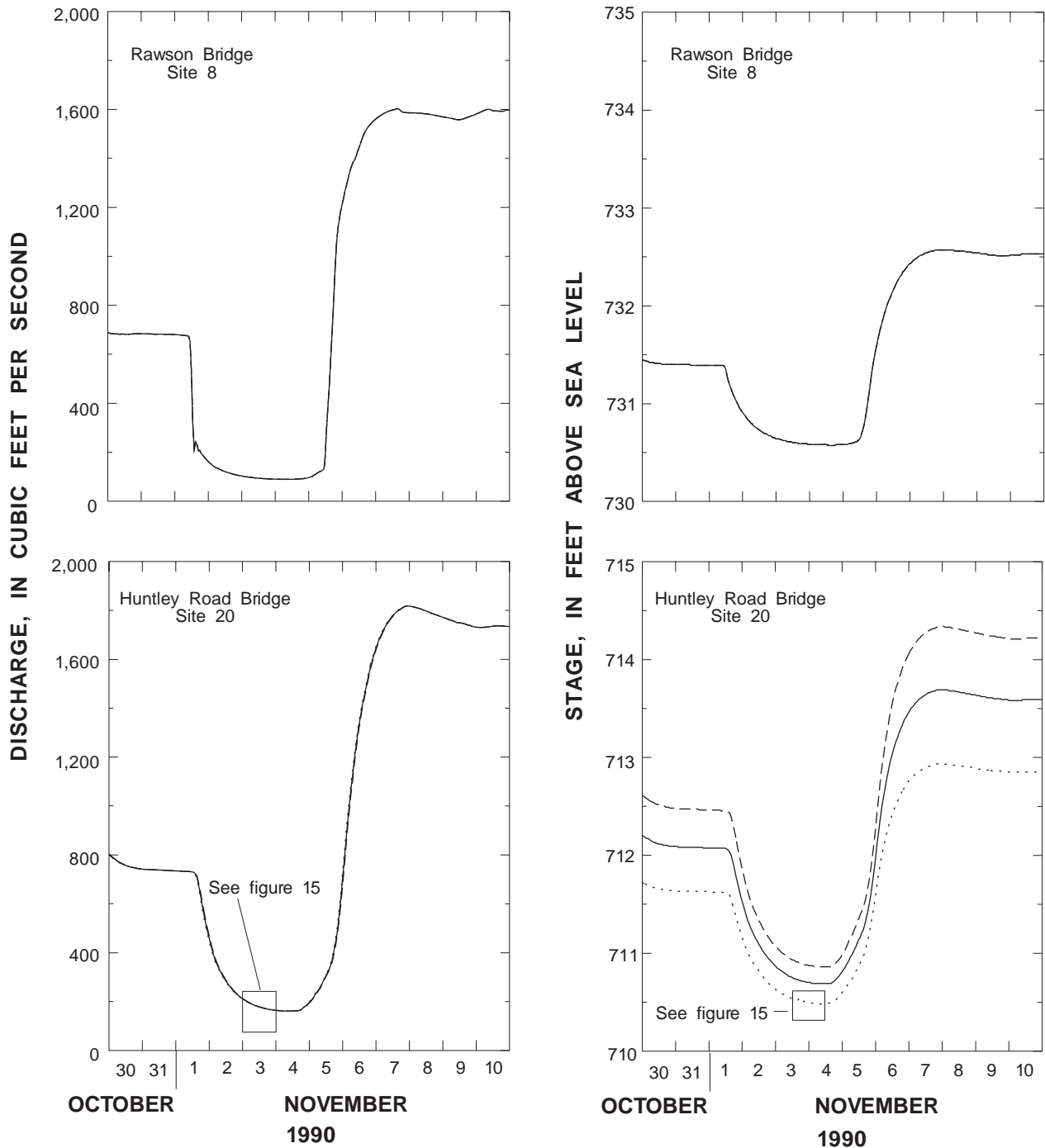


**EXPLANATION**

ROUGHNESS COEFFICIENT UPSTREAM FROM ALGONQUIN DAM

- Calibrated value
- - - 30-percent increase
- · · 30-percent decrease

**Figure 24.** Effect of varying the roughness coefficient by 30 percent upstream from Algonquin Dam on the Fox River in Illinois on simulated discharge and stage at selected sites upstream and downstream from the dam. (Site numbers are referenced to table 1.)



**EXPLANATION**

ROUGHNESS COEFFICIENT DOWNSTREAM FROM ALGONQUIN DAM

- Calibrated value
- - - 30-percent increase
- ..... 30-percent decrease

**Figure 25.** Effect of varying the roughness coefficient by 30 percent downstream from Algonquin Dam on the Fox River in Illinois on simulated discharge and stage at selected sites upstream and downstream from the dam. (Site numbers are referenced to table 1.)

Manning's  $n$  is used to adjust the stage for the erroneous discharges. For this reason, calibrating the river subreaches separately may be advisable if boundary conditions are available to select the best choice for Manning's  $n$  for each reach and avoid propagating errors downstream. Note that the change in Manning's  $n$  for the downstream reach has no effect on stage and discharge in the upstream reach because the effect of downstream flows cannot travel over and upstream from the dam. Ishii and Wilder (1993) have concurred with the suggestion of Lai and others (1992) that using stage as the boundary conditions for both ends of the model may result in greater sensitivity to Manning's  $n$ , which is a desirable condition for calibration.

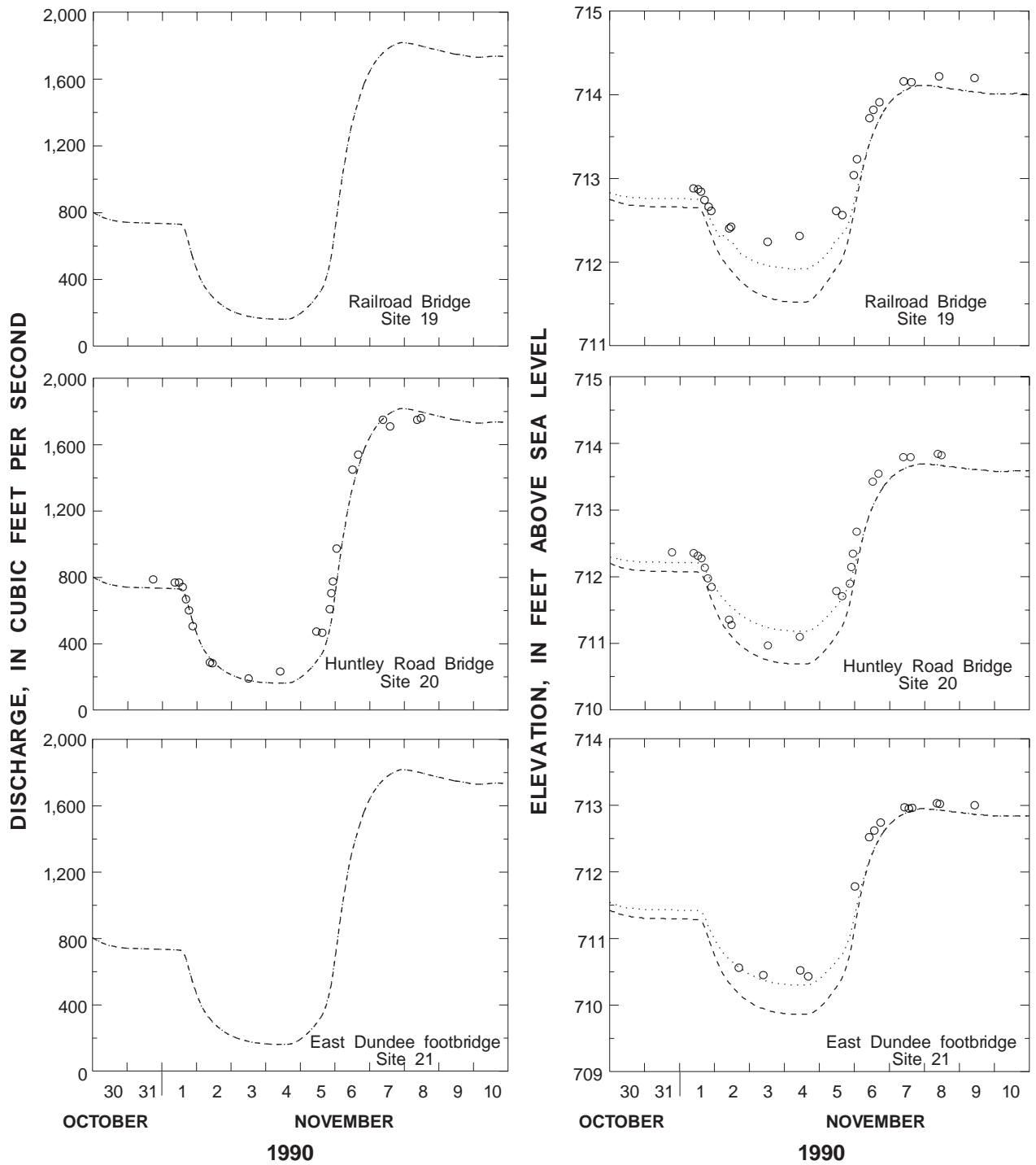
The effective variation in roughness with depth can be simulated with an option in FEQUTL to vary the value of Manning's  $n$  linearly with depth or with hydraulic depth. Because the verification results showed the greatest simulation errors in elevation during periods of shallow depths (figure 7), this option was tested by linearly increasing Manning's  $n$  from the calibrated value of 0.030 at 4 ft-depth to 0.130 at 0-ft depth from the cross section upstream from Railroad Bridge (site 19) to downstream from West Dundee piers (site 22) (fig. 26). Although the results could be improved by utilizing different effective depths and maximum values for Manning's  $n$  at different locations, a single type of variation was used to demonstrate the effect in general. At Railroad Bridge (site 19), the simulated variation in Manning's  $n$  is not large enough to cause the simulated elevation to match the measured elevations. It appears likely that the difference in elevations is due to inadequate representation of the head loss through the bridge as well as a possible increase in Manning's  $n$  at shallow depths as discussed in the "Hydraulic Geometry" section (see figure 17). At Huntley Road Bridge (site 20) the increase in Manning's  $n$  is excessive resulting in simulated stage exceeding measured stage. At the East Dundee foot-bridge (site 21), the variation in Manning's  $n$  appears to be optimal. These results are shown only to demonstrate the potential for improving the calibration by using the option for varying Manning's  $n$  with depth. An analysis of the physical reasonableness of the selected variation and verification using several other low-flow events would be required to verify the application of the option for calibration.

Because the stage is sensitive to the selection of Manning's  $n$ , the discharge area and velocity of the stream also may be expected to be sensitive. The effect

of increasing and decreasing Manning's  $n$  by 30 percent everywhere in the study reach on the dye transport simulation is shown in figure 27 for Rawson Bridge (site 8) and Huntley Road Bridge (site 20). The major effect is on the traveltime of the peak dye concentration, which increased by 1 hour for the increase in roughness and decreased by 1 hour for the decrease in roughness coefficient at Rawson Bridge, and increased and decreased by 3 hours for the respective increase and decrease in Manning's  $n$  at Huntley Road Bridge. The peak dye concentration is increased by 0.5 percent for the increase in roughness and by 2.6 percent for the decrease in roughness at Rawson Bridge, 6 mi downstream from the injection. At Huntley Road Bridge, 21 mi downstream from the injection site, the peak concentration is increased by 5.1 percent for the increase in roughness and by 10.3 percent for the decrease in roughness. An increase in peak concentration for a decrease in Manning's  $n$  may be explained by the decreased traveltime and consequent reduced attenuation in the dye peak concentration. The increase in peak concentration for an increase in Manning's  $n$  is more difficult to explain but may be an effect of the increase in the dynamic-wave celerity of the flood wave (which is proportional to the square root of the depth), which may result in a higher peak because of the reduced time for dilution. The unsteady nature of the flow precludes a simple analytical analysis of the traveltime and peak concentration results.

## EVALUATION OF THE MODEL

The flood-wave celerity and water velocity of an induced unsteady-flow wave on the Fox River in Illinois were accurately simulated using the dynamic-wave model FEQ indicating that the river geometry and roughness have been reasonably well described and that the dynamic-wave routines represent open-channel flow adequately. The Fox River was selected for the verification study because the low-gradient slope and large number of control structures were considered to provide a particularly rigorous test of the dynamic-wave model application. The FEQ model for the river was developed and calibrated prior to the verification study to maintain independence of the calibration phase from the verification phase of the study. The simulation results were evaluated in several different ways. Measured and simulated stage, discharge, and stage-discharge relations were compared. The accuracy of the simulated flood-wave celerity and



**EXPLANATION**

- CALIBRATED
- ..... ROUGHNESS COEFFICIENT VARIED WITH DEPTH
- RECORDED
- MEASURED

**Figure 26.** Effect of linear variation in the roughness coefficient from 0.030 at 4-ft depth to 0.130 at 0-ft depth at selected sites of the Fox River study reach in Illinois.

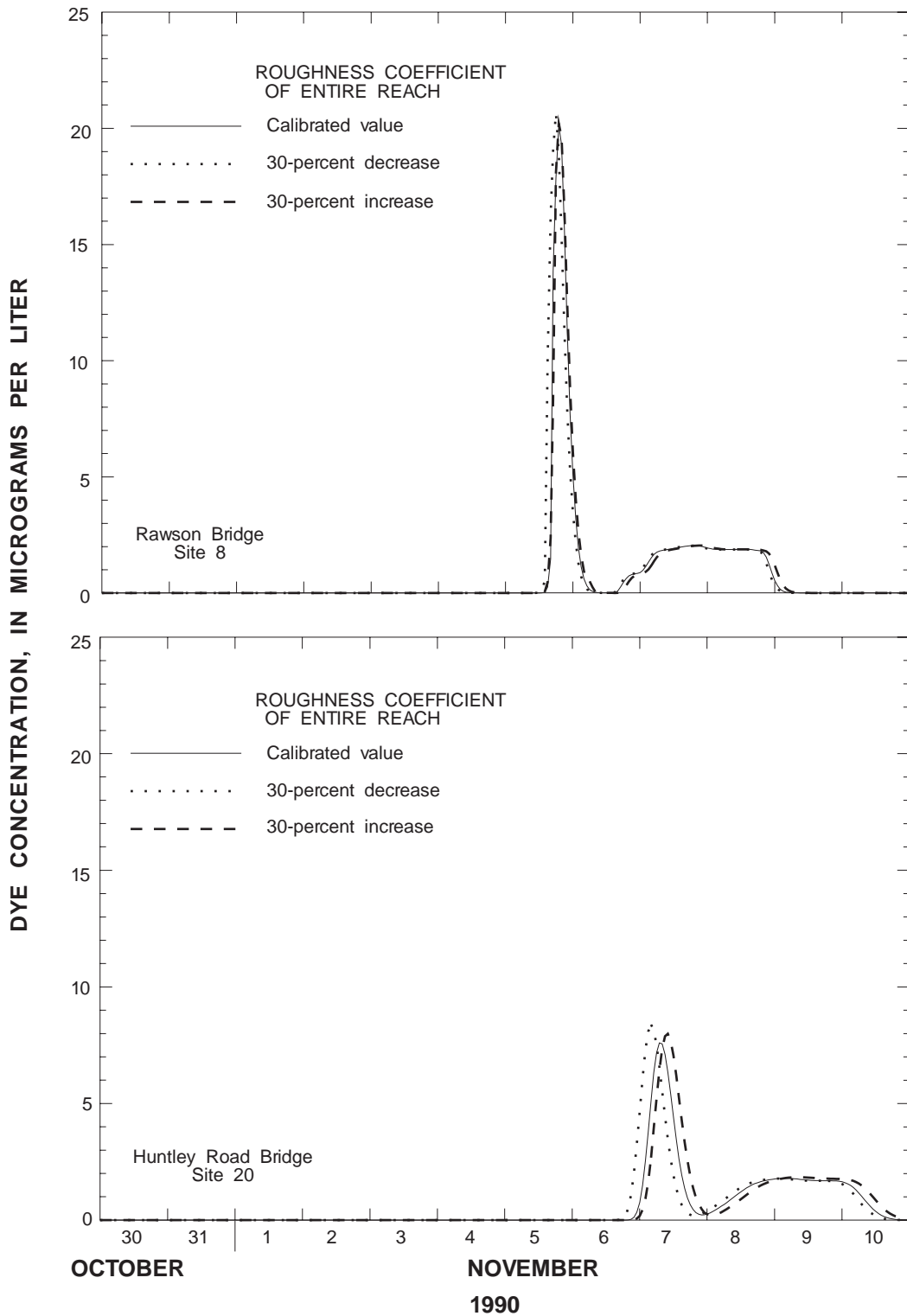


**Figure 27.** Effect of varying the roughness coefficient by 30 percent throughout the Fox River study reach on simulated dye concentration at selected sites in Illinois. (Site numbers are referenced to table 1.)

dynamic-wave celerity was inferred by using the simulated total flow field together with the dye-injection rate and concentration data measured in the field as input to the transport model, and comparing the simulated spatial and temporal dye-concentration distributions with measured dye-concentration distributions. The error in simulated traveltime was within the limit of resolution imposed by the frequency of dye-sample collection.

A high degree of robustness was demonstrated by the convergence of the model to an accurate solution within a limited number of iterations for a small convergence criterion even under widely varying initial conditions. The model sensitivity to time and distance steps was found to be relatively low for the study reach. The sensitivity of the model to the selection of the roughness coefficient was adequate and well within physically reasonable bounds. The model sensitivity to boundary datums depended on whether the upstream or downstream datum was varied, the locations of intervening dams, and the imposed boundary conditions used.

Several possible sources of error in the model input were investigated; none significantly affected the simulation of the overall dynamics of the induced flood wave. Potential sources of error in the input include the tributary inflows and other boundary conditions; the calibrated roughness coefficients, including the possible effective change in roughness at very shallow depths; the representations of dams and bridges; and errors in datum or other geometric features of the channel. Despite the possibility of some or all of these errors, the simulation results demonstrate the ability of the model to simulate the flood-wave celerity and to damp out errors in stage as the wave proceeds downstream and better geometric data are incorporated.

## **SUMMARY AND CONCLUSIONS**

A one-dimensional, unsteady-flow model, based on the Full de Saint-Venant Equations (FEQ) for dynamic flow in open channels, was verified for a 30.6-mi reach of the Fox River in northeastern Illinois. The model was calibrated prior to the study by the Illinois Department of Natural Resources, Office of Water Resources and Illinois State Water Survey. Thus, independence of the verification phase of the study from the calibration phase of the study was maintained. The calibrated model was used to simulate a period of

unsteady flow. Unsteady flows were introduced at the upstream end of the river reach by regulating the discharges of Stratton Dam during November 1990. The total flow field simulated by the model, together with dye-injection rate and concentration data measured at Stratton Dam, were used as input for a Branched Lagrangian Transport Model (BLTM). The simulation results from both models were compared graphically with discharge, stage, and (or) dye-concentration data collected during the unsteady-flow period at 8, 16, and 17 downstream locations, respectively. The simulated dynamic-wave celerity was inferred indirectly from the measured and simulated results for discharge, stage, and dye traveltime to have no significant error at any location. Differences during low-flow conditions between measured and simulated stage were less than about 0.2 foot at most of the sites, although differences up to 0.8 foot resulted at four sites where depths were shallow or head losses were inadequately represented through bridges. The differences may have resulted from the increase in effective roughness in the channel at very low depths that was not effectively modeled. Furthermore, accurate and representative measurements were difficult under some conditions of very low velocities or water-head buildup on the upstream side of bridges. The traveltime and concentration attenuation of the dye cloud were accurately simulated.

The effects of the physical and computational model parameters also are reported. Effective temporal resolution of the boundary-condition data was more important than the computational time increments used. The initial conditions were varied by 50 percent, and the model still converged to the correct solution within twelve 1-hour time steps. Deletion of bridges from the model caused no significant effects on the overall hydraulic routing and stage, although head losses at some bridges may have been inadequately represented. The effect of increasing distance-step size by about a factor of 3 caused no significant change in stage, but replacing cross sections with interpolated cross sections within river reach branches was found to change simulated stage as much as 0.7 ft depending on whether the remaining cross sections were representative of the local channel conditions. No significant effect on flood-wave celerity or discharge resulted from changes in distance step. Because of the low-head controlling dams throughout the study reach, sensitivity to error in gage datum depended on the type of boundary condition used and whether the datum error

was in the upstream or downstream boundary. The model was evaluated as accurate and robust for this application.

## REFERENCES CITED

- Barnes, H.H., 1967, Roughness characteristics of natural channels: U.S. Geological Survey Water-Supply Paper 1849, 213 p.
- Brater, E.F., and King, H.W., 1976, Handbook of hydraulics for the solution of hydraulic engineering problems (6th ed.): New York, McGraw-Hill, variably paginated.
- Chow, V.T., 1959, Open-channel hydraulics: New York, McGraw-Hill, 679 p.
- Chow, V.T., Maidment, D.R., and Mays, L.W., 1988, Applied hydrology: New York, McGraw-Hill, 572 p.
- Cunge, J.A., Holly, F.M., Jr., and Verwey, A., 1980, Practical aspects of computational river hydraulics: London, Pitman Publishing Limited, 420 p.
- Faye, R.E., and Cherry, R.N., 1980, Channel and dynamic flow characteristics of the Chattahoochee River, Buford Dam to Georgia Highway 141: U.S. Geological Survey Water-Supply Paper 2063, 66 p.
- Fisk, G.G., 1988, Discharge ratings for control structures at McHenry Dam on the Fox River, Illinois: U.S. Geological Survey Water-Resources Investigations Report 87-4226, 24 p.
- Federal Highway Administration, 1970, Hydraulics of bridge waterways: U.S. Department of Transportation, Hydraulic Design Series no. 1, 111 p.
- 1986, Bridge waterways analysis model: Research Report, U.S. Department of Transportation, Report No. FHWA/RD-86/106, 112 p.
- Franz, D.D., and Melching, C.S., in press, Full equations (FEQ) model for the solution of the full, dynamic equations of motion for one-dimensional unsteady flow in open channels and through control structures: U.S. Geological Survey Water-Resources Investigations Report 96-4240.
- Fread, D.L., 1975, Computation of stage-discharge relationships affected by unsteady flow: Water Resources Bulletin, v. 11, no. 2, American Water Resources Association, p. 213-228.
- Hulsing, Harry, 1967, Measurement of peak discharge at dams by indirect methods: U.S. Geological Survey Techniques of Water-Resources Investigations, book 3, chap. A5, 29 p.
- Hydraulic Engineering Center, 1982, HEC-2 Water Surface Profiles: U.S. Army Corps of Engineers, Water Resources Support Center, Davis, Calif., variably paginated.
- Ishii, A.L., and Wilder, J.E., 1993, Effect of boundary condition selection on unsteady-flow model calibration, in Proceedings of the XXV Congress of International Association for Hydraulic Research, Tokyo, p. 193-200.
- Jobson, H.E., 1987, Estimation of dispersion and first-order rate coefficients by numerical routing: Water Resources Research, v. 23, no. 1, p. 169-180.
- Jobson, H.E., and Schoellhamer, D.H., 1987, Users manual for a branched Lagrangian transport model: U.S. Geological Survey Water-Resources Investigations Report 87-4163, 73 p.
- Knapp, H.V., and Ortel, T.W., 1992, Effect of Stratton Dam operation on flood control along the Fox River and Fox Chain of Lakes: Illinois State Water Survey Contract Report 533, 79 p.
- Knapp, H.V., Ortel, T.W., and Larson, R.S., 1992, Hydrologic modeling of the Fox River Watershed: Illinois State Water Survey Contract Report 518, 89 p.
- Lai, Chintu, 1982, Numerical modeling of unsteady open-channel flow: Advances in Hydrosience, v. 14, Academic Press, p. 161-332.
- Lai, Chintu, Schaffranek, R.W., and Baltzer, R.A., 1992, Frictional resistance treatment in unsteady open-channel flow simulation, in Yen, B.C., ed, Channel Flow Resistance, Centennial of Manning's formula: Water Resources Publications, Littleton, Colo., p. 409-420.
- McCutcheon, S.C., 1989, Water Quality Modeling, Volume 1, Transport and Surface Exchange in Rivers: Boca Raton, FL, CRC Press, 334 p.
- Schaffranek, R.W., Baltzer, R.A., and Goldberg, D.E., 1981, A model for simulation of flow in singular and interconnected channels: U.S. Geological Survey Techniques of Water-Resources Investigations, book 7, chap. C3, 110 p.
- Schaffranek, R.W., ed., 1989, Proceedings of the Advanced Seminar on One-Dimensional, Open-Channel Flow and Transport Modeling, Bay St. Louis, Missouri, June 15-18, 1987: U.S. Geological Survey Water-Resources Investigations Report, 89-4061, 99 p.
- de Saint-Venant, Barre, 1871, Theory of unsteady water flow, with application to river floods and to propagation of tides in river channels: French Academy of Science, v. 73, p. 148-154, 237-240.
- Turner, M.J., 1994, Data-collection methods and data summary for verification of a one-dimensional, unsteady-flow model of the Fox River in Illinois: U.S. Geological Survey Open-File Report 93-483, 40 p.
- Xia, R., 1991, Sensitivity of flood-routing models to variations of momentum equation coefficients and terms: Ph.D. Thesis, Department of Civil Engineering, University of Illinois at Urbana-Champaign, 375 p.

---

# SELECTED SERIES OF U.S. GEOLOGICAL SURVEY PUBLICATIONS

---

## Periodicals

**Earthquakes & Volcanoes** (issued bimonthly).  
**Preliminary Determination of Epicenters** (issued monthly).

## Technical Books and Reports

**Professional Papers** are mainly comprehensive scientific reports of wide and lasting interest and importance to professional scientists and engineers. Included are reports on the results of resource studies and of topographic, hydrologic, and geologic investigations. They also include collections of related papers addressing different aspects of a single scientific topic.

**Bulletins** contain significant data and interpretations that are of lasting scientific interest but are generally more limited in scope or geographic coverage than Professional Papers. They include the results of resource studies and of geologic and topographic investigations, as well as collections of short papers related to a specific topic.

**Water-Supply Papers** are comprehensive reports that present significant interpretive results of hydrologic investigations of wide interest to professional geologists, hydrologists, and engineers. The series covers investigations in all phases of hydrology, including hydrogeology, availability of water, quality of water, and use of water.

**Circulars** present administrative information or important scientific information of wide popular interest in a format designed for distribution at no cost to the public. Information is usually of short-term interest.

**Water-Resources Investigations Reports** are papers of an interpretive nature made available to the public outside the formal USGS publications series. Copies are reproduced on request unlike formal USGS publications, and they are also available for public inspection at depositories indicated in USGS catalogs.

**Open-File Reports** include unpublished manuscript reports, maps, and other material that are made available for public consultation at depositories. They are a nonpermanent form of publication that may be cited in other publications as sources of information.

## Maps

**Geologic Quadrangle Maps** are multicolor geologic maps on topographic bases in 7.5- or 15-minute quadrangle formats (scales mainly 1:24,000 or 1:62,500) showing bedrock, surficial, or engineering geology. Maps generally include brief texts; some maps include structure and columnar sections only.

**Geophysical Investigations Maps** are on topographic or planimetric bases at various scales; they show results of surveys using geophysical techniques, such as gravity, magnetic, seismic, or radioactivity, which reflect subsurface structures that are of economic or geologic significance. Many maps include correlations with the geology.

**Miscellaneous Investigations Series Maps** are on planimetric or topographic bases of regular and irregular areas at various scales; they present a wide variety of format and subject matter. The series also includes 7.5-minute quadrangle photogeologic maps on planimetric bases that show geology as interpreted from aerial photographs. Series also includes maps of Mars and the Moon.

**Coal Investigations Maps** are geologic maps on topographic or planimetric bases at various scales showing bedrock or surficial geology, stratigraphy, and structural relations in certain coal-resource areas.

**Oil and Gas Investigations Charts** show stratigraphic information for certain oil and gas fields and other areas having petroleum potential.

**Miscellaneous Field Studies Maps** are multicolor or black-and-white maps on topographic or planimetric bases for quadrangle or irregular areas at various scales. Pre-1971 maps show bedrock geology in relation to specific mining or mineral-deposit problems; post-1971 maps are primarily black-and-white maps on various subjects such as environmental studies or wilderness mineral investigations.

**Hydrologic Investigations Atlases** are multicolored or black-and-white maps on topographic or planimetric bases presenting a wide range of geohydrologic data of both regular and irregular areas; principal scale is 1:24,000, and regional studies are at 1:250,000 scale or smaller.

## Catalogs

Permanent catalogs, as well as some others, giving comprehensive listings of U.S. Geological Survey publications are available under the conditions indicated below from the U.S. Geological Survey, Information Services, Box 25286, Federal Center, Denver, CO 80225. (See latest Price and Availability List.)

**“Publications of the Geological Survey, 1879–1961”** may be purchased by mail and over the counter in paperback book form and as a set of microfiche.

**“Publications of the Geological Survey, 1962–1970”** may be purchased by mail and over the counter in paperback book form and as a set of microfiche.

**“Publications of the U.S. Geological Survey, 1971–1981”** may be purchased by mail and over the counter in paperback book form (two volumes, publications listing and index) and as a set of microfiche.

**Supplements** for 1982, 1983, 1984, 1985, 1986, and for subsequent years since the last permanent catalog may be purchased by mail and over the counter in paperback book form.

**State catalogs, “List of U.S. Geological Survey Geologic and Water-Supply Reports and Maps For (State),”** may be purchased by mail and over the counter in paperback booklet form only.

**“Price and Availability List of U.S. Geological Survey Publications,”** issued annually, is available free of charge in paperback booklet form only.

**Selected copies of a monthly catalog “New Publications of the U.S. Geological Survey”** are available free of charge by mail or may be obtained over the counter in paperback booklet form only. Those wishing a free subscription to the monthly catalog “New Publications of the U.S. Geological Survey” should write to the U.S. Geological Survey, 582 National Center, Reston, VA 20192.

**Note**—Prices of Government publications listed in older catalogs, announcements, and publications may be incorrect. Therefore, the prices charged may differ from the prices in catalogs, announcements, and publications.

